Minimizing Variability of SARS-CoV-2 Wastewater Measurements and Advancing the Interpretation of Wastewater Surveillance Data

Nada Hegazy

Thesis submitted to the University of Ottawa
in partial fulfillment of the requirements for the degree of
Master of Applied Science in Environmental Engineering

Thesis Supervisors:
Dr. Robert Delatolla and Dr. Stéphanie Guilherme

uOttawa

Ottawa-Carleton Institute for Environmental Engineering (OCIENE)
Department of Civil Engineering
Faculty of Engineering
University of Ottawa

Abstract

Wastewater surveillance (WWS), included in the field of study of wastewater-based epidemiology (WBE), is the analysis of wastewaters to quantify community disease or use of chemicals by the community, such as pharmaceuticals and illicit drugs. WWS has historically been applied within the context of community public health through monitoring of pathogenic viral outbreaks such as polio and hepatitis A, as well as monitoring of illicit drug consumption. While WWS has been used for several decades, many of its contributions were largely unpopular within the public mainstream prior to the coronavirus disease in 2019 (COVID-19) pandemic. Since the onset of the pandemic, public health resources around the world were significantly afflicted by COVID-19. This elicited a prompt response by researchers to rapidly develop WWS for the application of severe acute respiratory syndrome-2 virus (SARS-CoV-2) WWS as a complementary epidemiological tool for population-wide monitoring of COVID-19 outbreaks. With the novelty of this technology, there are several challenges and gaps of knowledge that remain to be addressed in order to improve the reliability of WWS for SARS-CoV-2. Particularly, the effects of various constituents, endogenous and added, that commonly occur and are applied to wastewaters may result in the significant variability observed in WWS data sets, which in turn results in the uncertainty of the interpretation of WWS data sets of SARS-CoV-2 by various public health agencies throughout the pandemic.

This study is aimed to address the critical issue of data variability by investigating the effect of enhanced primary clarification with ferric-based chemical coagulants on the measurements of SARS-CoV-2 and the pepper mild mottle virus (PMMoV) WWS normalizing biomarker. It is believed that the addition of ferric ions via common coagulation treatment of primary sludge would interfere with the quantitative polymerase chain reaction (qPCR) amplification of viral RNA and could cause false-negative results. With 18.1% of the total population in Canada receiving wastewater that undergoes primary treatment including chemical precipitation/flocculation, and with proof of enrichment of SARS-CoV-2 and PMMoV RNA in untreated wastewater and settled primary sludge, it is important to elucidate whether ferric sulfate chemical coagulant is a potential source of data variability for population-wide WWS. With ferric sulfate concentrations ranging from 0 – 60 mg/L as Fe^{3+}, the PMMoV-normalized SARS-CoV-2 viral signal measurements were significantly reduced as a result of a significant elevation in the PMMoV viral signal

measurements. This is possibly due to the partitioning of PMMoV viral particles from the liquid phase to the solids phase of wastewater samples influenced by ferric sulfate at 60 mg/L as Fe^{3+} compared to the samples that were not treated with ferric sulfate.

This thesis also examined the evolving relation of WWS measurements to measurements of public health metrics to improve our current interpretation of SARS-CoV-2 WWS. The statistical correlations between wastewater PMMoV-normalized SARS-CoV-2 viral signal and clinical metrics indicative of disease incidence (laboratory-confirmed COVID-19 positive cases), and metrics indicative of disease burden (hospitalization, intensive care unit (ICU) admissions, and deaths) are investigated from the onset of the wildtype and the Alpha variant of concern (VOC) during limited vaccination immunization, through the onset of the Omicron BA.2 VOC in two strongly characterized sewersheds (Ottawa and Hamilton). WWS demonstrates to be a strong indicator of both disease incidence and disease burden during the period of limited vaccination immunization, and a moderate indicator of disease incidence, while remains a strong indicator of disease burden during the period of peak vaccination immunization (2-4 weeks after reception of 2 doses of the COVID-19 vaccine). Hospitalization-to-wastewater ratio is further shown to be a good indicator of VOC virulence when widespread clinical testing is limited.

Acknowledgments

To Dr. Robert Delatolla and Dr. Stéphanie Guilherme, thank you! I am tremendously grateful for your continued guidance, critique, and diligence, which allowed me to discover my potential in this challenging field. Thank you for supporting me on this journey and helping me become a better researcher.

To Patrick D'Aoust and Élisabeth Mercier, thank you for being great lab mates and wonderful friends! I greatly appreciate all the technical support you provided throughout this study, your help with collecting the wastewater samples, and your tremendous guidance with the nucleic acid extraction of SARS-CoV-2 RNA from wastewater samples. Your endless enthusiasm, invaluable discussions, and innovative ideas have greatly influenced my experience in the world of wastewater engineering and epidemiology.

I am thankful for the amazing friends I have made in the Wastewater Surveillance team at the University of Ottawa and for their collaborative efforts that tremendously contributed to the findings of this thesis. Special thanks to Aaron Cowan for sharing his knowledge and expertise in data analytics, to Zhihao (Howard) Zang for ensuring the timely arrival of wastewater samples to the University of Ottawa lab and for assisting with the nucleic acid extraction of SARS-CoV-2 RNA, to all of Xin Tian, Syeda Tasneem Towhid, Jian-Jun Jia, and Shen Wan for assisting with the RT-qPCR quantification of SARS-CoV-2 and PMMoV RNA. I would also like to acknowledge the assistance of Dr. Tyson Graber and his team from the Children's Hospital of Eastern Ontario Research Institute (CHEO-RI) for sharing their expertise in developing the experimental methodologies throughout this work. Of course, many thanks to Pervez Kabir, Juliet Ikem, and Huiyu Chen for all the learning and discussion we had with each other in the lab.

My thanks also extend to the Ottawa-Carleton Institute for Environmental Engineering and the Civil Engineering Department, its professors, and academic staff (Veronique, Luc, and Paula); each has helped me in their own way. I would also like to thank the University of Ottawa for granting me the admission scholarship; its financial support was key to completing this thesis.

Last and not least, my warmest appreciation goes to my parents, Heba Ashmawy and Elsayed Hegazy, for their infinite love and support in every step I take, and to my siblings for being my source of joy throughout this work. This thesis is dedicated to them.

Table of Contents

List of Figures

List of Tables

List of Abbreviations

Abbreviation	Description
5-HIAA	5-hydroxyinoleacetic acid
ANOVA	One-way analysis of variance
BOD	Biological oxygen demand
cBOD	Carbonaceous biological oxygen demand
CDC	Center for Disease Control and Prevention
CHAMO	Children's Hospital Academic Medical Organization
CHEO	Children's Hospital of Eastern Ontario
COD	Chemical oxygen demand
COVID-19	Coronavirus disease in 2019
crAssphage	Cross-assembly phage
ECCC	Environment and Climate Change Canada
GPEI	Global Polio Eradication Initiative
HCl	Hydrochloric acid
HIV	Human Immunodeficiency Virus
HW	Hospitalization-to-wastewater
ICU	Intensive care unit
MERS-CoV	Middle East Respiratory Syndrome Coronavirus
NP	Nasopharyngeal
OCIENE	Ottawa-Carleton Institute for Environmental Engineering
PMMoV	Pepper mild mottle virus
RNA	Ribonucleic acid
ROPEC	Robert O. Pickard Environmental Centre
RPM	Rotations per minute
RT-qPCR	Reverse transcription-quantitative polymerase chain reaction
SARS-CoV-2	Severe Acute Respiratory Syndrome Coronavirus-2
TKN	Total Kjeldahl nitrogen
TSS	Total suspended solids
VOC	Variant of concern
VSS	Volatile suspended solids
WBE	Wastewater-based epidemiology
WHO	World Health Organization
WRRF	Water resource recovery
WSI	Wastewater Surveillance Initiative
WWS	Wastewater-based surveillance

Chapter 1.

Introduction & Background

1.1 History of WWS

This study is conducted in the field of wastewater-based epidemiology (WBE) (also referred to as wastewater surveillance (WWS)); a population-wide approach that involves using municipal wastewater for real-time monitoring of public health status by collecting chemical and biological information. Measurement of microbial DNA or RNA in wastewater can suggest infectious disease outbreak in a population caused by viruses or bacteria. For the last four decades, humans have witnessed the emergence of some of the deadliest viral outbreaks caused by the Human Immunodeficiency Virus (HIV) (in 1981), Severe Acute Respiratory Syndrome Coronavirus (SARS-CoV) (in 2002), Influenza A virus subtype H1N1 (in 2009), Middle East Respiratory Syndrome Coronavirus (MERS-CoV) (in 2012), Ebola virus (in 2013), and Severe Acute Respiratory Syndrome Coronavirus-2 (SARS-CoV-2) (ongoing since the first detection in 2019) (Bloom and Cadarette, 2019; Qu et al., 2020; Wigginton and Boehm, 2020). The far-reaching consequences of the diseases caused by these viruses on public health safety have increased the importance of having an effective disease surveillance system. Commonly used infectious disease monitoring techniques include sentinel surveillance, clinical-based surveillance, questionnaires or surveys, hospital admission data, death rates due to disease complications, and human bio-monitoring (Sims and Kasprzyk-Hordern, 2020). While those techniques are greatly significant for infectious disease surveillance, they majorly rely on data acquisition from hospitals, clinics, public health units, and other sources which can be subject to biases, high cost, and limited representation of an entire population (Gracia-Lor et al., 2018). Countries with less-developed healthcare systems are particularly subject to underestimation of laboratory-identified cases due to poor reporting of healthcare data (Sims and Kasprzyk-Hordern, 2020). This poses the need for a surveillance technique that would provide real-time monitoring of population-wide public health

status while being economically feasible and could be applied in communities that lack healthcare resources.

WWS has been utilized for population-wide disease surveillance as early as the 1970s during the prevalence of poliovirus outbreaks. For instance, wildtype strains of poliovirus was measured in wastewater from two water resource recovery facilities (WRRFs) in Ottawa, Ontario, in 1974, indicating the presence of polio outbreaks within the community despite no reported positive cases of polio (Sattar and Westwood, 1977), demonstrating higher sensitivity of poliovirus detection in wastewater compared to clinical surveillance. From the1980s onwards, WWS of poliovirus has played a critical role in the worldwide initiative to eradicate polio under the World Health Organization (WHO) Global Polio Eradication Initiative (GPEI) program (Asghar et al., 2014; WHO, 2003). WWS has also been used to determine disease incidence of other viruses including enteroviruses (Brinkman et al., 2017) and measles (Benschop et al., 2017), and was further proven to provide an early warning of hepatitis A virus (HAV) (Hellmér et al., 2014), hepatitis E virus (HEV) (Miura et al., 2016), and norovirus outbreaks (Hellmér et al., 2014).

Contributions to WWS further include the monitoring of illicit drug consumption including cocaine, heroin, and methamphetamines (Boleda et al., 2007; Castiglioni et al., 2006; Kasprzyk-Hordern et al., 2008; Zuccato et al., 2008). WWS for illicit drug consumption was first achieved in 2005 when Zuccato et al. (2005) were able to extract and quantify cocaine in untreated wastewater samples to investigate population-wide cocaine usage (Zuccato et al., 2005). Before wastewater monitoring, trends in illicit drug abuse were primarily monitored by periodic drug-use surveys at a local or national level (Center for Behavioral Health Statistics and Quality, 2017; European Monitoring Centre for Drugs and Drug Addiction, 2002a, 2002b). These indicators, however, often provided unreliable data as they heavily relied on the respondents' truthfulness with no measures to account for errors derived from the avoidance of self-reporting or failure to report; thus, community-wide usage of drugs were not always properly captured (Daughton, 2001; Zuccato et al., 2005). As such, WWS is being continuously refined as a complementary tool for capturing drug abuse trends in various communities, and is currently being internationally supported by public health agencies in Europe ((EMCDDA) European Monitoring Centre for Drugs and Drug Addiction, 2020), Australia (Choi et al., 2019; Lai et al., 2018, 2016; O'Brien et

al., 2019; Ben J. Tscharke et al., 2016; Benjamin J. Tscharke et al., 2016), and in the USA (Halden et al., 2019).

In times of rising public health concerns, WWS was continuously proven to be an effective alternative for providing a real-time, anonymous, non-invasive, and sensitive measurement of community disease incidence or use of illicit drugs by the community for several decades. These characteristics of WWS, in combination with its low economical cost, further positions this surveillance tool to address some of the critical health disparities around the world, including regions with less developed health care systems (Government of Canada, 2020; Indigenous Services Canada, 2022; Medina et al., 2022; Public Health Ontario, 2020; Statistics Canada, 2020). These reported benefits, particularly its ability to act as an early warning indicator of community disease outbreaks, positions WWS as a promising population-wide surveillance tool in light of the coronavirus disease in 2019 (COVID-19) pandemic.

1.2 WWS of COVID-19

The novel COVID-19 disease was first reported in December 2019 as numerous patients were diagnosed with atypical pneumonia (He et al., 2020; WHO, 2020). The disease, which is caused by the SARS-CoV-2 virus began to spread very rapidly worldwide due to its high degree of infectiousness (Lu et al., 2020). By March 11th, 2020, the disease was declared a global pandemic by WHO (Yeo et al., 2020). The early stages of the pandemic during the onset of the wildtype and Alpha (B.1.1.7) variant of concern (VOC) (December 2019 through July 2020) had an immense impact on daily activities due to the severity of the COVID-19 illness, death, and the social and economic implications of restricted public gatherings and curfews placed by government agencies as means to control community spread of the virus. As the pandemic evolved over the past 27 months, the disease still poses a substantial global public health risk with newly emerging highly transmissible VOCs such as the Delta, and Omicron BA.1 and BA.2 VOCs, affecting millions worldwide (WHO, 2022a). By the time of writing this thesis (July 2022), SARS-CoV-2 has infected over 500 million people worldwide (~6.0% of the world population), and caused over 6 million deaths globally (1.2% of total infected cases) (WHO, 2022b).

The typical diagnostic test to confirm COVID-19 positivity is detecting SARS-CoV-2 RNA in nasopharyngeal (NP) swabs by reverse transcription-quantitative polymerase chain reaction

(RT-qPCR), or by symptom observation (Ahmed et al., 2020a; Huang et al., 2020). However, many countries have faced shortcomings in accurately determining the prevalence of COVID-19 since nasopharyngeal testing mostly targets symptomatic individuals while asymptomatic cases, which make up 20-30% of overall positive cases, may remain undetected (Long et al., 2020; Pan et al., 2020). Furthermore, the onset of COVID-19 disease symptoms is within 2 – 14 days after initial exposure to the virus (CDC, 2022). Contagiousness reportedly can begin days before infected individuals become symptomatic, accounting for 44% of COVID-19 transmission (He et al., 2020). As such, community transmission and exposure to the virus can occur unknowingly either before the onset of symptoms or by asymptomatic individuals and has consequently resulted in difficulties controlling the community spread of the virus. Hence, additional measures would be required for unbiased population-wide monitoring of COVID-19 (Daughton, 2009; Hill et al., 2021).

Early during the pandemic, individuals ill with COVID-19, symptomatic and asymptomatic were found to discharge SARS-CoV-2 viral RNA particles which ultimately reaches municipal wastewater treatment plants (Chen et al., 2020; Cheung et al., 2020; Park et al., 2021; Santos et al., 2020; Xing et al., 2020; Xu et al., 2020; Zhang et al., 2021). Medema et al (2020) was one of the earliest WWS works that determined a positive correlation between an increase in SARS-CoV-2 viral RNA signal in wastewater and increases in COVID-19 positive cases in the Netherlands (Medema et al., 2020). Numerous peer-reviewed literature further emerged confirming the detection of SARS-CoV-2 viral RNA in wastewater and is subsequently being monitored at various WRRFs around the world as a disease surveillance tool complementary to the standard disease surveillance metrics (Ahmed et al., 2020a; Bar-Or et al., 2020; Gonzalez et al., 2020; Haramoto et al., 2020; Kocamemi et al., 2020; La Rosa et al., 2021; Medema et al., 2020; Nemudryi et al., 2020a; Peccia et al., 2020; Randazzo et al., 2020b; Rimoldi et al., 2020; Sherchan et al., 2020; Wu et al., 2021; Wurtzer et al., 2020; Zhang et al., 2021). Additionally, various studies demonstrated that the SARS-CoV-2 viral RNA particles can be detected in wastewater 0 – 4 days prior to clinical testing of COVID-19 during the onset of the wildtype and Alpha VOC, thereby establishing WWS of SARS-CoV-2 as an effective predictor and indicator for disease incidence (D'Aoust et al., 2021a; Gerrity et al., 2021; Gonzalez et al., 2020; Graham et al., 2021; Medema et al., 2020; Peccia et al., 2020). These qualities in the context of a very serious global pandemic

have sparked keen interest world-wide to further develop and optimize WWS as an important epidemiological metric for disease surveillance (Figure 1.1).

By the time of writing this thesis (July 2022), WWS of SARS-CoV-2 is active worldwide in nearly 60 countries at over 3000 sites (COVIDPoops19, 2022). In Canada, there are approximately 250 locations being monitored using SARS-CoV-2 WWS. The Ontario Wastewater Surveillance Initiative (WSI) comprises 175 locations in Canada and is one of the largest SARS-CoV-2 surveillance systems in the world (Government of Ontario, 2022). The WSI program captures greater than 75% of the Ontario population, includes cities, First Nations, neighbourhoods, long term care facilities, shelters, university residences and airports. The WSI program analyzes wastewaters in all 34 public health jurisdictions and posts aggregated, regional measurements to the public world (Ontario Agency for Health Protection and Promotion (Public Health Ontario), 2022).

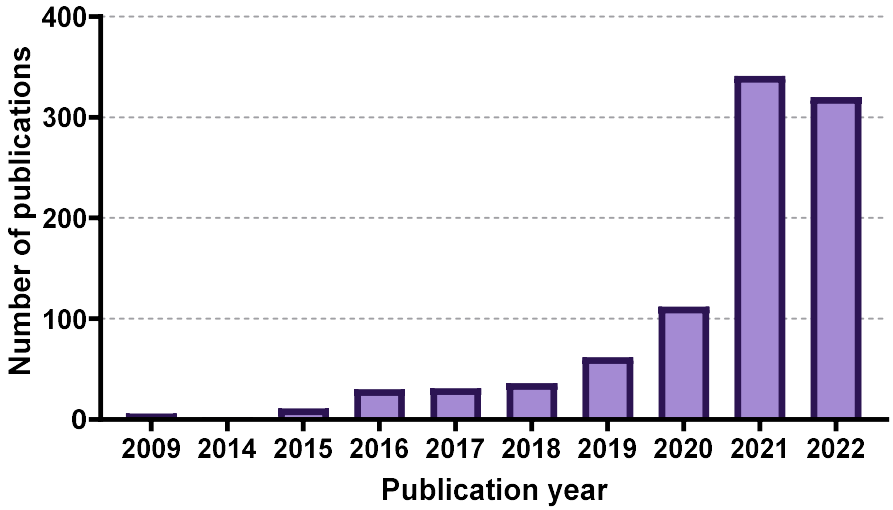

Figure 1.1: Number of peer-reviewed publications contributing to the WWS field over the last 12 years

1.2.1 Normalization of SARS-CoV-2 viral RNA signal

One of the recent developments in the field of WWS was accounting for day-to-day fluctuations in population size served by WRRFs when estimating for illicit drug consumption or incidence from viral infection over an extended period of time through normalization with hydrochemical parameters (such as ammonium (NH_4^+), chemical oxygen demand (COD),

biological oxygen demand (BOD), nitrogen (N), phosphorus (P)) (Been et al., 2014; Thomas et al., 2017), or human urine-biomarkers such as 5-hydroxyindoleacetic acid (5-HIAA), cotinine, and caffeine (Chen et al., 2014; Rico et al., 2017) in untreated wastewater. Normalization is further intended to remove biases in the longitudinal wastewater measurements due to fluctuations in WRRFs operations, and seasonal variations (i.e., raining or snowmelt events) that could influence mass flux of wastewater to enhance the utility of WWS data for interpretation of public health trends.

In the context of WWS for SARS-CoV-2 surveillance, biomarkers that have higher abundance in the solids fraction of wastewater would be optimal for the normalization of population-wide SARS-CoV-2 viral measurements since various WWS works suggest that SARS-CoV-2 biomass being largely localized in the solids fraction of wastewater (D'Aoust et al., 2021b; Graham et al., 2021; Kitamura et al., 2021; Peccia et al., 2020; Rosario et al., 2009). Such biomarkers include the pepper mild mottle virus (D'Aoust et al., 2021b, 2021a; Jafferali et al., 2021; Kitajima et al., 2018; Rosario et al., 2009; Wu et al., 2020a) and cross-assembly phage (crAssphage) (Crank et al., 2020; Polo et al., 2020). PMMoV viral RNA particles in wastewater solids consistently demonstrated substantial stability with low seasonal variations (D'Aoust et al., 2021b; Kitajima et al., 2018, 2014). With these properties, normalization of SARS-CoV-2 RNA viral particles with PMMoV was found to remove biases from day-to-day variability in wastewater qualities, as well as providing a trend that more strongly resembles incidence and disease burden of COVID-19 (D'Aoust et al., 2021a; Hegazy et al., 2022), compared to non-normalized SARS-CoV-2 viral signals (D'Aoust et al., 2021b). As such, SARS-CoV-2 viral RNA measurements were normalized with PMMoV throughout this study.

1.3 Current Limitations and Gap of Knowledge

Since the focus on WWS for disease surveillance has only begun to expand, there is presently no standardized approach to sampling, analyzing and interpreting WWS data. With respect to the sampling, SARS-CoV-2 viral RNA was successfully measured from wastewater collected directly from a municipal sewage system serving an urban population (Fongaro et al., 2021; Kitamura et al., 2021), and sewage systems serving a localized community (Bar-Or et al., 2022), solids fraction of wastewater influent (upstream of WRRF) (Ahmed et al., 2020a, 2020b; Haramoto et al., 2020;

Kitamura et al., 2021; Kumar et al., 2020; La Rosa et al., 2021, 2020; Nemudryi et al., 2020b; Randazzo et al., 2020b; Trottier et al., 2020; Wu et al., 2020b), final effluent after Upflow Anaerobic Sludge Blanket (UASB) (Kumar et al., 2020), and primary clarified sludge (D'Aoust et al., 2021b; Graham et al., 2021; Neault et al., 2020; Peccia et al., 2020; Philo et al., 2021; Zulli et al., 2022). Previous studies demonstrate higher sensitivity of SARS-CoV-2 RNA detection with solids-based viral extraction protocols, particularly from primary clarified sludge compared to wastewater influent (D'Aoust et al., 2021b; Graham et al., 2021). However, one source of variation in primary sludge qualities includes the use of metal-based coagulant during chemically enhanced primary treatment processes. Although coagulation has been previously used as a means for virus concentration in wastewater samples low in solids (Bar-Or et al., 2020; Barril et al., 2021; Randazzo et al., 2020b, 2020a), the effects of coagulation on RT-qPCR quantification of SARS-CoV-2 and the commonly used pepper mild mottle virus (PMMoV) biomarker (D'Aoust et al., 2021b, 2021a; Jafferali et al., 2021; Kitajima et al., 2018; Rosario et al., 2009; Wu et al., 2020a) remain unknown.

Furthermore, although wastewater surveillance has been widely implemented and continuously provided an accurate population-wide representation of the COVID-19 dynamics, there currently exists a gap of knowledge on the interpretation of WWS data as an indicator of disease incidence and disease burden during periods of peak natural and vaccination immunization and limited natural and vaccination immunization. Additionally, continuous population-wide diagnosis with PCR testing of NP swabs has presently become less applied in many countries due to the economic burden of testing, making it less representative of real-time community incidence.

1.4 Research Objectives & Significance of Work

The intent of this thesis is to address two key challenges in WWS of COVID-19: (i) variability in the data set, and (ii) interpretation of the WWS dataset. The specific objectives of this research are as follows:

1. Investigate the effect of enhanced primary clarification with ferric sulfate coagulant on the measurements of SARS-CoV-2 and PMMoV viral signals in the settled primary sludge.
2. Examine the dynamic relation between the SARS-CoV-2 viral signals in wastewater and

epidemiological metrics indicative of disease incidence (laboratory confirmed positive cases) and burden (hospitalizations, intensive care unit (ICU) admission, and deaths) through the course of the COVID-19 pandemic, including periods of peak and waned immunization (natural and vaccination induced).

Results granted from this work will help overcome the current limitations of WWS of the COVID-19 disease and advance its application in Canada and globally.

1.5 Thesis Structure

This thesis is subdivided into four chapters of which the first chapter is a manuscript that is in preparation for submission to a peer-reviewed journal, and the second chapter is submitted in the Science of the Total Environment peer reviewed journal. A description of the contents of each chapter is outlined below.

Chapter 1. *"Introduction & background"* presents a review of background and current developments of WWS for population-wide public health surveillance. This chapter highlights the importance of WWS as a complimentary tool for public health surveillance in addition to the current standard diagnostic surveillance methods. It further describes current limitations of WWS in the context of COVID-19 surveillance to illustrate the significance of the research and the objectives of the study, the scope and structure of the thesis.

Chapter 2. "*Impact of coagulation on SARS-CoV-2 and PMMoV viral signal in wastewater solids*" presents the effect of ferric sulfate coagulant addition on SARS-CoV-2 and PMMoV viral signals in wastewater solids by jar testing procedures to explore the possibility of data variation for WWS of SARS-CoV-2 from primary sludge produced by means of chemically enhanced primary clarification.

Manuscript to be submitted for publication:

N. Hegazy, X. Tian, P. M. D'Aoust, S. T. Towhid, É. Mercier, Z. Zhang, A. E. MacKenzie, T. E. Graber, S. Guilherme, and R. Delatolla "Impact of coagulation on SARS-CoV-2 and PMMoV viral signal in wastewater solids". In preparation to be submitted shortly.

Chapter 3. *"Understanding the dynamic relation between wastewater SARS-CoV-2 signal and clinical metrics throughout the pandemic"* presents a longitudinal study on the relation between WWS and four epidemiological metrics during the onset of the Alpha, Delta, and Omicron BA.1 and BA.2 VOCs concurring with periods of peak vaccination immunization and waned vaccination immunization in two Canadian communities.

Published in Science of the Total Environment:

N. Hegazy, A. Cowan, P. M. D'Aoust, É. Mercier, S. T. Towhid, J. Jia, S. Wan, Z. Zhang, M. P. Kabir, W. Fang, T. E. Graber, A. E. MacKenzie, S. Guilherme, R. Delatolla "Understanding the dynamic relation between wastewater SARS-CoV-2 signal and clinical metrics throughout the pandemic". Science of the Total Environment, 853, 2022, 158458.

Chapter 4. *"Conclusions and recommendations"* iterates on how the research objectives were met. Overall recommendations for future work are also provided.

1.6 Contribution of Authors

The thesis includes two manuscripts, which are based on the findings of this study. Both manuscripts are first-authored by me, with one manuscript currently in preparation for publication and the second published in the Science of the Total Environment peer-reviewed journal. The authors' contributions for each manuscript are described below:

Manuscript 1: N. Hegazy, X. Tian, P. M. D'Aoust, S. T. Towhid, É. Mercier, Z. Zhang, A. E. MacKenzie, T. E. Graber, S. Guilherme, and R. Delatolla *Impact of coagulation on SARS-CoV-2 and PMMoV viral signal in wastewater solids*. In preparation to be submitted shortly.

N. Hegazy: Conducted literature review, performed jar testing procedures, performed nucleic acid extraction of resulting solids pellets and supernatant fractions, performed formal analysis, and wrote the manuscript.

X. Tian: Assisted with jar testing experimental procedure, performed RT-qPCR for resulting solid pellets and supernatant fractions, assisted with formal analysis, and review and editing of the manuscript.

P. M. D'Aoust: Assisted with sample collection, provided expertise and guidance for experimental methodology, review and editing of the manuscript.

S. T. Towhid: Review and editing of the manuscript.

É. Mercier: Provided expertise and guidance for experimental methodology, and review and editing of the manuscript.

Z. Zhang: Review and editing of the manuscript.

A. E. MacKenzie: Provided expertise and guidance for experimental methodology, review and editing of the manuscript, and funding acquisition for the research.

T. E. Graber: Provided expertise and guidance for experimental methodology, review and editing of the manuscript.

S. Guilherme: Provided supervision in analysis and validation of results, and review and editing of the manuscript.

R. Delatolla: Provided expertise and guidance for experimental methodology, supervision in analysis and validation of results, editorial guidance and contribution, and funding acquisition for the research.

Manuscript 2: N. Hegazy, A. Cowan, P. M. D'Aoust, É. Mercier, S. T. Towhid, J. Jia, S. Wan, Z. Zhang, M. P. Kabir, W. Fang, T. E. Graber, A. E. MacKenzie, S. Guilherme, R. Delatolla *Understanding the dynamic relation between wastewater SARS-CoV-2 signal and clinical metrics throughout the pandemic.* Published in Science of the Total Environment.

N. Hegazy: Conducted literature review, performed nucleic acid extraction from primary sludge solids for a portion of the data, performed formal analysis and wrote the manuscript.

A. Cowan: Provided expertise and guidance in statistical data analysis, and review and editing of the manuscript.

P. M. D'Aoust: Provided expertise and guidance for experimental methodology, collection of wastewater samples, review and editing of the manuscript.

É. Mercier: Provided expertise and guidance for experimental methodology, assisted with experimental work through RT-qPCR extraction for a portion of the data, review and editing of the manuscript.

S. T. Towhid: Assisted with experimental work through RT-qPCR extraction for a portion of the data, review and editing of the manuscript.

J. Jia: Assisted with experimental work through RT-qPCR extraction for a portion of the data, review and editing of the manuscript.

S. Wan: Assisted with experimental work through RT-qPCR extraction for a portion of the data, review and editing of the manuscript.

Z. Zhang: Experimental work through nucleic acid extraction from primary sludge solids for a portion of the data, assistance with sample collection, review and editing of manuscript.

M. P. Kabir: Review and editing of the manuscript.

W. Fang: Review and editing of the manuscript.

T. E. Graber: Provided expertise and guidance for experimental methodology, review and editing of the manuscript.

Alex. E. MacKenzie: Provided expertise and guidance for experimental methodology, review and editing of the manuscript, and funding acquisition for the research.

S. Guilherme: Provided supervision in analysis and validation of results, and review and editing of the manuscript.

R. Delatolla: Provided expertise and guidance for experimental methodology, supervision in analysis and validation of results, editorial guidance and contribution, and funding acquisition for the research.

1.7 References

(EMCDDA) European Monitoring Centre for Drugs and Drug Addiction, 2020. Wastewater analysis and drugs: a European multi-city study. Lisbon, Portugal.

Ahmed, W., Angel, N., Edson, J., Bibby, K., Bivins, A., O'Brien, J.W., Choi, P.M., Kitajima, M., Simpson, S.L., Li, J., Tscharke, B., Verhagen, R., Smith, W.J.M., Zaugg, J., Dierens, L., Hugenholtz, P., Thomas, K. V., Mueller, J.F., 2020a. First confirmed detection of SARS-CoV-2 in untreated wastewater in Australia: A proof of concept for the wastewater surveillance of COVID-19 in the community. Sci. Total Environ. 728, 138764. https://doi.org/10.1016/j.scitotenv.2020.138764

Ahmed, W., Bertsch, P.M., Bivins, A., Bibby, K., Farkas, K., Gathercole, A., Haramoto, E., Gyawali, P., Korajkic, A., McMinn, B.R., Mueller, J.F., Simpson, S.L., Smith, W.J.M., Symonds, E.M., Thomas, K. V., Verhagen, R., Kitajima, M., 2020b. Comparison of virus concentration methods for the RT-qPCR-based recovery of murine hepatitis virus, a surrogate for SARS-CoV-2 from untreated wastewater. Sci. Total Environ. 739, 139960. https://doi.org/10.1016/J.SCITOTENV.2020.139960

Asghar, H., Diop, O.M., Weldegebriel, G., Malik, F., Shetty, S., El Bassioni, L., Akande, A.O., Al Maamoun, E., Zaidi, S., Adeniji, A.J., Burns, C.C., Deshpande, J., Oberste, M.S., Lowther, S.A., 2014. Environmental Surveillance for Polioviruses in the Global Polio Eradication Initiative. J. Infect. Dis. 210, S294–S303. https://doi.org/10.1093/INFDIS/JIU384

Bar-Or, I., Yaniv, K., Shagan, M., Ozer, E., Erster, O., Mendelson, E., Mannasse, B., Shirazi, R., Kramarsky-Winter, E., Nir, O., Abu-Ali, H., Ronen, Z., Rinott, E., Lewis, Y.E., Friedler, E., Bitkover, E., Paitan, Y., Berchenko, Y., Kushmaro, A., 2020. Regressing SARS-CoV-2 sewage measurements onto COVID-19 burden in the population: A proof-of-concept for quantitative environmental surveillance. medRxiv 1–11. https://doi.org/10.1101/2020.04.26.20073569

Bar-Or, I., Yaniv, K., Shagan, M., Ozer, E., Weil, M., Indenbaum, V., Elul, M., Erster, O., Mendelson, E., Mannasse, B., Shirazi, R., Kramarsky-Winter, E., Nir, O., Abu-Ali, H., Ronen, Z., Rinott, E., Lewis, Y.E., Friedler, E., Bitkover, E., Paitan, Y., Berchenko, Y., Kushmaro, A., 2022. Regressing SARS-CoV-2 Sewage Measurements Onto COVID-19 Burden in the Population: A Proof-of-Concept for Quantitative Environmental Surveillance. Front. Public Heal. 9, 2043. https://doi.org/10.3389/FPUBH.2021.561710/BIBTEX

Barril, P.A., Pianciola, L.A., Mazzeo, M., Ousset, M.J., Jaureguiberry, M.V., Alessandrello, M., Sánchez, G., Oteiza, J.M., 2021. Evaluation of viral concentration methods for SARS-CoV-2 recovery from wastewaters. Sci. Total Environ. 756, 144105. https://doi.org/10.1016/j.scitotenv.2020.144105

Been, F., Rossi, L., Ort, C., Rudaz, S., Olivier, ‖, Delémont, D., Esseiva, P., 2014. Population Normalization with Ammonium in Wastewater-Based Epidemiology: Application to Illicit Drug Monitoring. https://doi.org/10.1021/es5008388

Benschop, K.S.M., van der Avoort, H.G., Jusic, E., Vennema, H., van Binnendijk, R., Duizer, E., 2017. Polio and measles down the drain: Environmental enterovirus surveillance in the

Netherlands, 2005 to 2015. Appl. Environ. Microbiol. 83, 558–575. https://doi.org/10.1128/AEM.00558-17/FORMAT/EPUB

Bloom, D.E., Cadarette, D., 2019. Infectious disease threats in the twenty-first century: Strengthening the global response. Front. Immunol. 10, 549. https://doi.org/10.3389/FIMMU.2019.00549/BIBTEX

Boleda, M.R., Galceran, M.T., Ventura, F., 2007. Trace determination of cannabinoids and opiates in wastewater and surface waters by ultra-performance liquid chromatography–tandem mass spectrometry. J. Chromatogr. A 1175, 38–48. https://doi.org/10.1016/J.CHROMA.2007.10.029

Brinkman, N.E., Fout, G.S., Keely, S.P., 2017. Retrospective Surveillance of Wastewater To Examine Seasonal Dynamics of Enterovirus Infections. mSphere 2. https://doi.org/10.1128/MSPHERE.00099-17/SUPPL_FILE/SPH003172298SF9.PDF

Castiglioni, S., Zuccato, E., Crisci, E., Chiabrando, C., Fanelli, R., Bagnati, R., 2006. Identification and measurement of illicit drugs and their metabolites in urban wastewater by liquid chromatography-tandem mass spectrometry. Anal. Chem. 78, 8421–8429. https://doi.org/10.1021/AC061095B/ASSET/IMAGES/LARGE/AC061095BF00003.JPEG

CDC, 2022. Symptoms of COVID-19 | CDC [WWW Document]. URL https://www.cdc.gov/coronavirus/2019-ncov/symptoms-testing/symptoms.html (accessed 7.12.22).

Center for Behavioral Health Statistics and Quality, 2017. 1999-2015 National Surveys on Drug Use and Health: Small Area Estimation Dataset.

Chen, C., Kostakis, C., Gerber, J.P., Tscharke, B.J., Irvine, R.J., White, J.M., 2014. Towards finding a population biomarker for wastewater epidemiology studies. Sci. Total Environ. 487, 621–628. https://doi.org/10.1016/j.scitotenv.2013.11.075

Chen, Y., Chen, L., Deng, Q., Zhang, G., Wu, K., Ni, L., Yang, Y., Liu, B., Wang, W., Wei, C., Yang, J., Ye, G., Cheng, Z., 2020. The presence of SARS-CoV-2 RNA in the feces of COVID-19 patients. J. Med. Virol. 92, 833–840. https://doi.org/10.1002/jmv.25825

Cheung, K.S., Hung, I.F.N., Chan, P.P.Y., Lung, K.C., Tso, E., Liu, R., Ng, Y.Y., Chu, M.Y., Chung, T.W.H., Tam, A.R., Yip, C.C.Y., Leung, K.H., Fung, A.Y.F., Zhang, R.R., Lin, Y., Cheng, H.M., Zhang, A.J.X., To, K.K.W., Chan, K.H., Yuen, K.Y., Leung, W.K., 2020. Gastrointestinal Manifestations of SARS-CoV-2 Infection and Virus Load in Fecal Samples From a Hong Kong Cohort: Systematic Review and Meta-analysis. Gastroenterology 159, 81–95. https://doi.org/10.1053/j.gastro.2020.03.065

Choi, P.M., Tscharke, B., Samanipour, S., Hall, W.D., Gartner, C.E., Mueller, J.F., Thomas, K. V, O'brien, J.W., 2019. Social, demographic, and economic correlates of food and chemical consumption measured by wastewater-based epidemiology. Proc. Natl. Acad. Sci. U. S. A. 116, 21864–21873. https://doi.org/10.1073/pnas.1910242116

COVIDPoops19, 2022. Summary of global SARS-CoV-2 wastewater monitoring efforts by UC Merced researchers [WWW Document]. Univ. Calif. Merced. URL https://ucmerced.maps.arcgis.com/apps/dashboards/c778145ea5bb4daeb58d31afee389082 (accessed 6.6.22).

Crank, K., Li, X., North, D., Ferraro, G.B., Iaconelli, M., Mancini, P., La Rosa, G., Bibby, K., 2020. CrAssphage abundance and correlation with molecular viral markers in Italian wastewater. Water Res. 184, 116161. https://doi.org/10.1016/J.WATRES.2020.116161

D'Aoust, P.M., Graber, T.E., Mercier, E., Montpetit, D., Alexandrov, I., Neault, N., Baig, A.T., Mayne, J., Zhang, X., Alain, T., Servos, M.R., Srikanthan, N., MacKenzie, M., Figeys, D., Manuel, D., Jüni, P., MacKenzie, A.E., Delatolla, R., 2021a. Catching a resurgence: Increase in SARS-CoV-2 viral RNA identified in wastewater 48 h before COVID-19 clinical tests and 96 h before hospitalizations. Sci. Total Environ. 770. https://doi.org/10.1016/j.scitotenv.2021.145319

D'Aoust, P.M., Mercier, E., Montpetit, D., Jia, J.J., Alexandrov, I., Neault, N., Baig, A.T., Mayne, J., Zhang, X., Alain, T., Langlois, M.A., Servos, M.R., MacKenzie, M., Figeys, D., MacKenzie, A.E., Graber, T.E., Delatolla, R., 2021b. Quantitative analysis of SARS-CoV-2 RNA from wastewater solids in communities with low COVID-19 incidence and prevalence. Water Res. 188, 116560. https://doi.org/10.1016/j.watres.2020.116560

Daughton, C.G., 2009. Chemicals from the practice of healthcare: Challenges and unknowns posed by residues in the environment. Environ. Toxicol. Chem. 28, 2490–2494. https://doi.org/10.1897/09-138.1

Daughton, C.G., 2001. Illicit Drugs in Municipal Sewage: Proposed New Non-Intrusive Tool to Heighten Public Awareness of Societal Use of Illicit/Abused Drugs and their Potenital for Ecological Consequences, in: Pharmaceuticals and Personal Care Products in the Evironemnt: Scientific and Regulatory Issues. American Chemical Society, Washington D.C., pp. 348–364.

European Monitoring Centre for Drugs and Drug Addiction, 2002a. The State of the Drugs Problem in the European Union and Norway. Lisbon, Portugal.

European Monitoring Centre for Drugs and Drug Addiction, 2002b. Handbook for Surveys on Drug use Among the General Population. Lisbon, Protugal.

Fongaro, G., Stoco, P.H., Souza, D.S.M., Grisard, E.C., Magri, M.E., Rogovski, P., Schörner, M.A., Barazzetti, F.H., Christoff, A.P., de Oliveira, L.F.V., Bazzo, M.L., Wagner, G., Hernández, M., Rodríguez-Lázaro, D., 2021. The presence of SARS-CoV-2 RNA in human sewage in Santa Catarina, Brazil, November 2019. Sci. Total Environ. 778, 146198. https://doi.org/10.1016/J.SCITOTENV.2021.146198

Gerrity, D., Papp, K., Stoker, M., Sims, A., Frehner, W., 2021. Early-pandemic wastewater surveillance of SARS-CoV-2 in Southern Nevada: Methodology, occurrence, and incidence/prevalence considerations. Water Res. X 10, 100086. https://doi.org/10.1016/j.wroa.2020.100086

Gonzalez, R., Curtis, K., Bivins, A., Bibby, K., Weir, M.H., Yetka, K., Thompson, H., Keeling, D., Mitchell, J., Gonzalez, D., 2020. COVID-19 surveillance in Southeastern Virginia using wastewater-based epidemiology. Water Res. 186, 116296. https://doi.org/10.1016/j.watres.2020.116296

Government of Canada, 2020. Social inequalities in COVID-19 deaths in Canada [WWW Document]. URL https://health-infobase.canada.ca/covid-19/inequalities-deaths/ (accessed

9.23.22).

Government of Ontario, 2022. COVID-19 wastewater monitoring [WWW Document]. URL https://www.ontario.ca/page/covid-19-wastewater-monitoring (accessed 9.19.22).

Gracia-Lor, E., Rousis, N.I., Herna, F., Zuccato, E., Castiglioni, S., 2018. Wastewater-Based Epidemiology as a Novel Biomonitoring Tool to Evaluate Human Exposure To Pollutants. Environ. Sci. Technol. 52, 10224–10226. https://doi.org/10.1021/acs.est.8b01403

Graham, K.E., Loeb, S.K., Wolfe, M.K., Catoe, D., Sinnott-Armstrong, N., Kim, S., Yamahara, K.M., Sassoubre, L.M., Mendoza Grijalva, L.M., Roldan-Hernandez, L., Langenfeld, K., Wigginton, K.R., Boehm, A.B., 2021. SARS-CoV-2 RNA in Wastewater Settled Solids Is Associated with COVID-19 Cases in a Large Urban Sewershed. Environ. Sci. Technol. 55, 488–498. https://doi.org/10.1021/acs.est.0c06191

Halden, R.U., Terlinden, E., Kraberger, S., Scotch, M., Steele, J., Varsani, A., 2019. Tracking harmful chemicals and pathogens using the Human Health Observatory at ASU. Online J. Public Health Inform. 11. https://doi.org/10.5210/OJPHI.V11I1.9843

Haramoto, E., Malla, B., Thakali, O., Kitajima, M., 2020. First environmental surveillance for the presence of SARS-CoV-2 RNA in wastewater and river water in Japan. Sci. Total Environ. 737, 140405. https://doi.org/10.1016/J.SCITOTENV.2020.140405

He, X., Lau, E.H.Y., Wu, P., Deng, X., Wang, J., Hao, X., Lau, Y.C., Wong, J.Y., Guan, Y., Tan, X., Mo, X., Chen, Y., Liao, B., Chen, W., Hu, F., Zhang, Q., Zhong, M., Wu, Y., Zhao, L., Zhang, F., Cowling, B.J., Li, F., Leung, G.M., 2020. Temporal dynamics in viral shedding and transmissibility of COVID-19. Nat. Med. 26, 672–675. https://doi.org/10.1038/s41591-020-0869-5

Hegazy, N., Cowan, A., D'Aoust, P.M., Mercier, É., Towhid, S.T., Jia, J.-J., Wan, S., Zhang, Z., Kabir, M.P., Fang, W., Graber, T.E., MacKenzie, A.E., Guilherme, S., Delatolla, R., 2022. Understanding the dynamic relation between wastewater SARS-CoV-2 signal and clinical metrics throughout the pandemic. Sci. Total Environ. 853C, 158458. https://doi.org/10.1016/J.SCITOTENV.2022.158458

Hellmér, M., Paxéus, N., Magnius, L., Enache, L., Arnholm, B., Johansson, A., Bergström, T., Norder, H., 2014. Detection of pathogenic viruses in sewage provided early warnings of hepatitis A virus and norovirus outbreaks. Appl. Environ. Microbiol. 80, 6771–6781. https://doi.org/10.1128/AEM.01981-14

Hill, K., Zamyadi, A., Deere, D., Vanrolleghem, P.A., Crosbie, N.D., 2021. SARS-CoV-2 known and unknowns, implications for the water sector and wastewater-based epidemiology to support national responses worldwide: early review of global experiences with the COVID-19 pandemic. Water Qual. Res. J. 56, 57–67. https://doi.org/10.2166/WQRJ.2020.100

Huang, C., Wang, Y., Li, X., Ren, L., Zhao, J., Hu, Y., Zhang, L., Fan, G., Xu, J., Gu, X., Cheng, Z., Yu, T., Xia, J., Wei, Y., Wu, W., Xie, X., Yin, W., Li, H., Liu, M., Xiao, Y., Gao, H., Guo, L., Xie, J., Wang, G., Jiang, R., Gao, Z., Jin, Q., Wang, J., Cao, B., 2020. Clinical features of patients infected with 2019 novel coronavirus in Wuhan, China. Lancet 395, 497–506. https://doi.org/10.1016/S0140-6736(20)30183-5

Indigenous Services Canada, 2022. Confirmed cases of COVID-19 [WWW Document]. URL

https://www.sac-isc.gc.ca/eng/1598625105013/1598625167707 (accessed 9.23.22).

Jafferali, M.H., Khatami, K., Atasoy, M., Birgersson, M., Williams, C., Cetecioglu, Z., 2021. Benchmarking virus concentration methods for quantification of SARS-CoV-2 in raw wastewater. Sci. Total Environ. 755, 142939. https://doi.org/10.1016/J.SCITOTENV.2020.142939

Kasprzyk-Hordern, B., Dinsdale, R.M., Guwy, A.J., 2008. Multiresidue methods for the analysis of pharmaceuticals, personal care products and illicit drugs in surface water and wastewater by solid-phase extraction and ultra performance liquid chromatography–electrospray tandem mass spectrometry. Anal. Bioanal. Chem. 2008 3914 391, 1293–1308. https://doi.org/10.1007/S00216-008-1854-X

Kitajima, M., Iker, B.C., Pepper, I.L., Gerba, C.P., 2014. Relative abundance and treatment reduction of viruses during wastewater treatment processes — Identification of potential viral indicators. Sci. Total Environ. 488–489, 290–296. https://doi.org/10.1016/J.SCITOTENV.2014.04.087

Kitajima, M., Sassi, H.P., Torrey, J.R., 2018. Pepper mild mottle virus as a water quality indicator. npj Clean WaterClean Water 1. https://doi.org/10.1038/s41545-018-0019-5

Kitamura, K., Sadamasu, K., Muramatsu, M., Yoshida, H., 2021. Efficient detection of SARS-CoV-2 RNA in the solid fraction of wastewater. Sci. Total Environ. 763, 144587. https://doi.org/10.1016/j.scitotenv.2020.144587

Kocamemi, B.A., Kurt, H., Sait, A., Sarac, F., Saatci, A.M., Pakdemirli, B., 2020. SARS-CoV-2 Detection in Istanbul Wastewater Treatment Plant Sludges. medRxiv 2020.05.12.20099358. https://doi.org/10.1101/2020.05.12.20099358

Kumar, M., Patel, A.K., Shah, A. V., Raval, J., Rajpara, N., Joshi, M., Joshi, C.G., 2020. First proof of the capability of wastewater surveillance for COVID-19 in India through detection of genetic material of SARS-CoV-2. Sci. Total Environ. 746, 141326. https://doi.org/10.1016/J.SCITOTENV.2020.141326

La Rosa, G., Iaconelli, M., Mancini, P., Bonanno Ferraro, G., Veneri, C., Bonadonna, L., Lucentini, L., Suffredini, E., 2020. First detection of SARS-CoV-2 in untreated wastewaters in Italy. Sci. Total Environ. 736, 139652. https://doi.org/10.1016/J.SCITOTENV.2020.139652

La Rosa, G., Mancini, P., Bonanno Ferraro, G., Veneri, C., Iaconelli, M., Bonadonna, L., Lucentini, L., Suffredini, E., 2021. SARS-CoV-2 has been circulating in northern Italy since December 2019: Evidence from environmental monitoring. Sci. Total Environ. 750, 141711. https://doi.org/10.1016/j.scitotenv.2020.141711

Lai, F.Y., Gartner, C., Hall, W., Carter, S., O'Brien, J., Tscharke, B.J., Been, F., Gerber, C., White, J., Thai, P., Bruno, R., Prichard, J., Kirkbride, K.P., Mueller, J.F., 2018. Measuring spatial and temporal trends of nicotine and alcohol consumption in Australia using wastewater-based epidemiology. Addiction 113, 1127–1136. https://doi.org/10.1111/ADD.14157

Lai, F.Y., O'Brien, J.W., Thai, P.K., Hall, W., Chan, G., Bruno, R., Ort, C., Prichard, J., Carter, S., Anuj, S., Kirkbride, K.P., Gartner, C., Humphries, M., Mueller, J.F., 2016. Cocaine,

MDMA and methamphetamine residues in wastewater: Consumption trends (2009–2015) in South East Queensland, Australia. Sci. Total Environ. 568, 803–809. https://doi.org/10.1016/J.SCITOTENV.2016.05.181

Long, Q.-X., Tang, X.-J., Shi, Q.-L., Li, Q., Deng, H.-J., Yuan, J., Hu, J.-L., Xu, W., Zhang, Y., Lv, F.-J., Su, K., Zhang, F., Gong, J., Wu, B., Liu, X.-M., Li, J.-J., Qiu, J.-F., Chen, J., Huang, A.-L., 2020. Clinical and immunological assessment of asymptomatic SARS-CoV-2 infections. Nat. Med. 26, 1200–1204. https://doi.org/10.1038/s41591-020-0965-6

Lu, R., Zhao, X., Li, J., Niu, P., Yang, B., Wu, H., Wang, W., Song, H., Huang, B., Zhu, N., Bi, Y., Ma, X., Zhan, F., Wang, L., Hu, T., Zhou, H., Hu, Z., Zhou, W., Zhao, L., Chen, J., Meng, Y., Wang, J., Lin, Y., Yuan, J., Xie, Z., Ma, J., Liu, W.J., Wang, D., Xu, W., Holmes, E.C., Gao, G.F., Wu, G., Chen, W., Shi, W., Tan, W., 2020. Genomic characterisation and epidemiology of 2019 novel coronavirus: implications for virus origins and receptor binding. Lancet 395, 565–574. https://doi.org/10.1016/S0140-6736(20)30251-8

Medema, G., Heijnen, L., Elsinga, G., Italiaander, R., Brouwer, A., 2020. Presence of SARS-Coronavirus-2 RNA in Sewage and Correlation with Reported COVID-19 Prevalence in the Early Stage of the Epidemic in the Netherlands. Environ. Sci. Technol. Lett. 7, 511–516. https://doi.org/10.1021/acs.estlett.0c00357

Medina, C.Y., Kadonsky, K.F., Roman, F.A., Tariqi, A.Q., Sinclair, R.G., D'Aoust, P.M., Delatolla, R., Bischel, H.N., Naughton, C.C., 2022. The need of an environmental justice approach for wastewater based epidemiology for rural and disadvantaged communities: A review in California. Curr. Opin. Environ. Sci. Heal. 27. https://doi.org/10.1016/J.COESH.2022.100348

Miura, T., Lhomme, S., Le Saux, J.-C., Le Mehaute, P., Guillois, Y., Couturier, E., Izopet, J., Abranavel, F., Le Guyader, F.S., 2016. Detection of Hepatitis E Virus in Sewage After an Outbreak on a French Island. Food Environ. Virol. 8, 194–199. https://doi.org/10.1007/S12560-016-9241-9

Neault, N., Baig, A.T., Graber, T.E., D'Aoust, P.M., Mercier, E., Alexandrov, I., Crosby, D., Baird, S., Mayne, J., Pounds, T., MacKenzie, M., Figeys, D., MacKenzie, A., Delatolla, R., 2020. SARS-CoV-2 Protein in Wastewater Mirrors COVID-19 Prevalence. medRxiv 2020.09.01.20185280. https://doi.org/10.1101/2020.09.01.20185280

Nemudryi, A., Nemudraia, A., Wiegand, T., Surya, K., Buyukyoruk, M., Cicha, C., Vanderwood, K.K., Wilkinson, R., Wiedenheft, B., 2020a. Temporal Detection and Phylogenetic Assessment of SARS-CoV-2 in Municipal Wastewater. Cell Reports Med. 1, 100098. https://doi.org/10.1016/J.XCRM.2020.100098

Nemudryi, A., Nemudraia, A., Wiegand, T., Vanderwood, K.K., Wilkinson, R., Correspondence, B.W., Surya, K., Buyukyoruk, M., Cicha, C., Wiedenheft, B., 2020b. Temporal Detection and Phylogenetic Assessment of SARS-CoV-2 in Municipal Wastewater. Cell Reports Med. 1. https://doi.org/10.1016/j.xcrm.2020.100098

O'Brien, J.W., Grant, S., Banks, A.P.W., Bruno, R., Carter, S., Choi, P.M., Covaci, A., Crosbie, N.D., Gartner, C., Hall, W., Jiang, G., Kaserzon, S., Kirkbride, K.P., Lai, F.Y., Mackie, R., Marshall, J., Ort, C., Paxman, C., Prichard, J., Thai, P., Thomas, K. V., Tscharke, B.,

Mueller, J.F., 2019. A National Wastewater Monitoring Program for a better understanding of public health: A case study using the Australian Census. Environ. Int. 122, 400–411. https://doi.org/10.1016/J.ENVINT.2018.12.003

Ontario Agency for Health Protection and Promotion (Public Health Ontario), 2022. COVID-19 wastewater surveillance in Ontario [WWW Document]. King's Print. Ontario. https://doi.org/10.47326/OCSAT.DASHBOARD.2021.1.0

Pan, X., Chen, D., Xia, Y., Wu, X., Li, T., Ou, X., Zhou, L., Liu, J., 2020. Asymptomatic cases in a family cluster with SARS-CoV-2 infection. Lancet Infect. Dis. 20, 410–411. https://doi.org/10.1016/S1473-3099(20)30114-6

Park, S. kyung, Lee, C.W., Park, D. Il, Woo, H.Y., Cheong, H.S., Shin, H.C., Ahn, K., Kwon, M.J., Joo, E.J., 2021. Detection of SARS-CoV-2 in Fecal Samples From Patients With Asymptomatic and Mild COVID-19 in Korea. Clin. Gastroenterol. Hepatol. 19, 1387-1394.e2. https://doi.org/10.1016/J.CGH.2020.06.005

Peccia, J., Zulli, A., Brackney, D.E., Grubaugh, N.D., Kaplan, E.H., Casanovas-Massana, A., Ko, A.I., Malik, A.A., Wang, D., Wang, M., Warren, J.L., Weinberger, D.M., Arnold, W., Omer, S.B., 2020. Measurement of SARS-CoV-2 RNA in wastewater tracks community infection dynamics. Nat. Biotechnol. 38, 1164–1167. https://doi.org/10.1038/s41587-020-0684-z

Philo, S.E., Keim, E.K., Swanstrom, R., Ong, A.Q.W., Burnor, E.A., Kossik, A.L., Harrison, J.C., Demeke, B.A., Zhou, N.A., Beck, N.K., Shirai, J.H., Meschke, J.S., 2021. A comparison of SARS-CoV-2 wastewater concentration methods for environmental surveillance. Sci. Total Environ. 760, 144215. https://doi.org/10.1016/J.SCITOTENV.2020.144215

Polo, D., Quintela-Baluja, M., Corbishley, A., Jones, D.L., Singer, A.C., Graham, D.W., Romalde, J.L., 2020. Making waves: Wastewater-based epidemiology for COVID-19 – approaches and challenges for surveillance and prediction. Water Res. 186, 116404. https://doi.org/10.1016/J.WATRES.2020.116404

Public Health Ontario, 2020. COVID-19 in Ontario: A Focus on Neighbourhood Material Deprivation, February 26, 2020 to December 13, 2021.

Qu, G., Li, X., Hu, L., Jiang, G., 2020. An Imperative Need for Research on the Role of Environmental Factors in Transmission of Novel Coronavirus (COVID-19). Environ. Sci. Technol. 54, 3730–3732. https://doi.org/10.1021/ACS.EST.0C01102/ASSET/IMAGES/ACS.EST.0C01102.SOCIAL.JPEG_V03

Randazzo, W., Cuevas-Ferrando, E., Sanjuán, R., Domingo-Calap, P., Sánchez, G., 2020a. Metropolitan wastewater analysis for COVID-19 epidemiological surveillance. Int. J. Hyg. Environ. Heal. 230. https://doi.org/10.1101/2020.04.23.20076679

Randazzo, W., Truchado, P., Cuevas-Ferrando, E., Simón, P., Allende, A., Sánchez, G., 2020b. SARS-CoV-2 RNA in wastewater anticipated COVID-19 occurrence in a low prevalence area. Water Res. 181. https://doi.org/10.1016/j.watres.2020.115942

Rico, M., Andrés-Costa, J., Picó, Y., 2017. Estimating population size in wastewater-based

epidemiology. Valencia metropolitan area as a case study. J. Hazard. Mater. 323, 156–165. https://doi.org/10.1016/j.jhazmat.2016.05.079

Rimoldi, S.G., Stefani, F., Gigantiello, A., Polesello, S., Comandatore, F., Mileto, D., Maresca, M., Longobardi, C., Mancon, A., Romeri, F., Pagani, C., Cappelli, F., Roscioli, C., Moja, L., Gismondo, M.R., Salerno, F., 2020. Presence and infectivity of SARS-CoV-2 virus in wastewaters and rivers. Sci. Total Environ. 744, 140911. https://doi.org/10.1016/J.SCITOTENV.2020.140911

Rosario, K., Symonds, E.M., Sinigalliano, C., Stewart, J., Breitbart, M., Petersburg, S., 2009. Pepper Mild Mottle Virus as an Indicator of Fecal Pollution. Appl. Environ. Microbiol. 75, 7261–7267. https://doi.org/10.1128/AEM.00410-09

Santos, V.S., Gurgel, R.Q., Cuevas, L.E., Martins-Filho, P.R., 2020. Prolonged fecal shedding of SARS-CoV-2 in pediatric patients. A quantitative evidence synthesis. J. Pediatr. Gastroenterol. Nutr. 71, 150–152. https://doi.org/10.1097/MPG.0000000000002798

Sattar, S.A., Westwood, J.C.N., 1977. Isolation of apparently wild strains of poliovirus type 1 from sewage in the Ottawa area. Can. Med. Assoc. J. 116, 25.

Sherchan, S.P., Shahin, S., Ward, L.M., Tandukar, S., Aw, T.G., Schmitz, B., Ahmed, W., Kitajima, M., 2020. First detection of SARS-CoV-2 RNA in wastewater in North America: A study in Louisiana, USA. Sci. Total Environ. 743, 140621. https://doi.org/10.1016/J.SCITOTENV.2020.140621

Sims, N., Kasprzyk-Hordern, B., 2020. Future perspectives of wastewater-based epidemiology: Monitoring infectious disease spread and resistance to the community level. Environ. Int. 139, 105689. https://doi.org/10.1016/J.ENVINT.2020.105689

Statistics Canada, 2020. COVID-19 mortality rates in Canada's ethno-cultural neighbourhoods [WWW Document]. URL https://www150.statcan.gc.ca/n1/pub/45-28-0001/2020001/article/00079-eng.htm (accessed 9.23.22).

Thomas, K. V., Amador, A., Baz-Lomba, J.A., Reid, M., 2017. Use of Mobile Device Data To Better Estimate Dynamic Population Size for Wastewater-Based Epidemiology. Environ. Sci. Technol. 51, 11363–11370. https://doi.org/10.1021/ACS.EST.7B02538/ASSET/IMAGES/LARGE/ES-2017-02538Y_0009.JPEG

Trottier, J., Darques, R., Ait Mouheb, N., Partiot, E., Bakhache, W., Deffieu, M.S., Gaudin, R., 2020. Post-lockdown detection of SARS-CoV-2 RNA in the wastewater of Montpellier, France. One Heal. 10, 100157. https://doi.org/10.1016/J.ONEHLT.2020.100157

Tscharke, Benjamin J., Chen, C., Gerber, J.P., White, J.M., 2016. Temporal trends in drug use in Adelaide, South Australia by wastewater analysis. Sci. Total Environ. 565, 384–391. https://doi.org/10.1016/J.SCITOTENV.2016.04.183

Tscharke, Ben J., White, J.M., Gerber, J.P., 2016. Estimates of tobacco use by wastewater analysis of anabasine and anatabine. Drug Test. Anal. 8, 702–707. https://doi.org/10.1002/DTA.1842

WHO, 2022a. Tracking SARS-CoV-2 variants [WWW Document]. URL

https://www.who.int/en/activities/tracking-SARS-CoV-2-variants/ (accessed 7.25.22).

WHO, 2022b. WHO Coronavirus (COVID-19) Dashboard With Vaccination Data [WWW Document]. URL https://covid19.who.int/

WHO, 2020. Novel coronavirus (2019-nCoV) situation report - 1 [WWW Document]. URL https://www.who.int/docs/default-source/coronaviruse/situation-reports/20200121-sitrep-1-2019-ncov.pdf (accessed 5.28.21).

WHO, 2003. WHO Guidelines for environmental surveillance of poliovirus circulation. Dep. Vaccines Biol.

Wigginton, K.R., Boehm, A.B., 2020. Environmental Engineers and Scientists Have Important Roles to Play in Stemming Outbreaks and Pandemics Caused by Enveloped Viruses. Environ. Sci. Technol. 54, 3736–3739. https://doi.org/10.1021/ACS.EST.0C01476

Wu, F., Xiao, A., Zhang, J., Moniz, K., Endo, N., Armas, F., Bushman, M., Chai, P.R., Duvallet, C., Erickson, T.B., Foppe, K., Ghaeli, N., Gu, X., Hanage, W.P., Huang, K.H., Lee, W.L., Matus, M., McElroy, K.A., Rhode, S.F., Wuertz, S., Thompson, J., Alm, E.J., 2021. Wastewater Surveillance of SARS-CoV-2 across 40 U.S. states. medRxiv 1–13. https://doi.org/10.1101/2021.03.10.21253235

Wu, F., Zhang, J., Xiao, A., Gu, X., Lee, W.L., Armas, F., Kauffman, K., Hanage, W., Matus, M., Ghaeli, N., Endo, N., Duvallet, C., Poyet, M., Moniz, K., Washburne, A.D., Erickson, T.B., Chai, P.R., Thompson, J., Alm, E.J., 2020a. SARS-CoV-2 Titers in Wastewater Are Higher than Expected from Clinically Confirmed Cases. Am. Soc. Microbiol. 5. https://doi.org/10.1128/msystems.00614-20

Wu, F., Zhang, J., Xiao, A., Gu, X., Lin Lee, W., Armas, F., Kauffman, K., Hanage, W., Matus, M., Ghaeli, N., Endo, N., Duvallet, C., Poyet, M., Moniz, K., Washburne, A.D., Erickson, T.B., Chai, P.R., Thompson, J., Alm, E.J., Xiao contributed equally, A., Wu, C.F., 2020b. SARS-CoV-2 Titers in Wastewater Are Higher than Expected from Clinically Confirmed Cases. https://doi.org/10.1128/mSystems.00614-20

Wurtzer, S., Marechal, V., Mouchel, J., Maday, Y., Teyssou, R., Richard, E., Almayrac, J., Moulin, L., 2020. Evaluation of lockdown impact on SARS-CoV-2 dynamics through viral genome quantification in Paris wastewaters. medRxiv 2020.04.12.20062679. https://doi.org/10.1101/2020.04.12.20062679

Xing, Y.H., Ni, W., Wu, Q., Li, W.J., Li, G.J., Wang, W. Di, Tong, J.N., Song, X.F., Wing-Kin Wong, G., Xing, Q.S., 2020. Prolonged viral shedding in feces of pediatric patients with coronavirus disease 2019. J. Microbiol. Immunol. Infect. https://doi.org/10.1016/j.jmii.2020.03.021

Xu, Y., Li, X., Zhu, B., Liang, H., Fang, C., Gong, Y., Guo, Q., Sun, X., Zhao, D., Shen, J., Zhang, H., Liu, H., Xia, H., Tang, J., Zhang, K., Gong, S., 2020. Characteristics of pediatric SARS-CoV-2 infection and potential evidence for persistent fecal viral shedding. Nat. Med. 26, 502–505. https://doi.org/10.1038/s41591-020-0817-4

Yeo, C., Kaushal, S., Yeo, D., 2020. Enteric involvement of coronaviruses: is faecal–oral transmission of SARS-CoV-2 possible? Lancet Gastroenterol. Hepatol. https://doi.org/10.1016/S2468-1253(20)30048-0

Zhang, Y., Cen, M., Hu, M., Du, L., Hu, W., Kim, J.J., Dai, N., 2021. Prevalence and Persistent Shedding of Fecal SARS-CoV-2 RNA in Patients With COVID-19 Infection: A Systematic Review and Meta-analysis. Clin. Transl. Gastroenterol. 12, e00343. https://doi.org/10.14309/CTG.0000000000000343

Zuccato, E., Chiabrando, C., Castiglioni, S., Bagnati, R., Fanelli, R., 2008. Estimating community drug abuse by wastewater analysis. Environ. Health Perspect. 116, 1027–1032. https://doi.org/10.1289/EHP.11022

Zuccato, E., Chiabrando, C., Castiglioni, S., Calamari, D., Bagnati, R., Schiarea, S., Fanelli, R., 2005. Environmental Health: A Global Access Science Source Cocaine in surface waters: a new evidence-based tool to monitor community drug abuse. Environ. Heal. 4. https://doi.org/10.1186/1476-069X-4-14

Zulli, A., Pan, A., Bart, S.M., Crawford, F.W., Kaplan, E.H., Cartter, M., Ko, A.I., Sanchez, M., Brown, C., Cozens, D., Brackney, D.E., Peccia, J., 2022. Predicting daily COVID-19 case rates from SARS-CoV-2 RNA concentrations across a diversity of wastewater catchments. FEMS Microbes 2, 22. https://doi.org/10.1093/FEMSMC/XTAB022

This chapter is a manuscript prepared for refereed journal publication

Chapter 2.

Impact of Coagulation on SARS-CoV-2 & PMMoV Viral Signal in Wastewater Solids

Nada Hegazy[1], Xin Tian[1], Patrick M. D'Aoust[1], Syeda Tasneem Towhid[1], Élisabeth Mercier[1], Zhihao Zhang[1], Alex E. MacKenzie[2], Tyson E. Graber[2], Stéphanie Guilherme[1], and Robert Delatolla[1]*

1: Department of Civil Engineering, University of Ottawa
161 Louis Pasteur Street, Ottawa, ON, K1N 6N5, Canada

2: Children's Hospital of Eastern Ontario Research Institute
401 Smyth Rd., Ottawa, ON, K1H 5B2, Canada

*Corresponding author: Tel: (613) 562-5800 Ext.2677; E-mail: Robert.Delatolla@uOttawa.ca

Abstract

Wastewater surveillance (WWS) is receiving interest from researchers, scientists, and public health units for its application in monitoring active COVID-19 cases and its capability to provide early warning of community outbreaks. Detection of SARS-CoV-2 RNA in primary municipal sludge and normalization of the viral signal with pepper mild mottle virus (PMMoV) has been shown to be a sensitive means of COVID-19 disease surveillance in communities. While WWS of SARS-CoV-2 has been widely applied worldwide, a knowledge gap exists concerning the effects of enhanced primary clarification with the coagulation process on SARS-CoV-2 and PMMoV quantification. Ferric-based chemical coagulants are extensively used in enhanced clarification, particularly for phosphorus removal, in North America. This study examines the effects of coagulation with ferric sulfate on the measurement of SARS-CoV-2 and PMMoV viral signals in solids. Wastewater with Fe^{3+} concentrations ranging from 0 to 60 mg/L caused no change in N1 and N2 gene region measurements in wastewater solids. Fe^{3+} concentrations above 0 mg/L

however were shown to be associated with a statistically significant increase in PMMoV viral signals, which consequently resulted in the underestimation of PMMoV normalized SARS-CoV-2 viral signals (N1 and N2 copies/copies of PMMoV). pH reduction associated with adding coagulant was not associated with this increase in PMMoV measurements. Thus, the increase in PMMoV measurements is indicative that coagulation causes PMMoV to partition to the solids of wastewaters from an existing portion of the PMMoV virus in the bulk liquid phase of wastewaters.

***Keywords**:* post-grit wastewater; wastewater surveillance; coagulation; normalization, partitioning

2.1 Introduction

Wastewater surveillance (WWS) efforts for monitoring active COVID-19 positive cases are ongoing worldwide and are playing a major role in the early detection of community outbreaks (Ahmed et al., 2020a; Arora et al., 2020; Bivins et al., 2020; D'Aoust et al., 2021a; Gonzalez et al., 2020; La Rosa et al., 2021; Mao et al., 2020; Medema et al., 2020; Polo et al., 2020; Randazzo et al., 2020a, 2020b; Sims and Kasprzyk-Hordern, 2020; Thompson et al., 2020; Wu et al., 2020). Solids-based viral extraction protocols for measuring SARS-CoV-2 in wastewater have shown to perform well with samples rich in solids such as primary sludge, raw wastewater influent, and sewage (Balboa et al., 2020; D'Aoust et al., 2021b; Graham et al., 2021; Peccia et al., 2020; Petala et al., 2021; Westhaus et al., 2021; Wu et al., 2020). Previous studies suggest higher sensitivity of SARS-CoV-2 RNA detection from testing primary sludge compared to testing influent (D'Aoust et al., 2021b; Graham et al., 2021).

The design and operation of primary sludge treatment processes may impact the sensitivity of SARS-CoV-2 measurements in wastewater. One such design and operational consideration is the addition of chemical coagulants in enhanced primary clarification treatment. Enhanced primary sludge treatment is the process of adding coagulants to primary clarifier units (Metcalf and Eddy, 2014; Shewa and Dagnew, 2020), to enhance the removal of suspended solids and phosphorus from wastewater (Cornel and Schaum, 2009; Metcalf and Eddy, 2014; Shewa and Dagnew, 2020). In Canada, 18.1% of the total population received wastewater with primary treatment which includes chemical precipitation/flocculation (ECCC, 2011). Chemical elimination of phosphorus and suspended solids during primary clarification is commonly achieved with trivalent metal

coagulants, mainly ferric-based salts (e.g. sulfate or chloride) or dissolved aluminum (alum i.e., aluminum sulfate) (Crittenden et al., 2012; Metcalf and Eddy, 2014). Ferric salts in particular are extensively used for removing phosphorus during primary clarification across North America (Crittenden et al., 2012; Davis, 2010; ECCC, 2010; Mckinnon et al., 2018; Toronto Water, 2009; U.S. EPA, 2000; Yeoman et al., 1988) and the UK (Carliell-Marquet et al., 2010). Optimal ferric sulfate dosage (usually expressed as the concentration of Fe^{3+}) in primary treatment range between 5 and 250 mg/L as Fe^{3+} depending on raw water quality and treatment objectives (Crittenden et al., 2012; Pal, 2017); in conventional enhanced primary clarification systems, the optimal ferric sulfate dosage range between 5 and 60 mg/L as Fe^{3+} (Dong et al., 2019; Pal, 2017). Ferric and aluminum ions may also be added to wastewater conveyance systems and ultimately to water resource recovery facilities (WRRFs) from the discharge of drinking water treatment plant effluent in sewersheds (where drinking water plants may use these same or similar coagulants in their water production processes).

Earlier wastewater-based epidemiology studies relied on the "aluminum hydroxide adsorption-precipitation" method to examine for SARS-CoV-2 RNA measurements in wastewater with low solids (post-grit wastewater) (Bar-Or et al., 2020; Barril et al., 2021; Randazzo et al., 2020b, 2020a). This method has been historically used to concentrate poliovirus in post-grit wastewater and it involves the addition of aluminum-based coagulant, followed by agitation and sedimentation of aluminum-bound solids that are then collected and analyzed by PCR (Cuevas-Ferrando et al., 2020). However, evidence suggests that wastewater samples contaminated with ferric and aluminum ions were found to interfere with qPCR amplification for the detection of viruses (Combs et al., 2015; Dalecka and Mezule, 2018; Kuffel et al., 2021), and could cause false-negative results (Graham et al., 2021; Kitajima et al., 2018; Rock et al., 2010; Schrader et al., 2012). Ferric-based precipitation has also been used in previous studies to effectively concentrates viruses from wastewater and sewage (Farrah and Preston, 1985; John et al., 2011; Payment et al., 1984; Randazzo et al., 2019; Sobsey et al., 1997). However, these practices have not been used to concentrate SARS-CoV-2 and pepper mild mottle virus (PMMoV) RNA in wastewaters. PMMoV-normalization of SARS-CoV-2 is believed to be important in representing the true community prevalence of COVID-19 clinical positive cases as PMMoV can effectively reflect wastewater variability and fecal mass flux (D'Aoust et al., 2021b; Graham et al., 2021; Kitamura et al., 2021; Wolfe et al., 2021a; Wu et al., 2021). Therefore, the effects of enhanced primary clarification with

ferric-based coagulants remain unknown for detecting and quantifying SARS-CoV-2, as well as normalization against human-associated indicator viruses such as PMMoV (Feng et al., 2021; Simpson et al., 2021; Whitney et al., 2021; Wolfe et al., 2021a, 2021b; Wu et al., 2020).

An additional factor that may indirectly influence SARS-CoV-2 and PMMoV RNA detection sensitivity is the drop in pH that occurs when a coagulant is added (Crittenden et al., 2012). Viral particles increase their propensity for binding to wastewater colloids at lower pH due to associated changes in ionic strength and surface charges at various lower pH values (Walshe et al., 2010). Independently of the reduction in pH, the neutralization of negatively charged wastewater colloids that initiates coagulation (Crittenden et al., 2012) can also affect how SARS-CoV-2 and PMMoV bind to the solid phase. Moreover, differences in surface morphology, such as the presence of an enveloped virus, along with the properties of SARS-CoV-2 and PMMoV virions could influence virus adsorption as well as partitioning between the liquid and solid phases of wastewater (Lee et al., 2016; Xagoraraki et al., 2014). Enveloped viruses, such as SARS-CoV-2, preferentially adsorb to wastewater solids compared to non-enveloped viruses (Kampf et al., 2020; Kumar et al., 2021; Ye et al., 2016). Meanwhile, the lack of an envelope, such as with PMMoV virion particles, may also influence the virus' partitioning to solids or the liquid phase of wastewaters. It has been observed that non-enveloped viruses are more likely to partition to the liquid phase compared to enveloped viruses (Kitamura et al., 2021; Ye et al., 2016). Although both SARS-CoV-2 RNA (D'Aoust et al., 2021b; Graham et al., 2021; Kitamura et al., 2021; Peccia et al., 2020; Rosario et al., 2009) and PMMoV viral RNA (D'Aoust et al., 2021b; Jafferali et al., 2021; Kitajima et al., 2018; Rosario et al., 2009; Wu et al., 2020) were consistently detected at high concentrations in the solids fraction of wastewater, the effects of the partitioning of SARS-CoV-2 and PMMoV viruses from the solid phase to the liquid phase caused by the addition of trivalent metal coagulants and associated pH changes have not been previously explored. Hence, a knowledge gap regarding the effects of coagulation in primary sludge clarifiers on SARS-CoV-2 and PMMoV wastewater measurements exists and is necessary to apply wastewater surveillance as a means of community prevalence of COVID-19 or incidence in communities.

The implications of coagulation in primary clarifiers on the measurement of SARS-CoV-2 and PMMoV viral tracking in wastewaters remains unknown and needs to be elucidated to improve the ability of COVID-19 WWS for prevalence or incidence of community COVID-19 disease.

Further, the impact of addition and increasing ferric sulfate dosage (Fe^{3+}), a common primary sludge coagulant, on SARS-CoV-2 RNA and PMMoV RNA will improve our understanding of the partitioning of these biological targets in primary sludge wastewaters. The specific objectives of this study are therefore to quantify the effects of Fe^{3+} and the corresponding pH changes on N1 and N2 SARS-CoV-2 gene region measurements as well as PMMoV measurements in primary sludge wastewaters and to use the results of Fe^{3+} addition on SARS-CoV-2 RNA and PMMoV RNA measurements in primary sludge to advance the current understanding of the partitioning of these targets in primary sludge wastewaters.

2.2 Materials and Methods

2.2.1 Wastewater source and collection

A total of 22.5 L of post-grit unit wastewater was collected on Feb. 22nd, Mar. 23rd, and May 2nd, 2021, from the City of Ottawa's (Ontario, Canada) WRRF, Robert O. Pickard Environmental Centre (ROPEC). Grab samples were collected from the outflow of the grit removal unit (post-grit wastewater) using an ISCO 6700 series sampler (Teledyne ISCO Lincoln, NE, USA). The Ottawa WRRF treats wastewater collected from approximately 936,382 people and has an average wastewater flow rate of 545 million litres per day. Post-grit samples were collected in this study for various coagulant concentrations to be added to the harvested post-grit wastewaters to produce primary sludge samples of various coagulant concentrations. Samples were immediately transported to the laboratory for storage following collection. During transportation, the samples were kept cold on ice, and they were then stored at 4°C in a refrigerator for up to 24 hours before processing.

The physico-chemical characteristics of the influent samples were measured by the city of Ottawa WRRF as per standard methods common to wastewaters (APHA American Public Health Association, 2017). These properties include volatile suspended solids (VSS), total suspended solids (TSS), carbonaceous biological oxygen demand (cBOD), chemical oxygen demand (COD), total Kjeldahl nitrogen (TKN), and conductivity.

2.2.2 Jar test: effect of ferric sulfate dosing on SARS-CoV-2 and PMMoV viral signals

To simulate primary clarification and coagulation processes at a lab-scale, jar testing of wastewater is often performed (American Water Works Association, 2011). Post-grit wastewater from the samples harvested from the Ottawa WRRF on Feb. 22nd, Mar. 23rd, and May 2nd were dosed with ferric sulfate ($Fe_2(SO_4)_3$) and mixed within jar test apparatus at five concentrations to produce sedimented solids akin to primary sludge to be analyzed for SARS-CoV-2 and PMMoV viral signals. Each jar test consisted of a batch experiment involving rapid mixing, slow mixing, and sedimentation in standard jar test apparatus (Orbeco-Hellige six-paddle stirrer, FL, USA) to simulate a conventional primary clarification and coagulation process (Figure 2.1). The post-grit samples were first well homogenized (well-mixed samples to resuspend solids within the wastewater matrix) and then 500 mL of the samples were aliquoted into disinfected jar test B-KER^2 laboratory 1000 mL beakers (Phipps & Bird PN 7790630, VA, USA). The beakers and the paddle stirrers were disinfected with 5% bleach solution (5 min contact time) and 70% ethanol (5 min contact) and then rinsed with tap water prior to use. Ferric sulfate coagulant solution was prepared from acidified ferric sulfate stock coagulant (12% concentration as Fe^{3+}).

Sedimented solids from the post-grit samples collected on Feb. 22nd, Mar. 23rd, and May 2nd, 2021, were analyzed for SARS-CoV-2 and PMMoV measurements at various ferric sulfate coagulant concentrations. The coagulation process of the post-grit samples was initiated by undergoing rapid mixing at 100 rotations per minute (RPM) for one minute immediately after the beakers with the 500 mL of homogenized samples were dosed with ferric sulfate, followed by 15 min of slow mixing at 40 RPM. Immediately thereafter, the mixing pedals were removed from the beakers for a 30 min sedimentation period to allow large flocs to settle down. Finally, a 10 mL pipettor with a broad (disposable) pipette tip was used to preferentially aspirate 40 mL of the sedimented solids fraction at the bottom of the beakers into a 40 mL disinfected centrifuge tube. The post-grit sample harvested on Feb. 22nd, 2021, was dosed with the ferric sulfate solution to produce final concentrations of 0, 5, 15, 30, and 60 mg/L as Fe^{3+}. Each of these five concentrations was prepared in triplicate, resulting in 15 samples analyzed from the wastewater harvested on Feb. 22nd, 2021. Samples collected on Mar. 23rd and May 2nd, 2021, were dosed with ferric sulfate to produce final concentrations of 0 and 60 mg/L Fe^{3+}, again with each concentration being produced

in triplicate. The 6 samples produced from the wastewater harvested on Mar. 23rd and again the 6 samples from May 2nd were run as complete test replicates to the Feb. 22nd samples to ensure that the variation in wastewater samples did not alter the findings of the study.

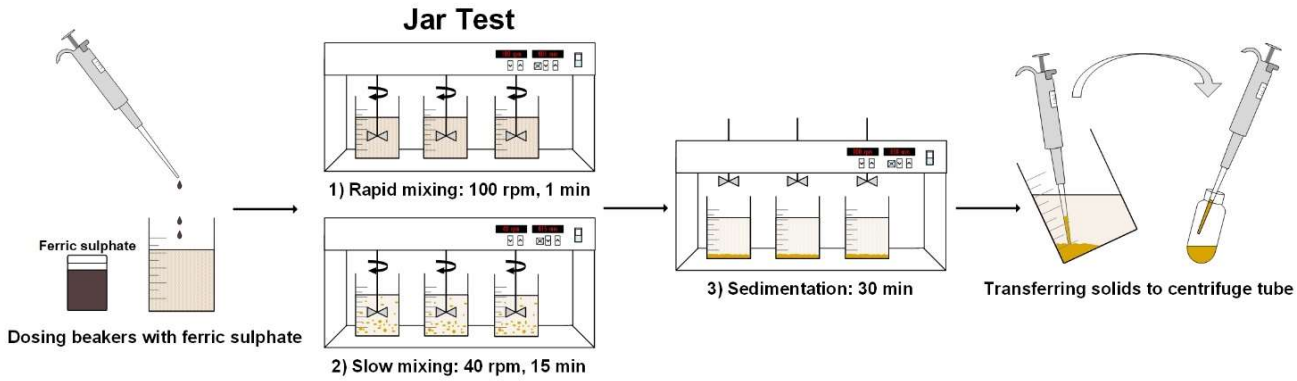

Figure 2.1: Jar test method used in this study

2.2.2.1 Jar test: effect of pH change

An identical procedure to the jar test method described above to determine the effect of ferric sulfate on wastewater viral measurements (Figure 2.1) was conducted to test the indirect effects of pH changes that are associated with adding ferric sulfate, except that the jar test beakers were slowly dosed with 34,460 mg/L hydrochloric acid (HCl) in place of ferric sulfate. These tests allowed for the effects of changes in the wastewater pH on SARS-CoV-2 and PMMoV due to ferric sulfate dosing to be isolated from the effects of the ferric ion (Fe^{3+}) itself. Immediately after the 30 min sedimentation of the post-grit wastewater collected on Feb. 22nd with 0, 5, 15, 30, and 60 mg/L as Fe^{3+}, the wastewater pH for each sample replicate was measured using an HQ430d pH meter (Hach, CO, USA). As there was a minimal change in pH between each ferric sulfate concentration, only the pH for wastewater without coagulant (average pH of 7.6 ± 0.1) and wastewater with 60 mg/L as Fe^{3+} (average pH of 6.6 ± 0.2) were investigated. Each of these two conditions was prepared in triplicate, resulting in an additional 6 samples analyzed from the wastewater sample harvested on Feb. 22nd. Three of the six beakers with 500 mL of homogenized post-grit samples were dosed slowly with 34,460 mg/L HCl until a pH of 6.6 was reached (HQ430d pH meter, CO, USA), which was equivalent to the average pH recorded during dosing to 60 mg/L as Fe^{3+}, while the remaining three post-grit sample replicates remained untreated to maintain a pH of 7.6; equivalent to the 0 mg/L as Fe^{3+} dosing. Following the 30 min sedimentation period, 40

mL of the sedimented solids were aspirated in a 40 mL centrifuge tube and were processed immediately for viral extraction and RT-qPCR quantification. The effect of pH change on SARS-CoV-2 and PMMoV measurements was only conducted for the aliquoted post-grit samples from Feb. 22nd, 2021, as results show no notable effects on the PMMoV-normalized SARS-CoV-2 measurements and were isolated from the effects of the coagulation process with ferric sulfate.

2.2.2.2 Jar test: effect of ferric sulfate dosing on virus partitioning

This study further investigates the influence of ferric sulfate dosages on the partitioning of SARS-CoV-2 and PMMoV RNA between the solid and liquid fractions of wastewater. An identical jar-testing procedure to the preceding experiments was performed with post-grit wastewater samples collected on Mar. 23rd and May 2nd, 2021; in this case, the jar tests were only dosed at 0 and 60 mg/L as Fe^{3+} with each concentration being performed in triplicate, resulting in 6 beakers for each sample collection day. The SARS-CoV-2 and PMMoV viral signals in the wastewater from both days were analyzed in both the sedimented solids fraction and the supernatant (liquid) fraction. After the 30 min sedimentation period for all samples and prior to aspiration of the sedimented solids, a 10 mL pipettor was used to collect 15 mL of the supernatant at different depths of the beaker to homogenize the supernatant samples, but without resuspension of the sedimented solids. Supernatant samples were collected before collecting the sedimented solids samples after the 30 min sedimentation period to ensure no resuspension of solid wastewater particles into the supernatant samples such that subsequent SARS-CoV-2 and PMMoV measurements are from the liquid phase of the wastewater only. From the jar test conducted for the post-grit wastewater collected on Mar. 23rd, 2021, supernatant samples were only collected from the beakers directly after the 30 min sedimentation period (settled supernatant), resulting in 6 supernatant samples that were processed in parallel with the 6 sedimented solids samples for viral extraction and RT-qPCR amplification, resulting in a total of 12 samples. As for the jar test conducted for post-grit wastewater collected on May 2nd, 2021, the resulting supernatant from the centrifugation (centrifuged supernatant) of the subsequent solids pellet was also collected in addition to the settled supernatant to investigate whether SARS-CoV-2 and PMMoV viral particles are localized within a certain fraction of the liquid phase, resulting in 12 supernatant samples that were processed in parallel with the 6 sedimented solids samples from May 2nd post-grit wastewater for a total of 18 samples (Figure 2.2). The supernatant samples were processed for viral extraction

and RT-qPCR quantification using the same protocol that was applied for the solids pellet, except that the supernatant samples did not undergo a separate centrifugation stage.

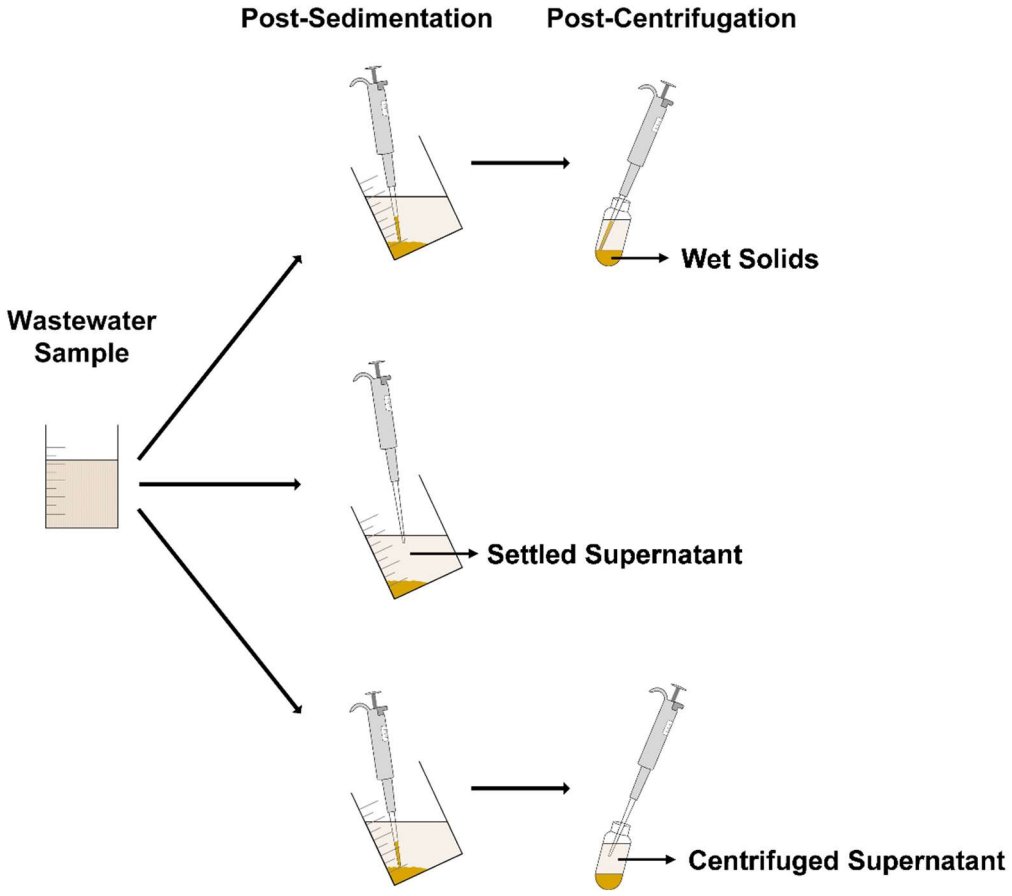

Figure 2.2: Wastewater sample fractions post-sedimentation and post-centrifugation analyzed in this study

2.2.3 Sample concentration viral extraction and RT-qPCR quantification

The sedimented solids samples were concentrated by centrifuging the samples at 10,000 × g for 45 min at 4°C. The supernatant was decanted to isolate the sedimented solids fraction and the sample was centrifuged once more at 10,000 × g for 5 min at 4°C to isolate the centrifuged solids pellet (also referred to as wet solids). Sample pellets inside the 40 mL centrifuge were massed and the total pellet weight was recorded, and then 0.250 ± 0.05 g of the sample pellets were immediately processed for viral extraction and RT-qPCR quantification. RNA was extracted using a Qiagen RNeasy PowerMicrobiome extraction kit (PN 26000-50, MD, USA) on a QIAcube

Connect automated extraction platform with a modified methodology previously described using the RNeasy PowerMicrobiome Kit (Qiagen, Germantown, MD) (D'Aoust et al., 2021b, 2021c). RT-qPCR quantification was performed for the SARS-CoV-2 N1 and N2 gene regions, as well as the replication-associated gene region of the pepper mild mottle virus (PMMoV), where measurements of PMMoV involved 1/10 dilution of samples. Each PCR reaction well consisted of 1.5 µL of RNA template and each sample was analyzed in triplicates; referred to as "biological replicates" throughout this study. The primer and probe combinations that were used in this study are shown in Table 2.3S (Supplementary Material). To check for inhibition, the samples were diluted by a factor of four and then a factor of ten and were compared with undiluted samples for corresponding drops in PMMoV signal. The assay limit of detection (ALOD, ≥ 95% detection) was determined to be approximately 2 copies/reaction (D'Aoust et al., 2021b). To avoid contamination, RNA extraction and RT-qPCR were performed in separate laboratories in Class 2 biosafety cabinets. The resulting SARS-CoV-2 N1 and N2 viral signals, as well as PMMoV viral signals in this study, are represented as N1, N2, and PMMoV genomic copies (or copies) per gram of extracted wastewater concentrated solids (0.250 ± 0.05 g) and N1, N2 and PMMoV copies per sample-volume basis (500 mL). The PMMoV-normalized SARS-CoV-2 viral signals measured in wastewater during this study are expressed as N1 and N2 copies/copies of PMMoV.

2.2.4 Quantification of total solids (TS)

For each jar-test triplicate on all the sample collection days in this study, total solids (TS) were measured before the beakers were dosed with ferric sulfate and after the 30 min sedimentation period to validate that the 500 mL post-grit wastewater sample triplicates for each ferric sulfate concentration analyzed had identical homogenization. Prior to dosing the post-grit wastewater samples with ferric sulfate, a 10 mL pipettor with a broad pipette tip was used to collect 20 mL of the homogenized post-grit wastewater sample from each beaker into a separate 75 mL aluminum weighing dish (Fisher Scientific, PA, USA) that was massed prior to use and labelled for each sample. The weighing dishes were then left in a furnace (VWR International, PA, USA) at 133°C for at least 24 hrs so that only the total solids would remain in the weighing dishes. An identical procedure was undertaken to measure the TS in the wastewater after the 30 min sedimentation period without resuspension of the sedimented solids. The weighting dishes were massed once more after removing from the furnace and the TS concentration (mg/L) for each sample replicate,

before and after coagulation, was calculated by taking the difference in masses of the empty weighing dishes and weighing dishes with TS.

2.3 Statistical Analysis

To test for statistically significant changes between SARS-CoV-2 N1 and N2 signals, as well as PMMoV signals of the differing five ferric sulfate dosed concentrations in the resulting sedimented solids fraction and the supernatant fractions, a one-way analysis of variance (ANOVA) was performed with a *p*-value of 0.05 or lower indicating statistical significance. ANOVA was also used to determine the statistical significance of SARS-CoV-2 and PMMoV RNA viral detection due to a change in pH. Throughout this study, the linear association (R^2) between the SARS-CoV-2 N1 and N2 and PMMoV viral signal measurements, and the ferric sulfate dosed concentrations, were determined cumulatively with respect to all individual resulting data.

2.4 Results and Discussion

2.4.1 Characteristics of Ottawa post-grit wastewater

The physico-chemical characteristics of the post-grit wastewater samples collected from the Ottawa WRRF exhibited low variations across the three distinct sampling dates (Table 2.1). It is noted that wastewater parameters are measured every second day at the Ottawa WRRF, and hence the parameters corresponding to the sampling dates of Mar. 23rd and May 2nd of this study were calculated by averaging the wastewater measurements performed on the day prior and following those sampling dates.

Table 2.1: Physico-chemical characteristics of post-grit samples collected at the Ottawa (Ontario, Canada) WRRF on the sampling dates during this study.

Wastewater characteristics	**Feb. 22nd**	**Mar. 22nd – 24th (avg. ± standard dev.)**	**May 1st – 3rd (avg ± standard dev.)**
VSS (mg/L)	270	219 ± 52	353 ± 152
cBOD (mg/L)	201	164 ± 7	243 ± 79
COD (mg/L)	660	488 ± 77	693 ± 302
TSS (mg/L)	323	289 ± 72	348 ± 53
TKN (mg/L)	53.7	36.6 ± 0.9	44.3 ± 4.5
Conductivity (µS/cm)	1,234	1,606 ± 143	1,392 ± 51

PMMoV-normalized SARS-CoV-2 RNA measured in post-grit wastewater collected on Feb. 22nd, Mar. 23rd, and May 2nd from the Ottawa WRRF (with no influence of coagulation) were 2.8 x 10^{-4} ± 7.5 x 10^{-5} N1-N2 avg. copies/copies PMMoV, 2.6 x10^{-4} ± 4.8 x 10^{-5} N1-N2 avg. copies/copies PMMoV, and 2.6 x 10^{-4} ± 2.0 x 10^{-5} N1-N2 avg. copies/copies PMMoV, respectively. In comparison with primary sludge collected from the Ottawa WRRF on Feb. 22nd and Mar. 23rd 2021 for subsequent WWS of COVID-19 in Ottawa, the PMMoV normalized SARS-CoV-2 RNA measurements (five-day midpoint average provided in brackets) were 3.2 x 10^{-4} N1-N2 avg. copies/copies PMMoV (2.9 x 10^{-4} avg. N1-N2 copies/copies PMMoV), 9.3 x 10^{-5} N1-N2 avg. copies/copies PMMoV (2.3 x 10^{-4} avg. N1-N2 copies/copies PMMoV), respectively (Figure 2.3). Primary sludge was not sampled on May 2nd for SARS-CoV-2 and PMMoV RNA quantification. Finally, the PMMoV-normalized SARS-CoV-2 RNA measured in primary sludge collected from the Ottawa WRRF from June 1st, 2020, through May 4rth 2021 ranged from 4.8 x 10^{-6} – 2.5 x 10^{-3} N1-N2 copies/copies PMMoV (avg. 4.2 x 10^{-4} ± 3.4 x 10^{-4} N1-N2 copies/copies PMMoV) (Figure 2.3). By comparison of the viral measurements in the post-grit influent from this study and in the primary sludge collected from the Ottawa WRRF, the viral signal measurements expressed as N1 and N2 copies/g, PMMoV copies/g, and the N1 and N2 copies/copies of PMMoV measurements in the post-grit samples were within similar magnitudes as measurements in the primary sludge for each sampling date (Table 2.2); it is noteworthy that in this study, grab samples of post-grit wastewater were used while the subsequent WWS of SARS-CoV-2 in Ottawa uses 24-hour composite samples. The N1 and N2 copies/L and PMMoV copies/L in the post-grit samples were two orders of magnitude lower compared to subsequent measurements in primary sludge; this is likely due to the volumetric flow of primary sludge leaving the primary clarifier being two magnitudes lower compared to the post grit volumetric flow entering the primary clarifier.

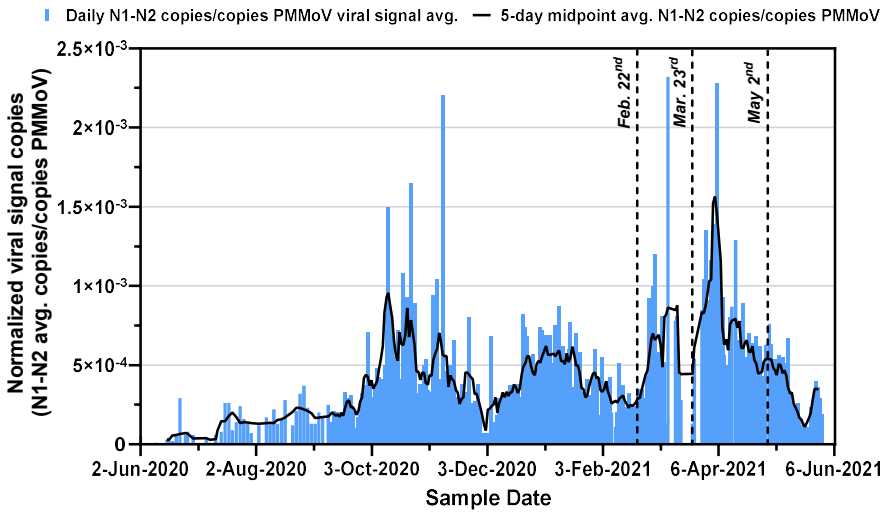

Figure 2.3: PMMoV-normalized SARS-CoV-2 viral signals measured in primary sludge collected at the Ottawa (Ontario, Canada) WRRF. The collection dates for post-grit wastewater are outlined.

Table 2.2: Viral signal measurements from post-grit samples from this study, and primary sludge from subsequent SARS-CoV-2 studies at Ottawa (Ontario, Canada) WRRF.

		Feb. 22nd, 2021		Mar. 23rd, 2021		May 2nd, 2021	
		Post-grit Wastewater	Primary Sludge	Post-grit Wastewater	Primary Sludge	Post-grit Wastewater	*Primary Sludge
Copies/g	N1	3.0×10^3	4.1×10^3	3.0×10^3	7.1×10^3	1.3×10^4	$8.1 \times 10^3 \pm 1.7 \times 10^3$
	N2	3.0×10^3	4.1×10^3	4.0×10^3	3.3×10^3	1.1×10^4	$7.9 \times 10^3 \pm 4.5 \times 10^3$
	PMMoV	1.0×10^7	1.3×10^7	1.4×10^7	5.6×10^7	4.5×10^6	$1.2 \times 10^7 \pm 4.0 \times 10^6$
Copies/L	N1	4.3×10^3	5.7×10^5	3.1×10^3	9.7×10^5	1.5×10^4	$1.3 \times 10^6 \pm 3.9 \times 10^5$
	N2	4.3×10^3	5.4×10^5	4.1×10^3	4.5×10^5	1.1×10^4	$1.3 \times 10^6 \pm 8.3 \times 10^5$
	PMMoV	1.5×10^7	1.7×10^9	1.2×10^7	7.6×10^9	4.9×10^6	$1.9 \times 10^9 \pm 8.2 \times 10^8$
Copies/copies PMMoV	N1	2.9×10^{-4}	3.3×10^{-4}	2.0×10^{-4}	1.3×10^{-4}	2.1×10^{-4}	$6.9 \times 10^{-4} \pm 9.0 \times 10^{-5}$
	N2	2.9×10^{-4}	3.2×10^{-4}	3.2×10^{-4}	6.0×10^{-5}	3.2×10^{-4}	$6.3 \times 10^{-4} \pm 1.6 \times 10^{-4}$
Daily COVID-19 positive cases		31		95		118	
Percentage Positivity		1.4%		3.3%		6.9%	

** Avg. ± standard deviation between measurements on May 1st and May 3rd as no primary sludge on May 2nd was collected and analyzed*

The daily COVID-19 positive cases (five-day midpoint average in brackets) reported by Ottawa Public Health (OPH) on Feb. 22nd, Mar. 23rd, and May 2nd, 2021, were 31 (46.0 ± 12.3), 95 (88.6 ± 22.8), and 118 (121.2 ± 21.8), respectively (Table 2.2). The daily COVID-19 positive

cases (five-day midpoint average in brackets) between June 1st, 2020, through May 4th, 2021, ranged from 0 to 682 (62.2 ± 82). The daily percentage test positivity (five-day midpoint average) reported by the Ontario Laboratories Information System (OLIS) on Feb. 22nd, Mar. 23rd, and May 2nd, 2021, were 1.4% (2.1%), 3.3% (4.0%), and 6.9% (8.2%), respectively (Table 2.2). The daily percentage test positivity (five-day midpoint average in brackets) from Jun. 1st, 2020, through May 2021 ranged from 0.0% to 16.8% (2.6% ± 2.9%).

2.4.2 Effects of ferric sulfate coagulant on SARS-CoV-2 and PMMoV viral signals in wastewater

The effects of coagulation with ferric sulfate at 0, 5, 15, 30, and 60 mg/L as Fe^{3+} on the detection of SARS-CoV-2 N1 and N2 and PMMoV viral signals in sedimented solids were investigated with the post-grit sample collected on Feb. 22nd, 2021. RT-qPCR analysis of the resulting solids pellets for each biological replicate displayed oscillations between 1460 and 6700 N1 and N2 copies/g without a notable change in trend at all five Fe^{3+} concentrations (Figure 2.4). As such, findings suggest no significant effects of ferric sulfate coagulant dosage on N1 copies/g measurements (Figure 2.4 A), and in N2 copies/g measurements, except for the N2 copies/g measurements at 5 mg/L Fe^{3+} which is a likely outlier (Figure 2.4 B). The N1 and N2 copies/L measurements exhibited a statistically significant change across the five Fe^{3+} ($p < 0.05$) which is likely attributed to the differing pellet weights obtained throughout all the five Fe^{3+} concentrations (Table 2.4S in Supplementary Material). Nonetheless, a very weak linear association remains between the increasing Fe^{3+} concentrations and the SARS-CoV-2 N1 and N2 copies/L (Figure 2.4 D and E). Hence, ferric sulfate dosages exhibited no significant effect on the SARS-CoV-2 RNA viral signal measurements in sedimented solids.

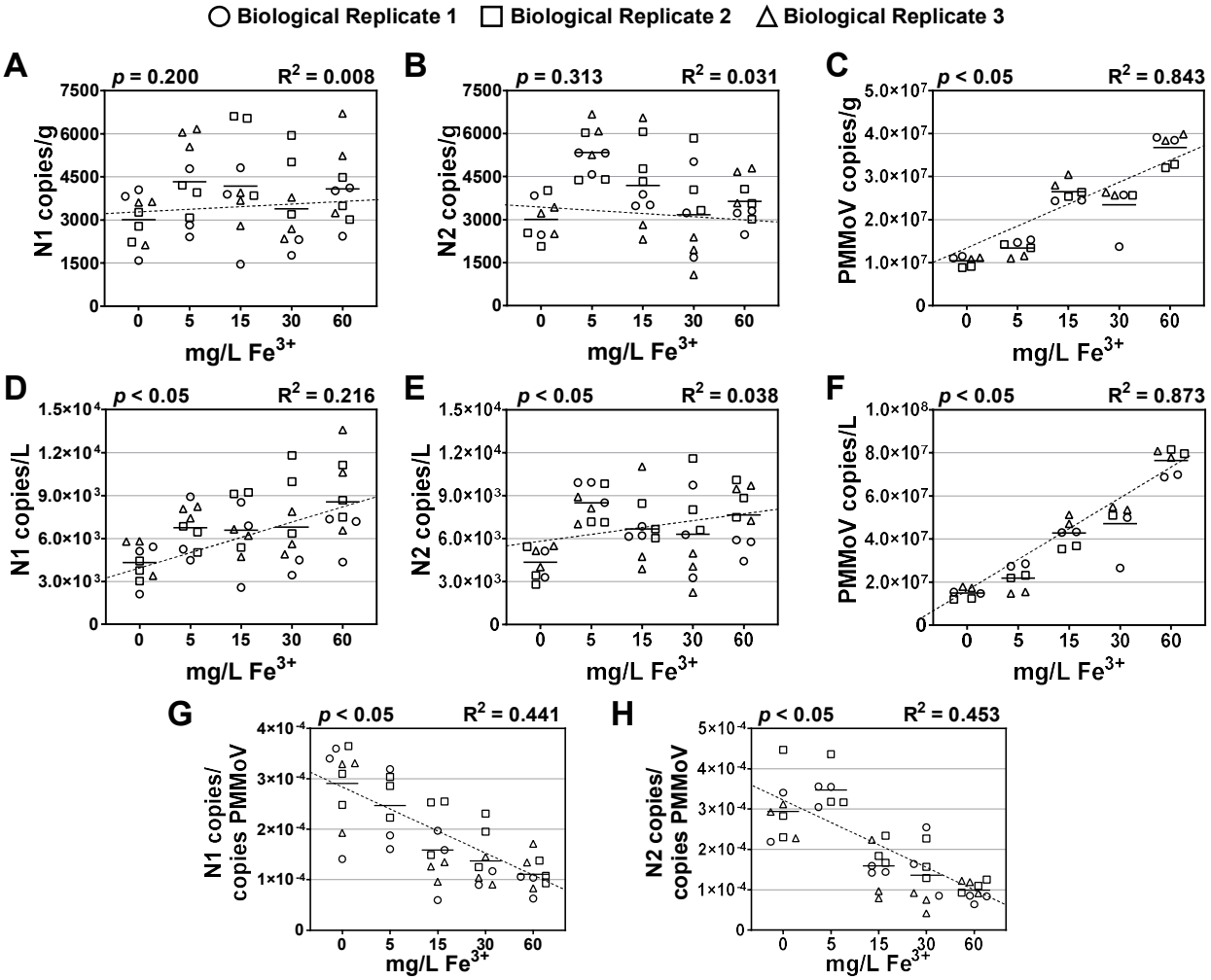

Figure 2.4: Effect of increasing coagulant concentrations on: (A) N1 copies/g extracted mass, (B) N2 copies/g extracted mass, (C) PMMoV copies/g of extracted mass, (D) N1 copies/L of total sample volume, (E) N2 copies/L of total sample volume, (F) PMMoV copies/L total sample volume, (G) N1 copies/copies PMMoV, and (H) N2 copies/copies PMMoV.

PMMoV viral signals in sedimented solids from the post-grit wastewater that was collected from the Ottawa WRRF on Feb. 22nd, 2021, were detected at all five Fe^{3+} concentrations. Unlike the observations for the N1 and N2 gene region measurements, coagulation with ferric sulfate significantly affected the PMMoV viral signal measurements in the sedimented solids (Figure 2.4 C and F). Measurements represented in PMMoV copies/g and PMMoV copies/L displayed a statistically significant increase with increasing Fe^{3+} concentrations ($p < 0.05$) (Figure 2.4 C and F). Higher PMMoV measurements in wastewater were previously associated with higher fractions of solids in wastewater (Kitamura et al., 2021). However, in this study, the PMMoV copies/g and

copies/L measurements have a stronger linear dependence on Fe^{3+} concentrations ($R^2 = 0.843$ and $R^2 = 0.873$) (Figure 2.4 C and F, respectively)) compared to the resulting settled solids pellet at all five Fe^{3+} concentrations ($R^2 = 0.377$ and $R^2 = 0.638$) (Figure 2.9S A and B, respectively), respectively, in Supplemental Material). Hence, the significant elevations of PMMoV viral measurements in the sedimented solids are more strongly associated with the increased coagulant concentration in the post-grit wastewater samples collected on Feb. 22nd, 2021. Consequently, the increased Fe^{3+} dosages were shown to significantly reduce the PMMoV-normalized SARS-CoV-2 N1 and N2 viral measurement in the sedimented solids samples ($p < 0.05$) (Figure 2.4 G and H). This suggests that coagulation with ferric sulfate could cause a significant under-representation of PMMoV-normalized SARS-CoV-2 viral measurements in sedimented solids in WWS applications.

There is no previous literature that explored the effects of trivalent metal coagulant addition on the electrostatic interaction between wastewater solids and PMMoV viral particles. Since PMMoV RNA was previously measured in both the wastewater solids fraction and the supernatant fraction (Kim et al., 2021; Kitamura et al., 2021), it is hypothesized that the change in PMMoV viral measurements associated with the increasing Fe^{3+} concentrations is likely attributed to alterations in electrostatic interactions between PMMoV RNA particles and the sedimented wastewater solids. Change in the virus' surface charge was reported to affect their propensity for binding to wastewater colloids from the liquid phase (Walshe et al., 2010; Ye et al., 2016). Virus' surface charges are influenced either by: i) pH change (Walshe et al., 2010) or ii) by a direct change in surface charge caused by the interaction between Fe^{3+} ions and the wastewater colloids during the coagulation process (Crittenden et al., 2012). In this study, those two hypotheses are explored by i) testing the effects of the consecutive pH drop associated with the increased Fe^{3+} dosages in the post-grit samples collected on Feb. 22nd, 2021, and ii) by measuring the SARS-CoV-2 and PMMoV RNA in the supernatant fractions of the wastewater at increasing Fe^{3+} concentrations in the post-grit wastewater samples collected on Mar. 23rd and May 2nd, 2021.

2.4.3 Effects of pH change on SARS-CoV-2 and PMMoV viral signals measurements

This study further explored whether the pH drop associated with the increased Fe^{3+} dosages affects SARS-CoV-2 and PMMoV copies. For the post-grit wastewater collected on Feb. 22nd, 2021, the recorded pH for all five Fe^{3+} concentrations after 30 min of sedimentation has dropped

from 7.6 ± 0.1 (at 0 mg/L Fe^{3+}) to 6.6 ± 0.2 (at 60 mg/L Fe^{3+}), which lie within the optimal operating pH range of 5.0 - 8.5 for ferric precipitation during enhanced primary clarification (Crittenden et al., 2012). Measurements of SARS-CoV-2 N1 and N2 gene regions and the PMMoV biomarker were both detected in the sedimented solids of all six samples (Figure 2.5). Measurements of N1 and N2 copies/g showed no significant change between the two pH conditions (Figure 2.5 A and B). However, measurements of PMMoV copies/g showed a statistically significant drop in the samples at pH 6.6 ($p < 0.05$) compared to samples at pH 7.6 (Figure 2.5 C). This finding runs contrary to the original hypothesis that reducing the sample pH would result in a higher PMMoV viral signal in solids since viral particles reportedly bind better to wastewater colloids at lower pH due to a reduction in the negativity of the virus (Walshe et al., 2010). PMMoV viral particles are negatively charged at an environmental pH above 3.8 (Charles P. Gerba, 1984; Kitajima et al., 2018; Michen and Graule, 2010; Shirasaki et al., 2017; Vega, 2006; Wetter et al., 1984); thus, PMMoV surface charge at the sample with pH 7.6 would likely be more negative than at sample with pH 6.6. Since wastewater solids are usually negatively charged as well, it would be expected that PMMoV RNA in samples with pH 6.6 (less negative surface charge) to have better binding to wastewater solids. However, it was found in previous studies that wastewater acidification could reduce virus recovery in wastewater solids due to possible degradation or alteration in the virus' integrity (Ahmed et al., 2020b). Despite these changes in the PMMoV RNA measurements, the PMMoV-normalized SARS-CoV-2 N1 and N2 gene regions associated with these measurements are shown to not be significantly affected by this change in the measured PMMoV in the solids (Figure 2.5 D and E). Therefore, the pH drop associated with the Fe^{3+} addition is isolated from the decreasing trends in the PMMoV-normalized SARS-CoV-2 measurements in the wastewater solids with increasing Fe^{3+} dosages (Figure 2.4 C and F).

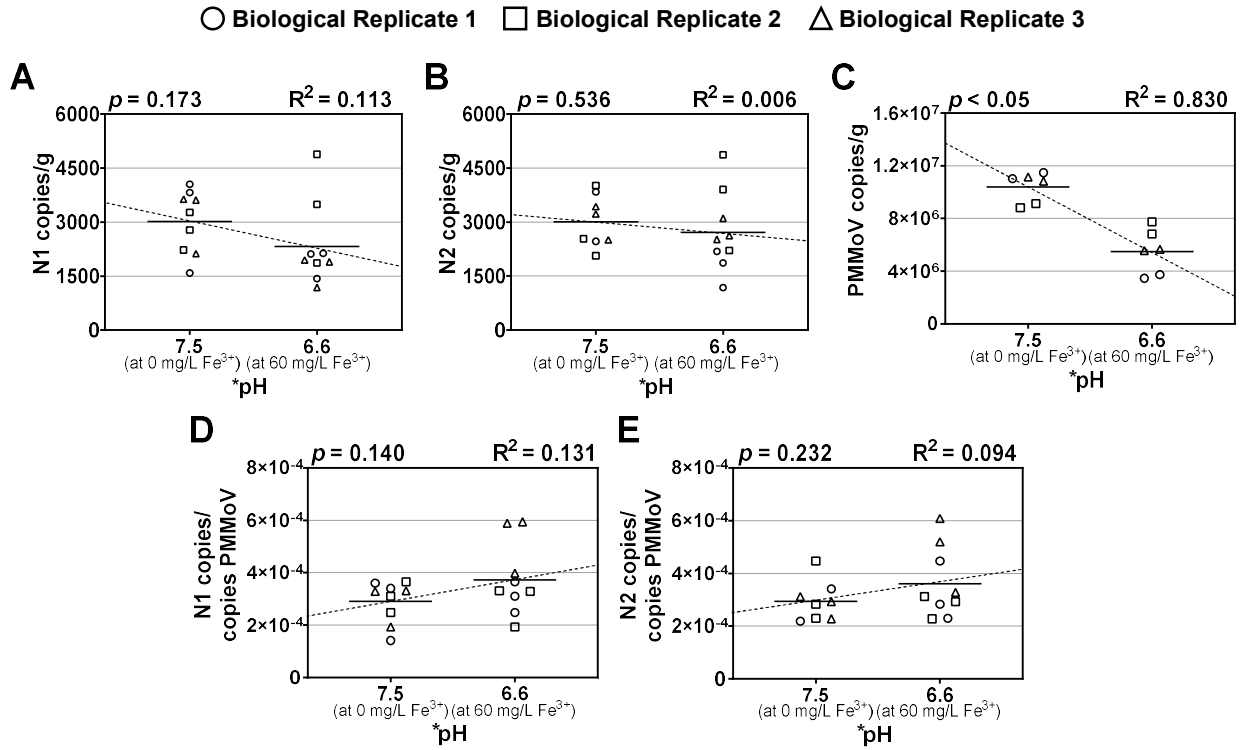

** pH on the x-axis is shown to be decreasing to corresponding to the increasing Fe^{3+} concentrations.*

Figure 2.5: Effect of pH change on (A) N1 copies/g of extracted mass, (B)N2 copies/g of extracted mass, (C) PMMoV copies/g of extracted mass, (D) N1 copies/copies PMMoV, and (E) N2 copies/copies PMMoV.

2.4.4 Partitioning of PMMoV signals between wastewater solids and supernatant

This study further investigates the differences in SARS-CoV-2 and PMMoV viral measurements between the sedimented solids and supernatant fraction after the jar testing of post-grit wastewater collected on Mar. 23rd, 2021. RT-qPCR measurements of SARS-CoV-2 N1 copies/g and N2 copies/g in sedimented solids exhibited no significant change with a dosage of 60 mg/L Fe^{3+} dosage (p = 0.557 and p = 0.519, respectively) (Figure 2.6 A and B), similarly to the viral measurement trend in the post-grit wastewater collected on Feb. 22nd, 2021 (Figure 2.4). The N1 and N2 copies/L were significantly higher in sedimented solids with 60 mg/L Fe^{3+} dosages compared to the samples without coagulant ($p < 0.05$) (Figure 2.6 D and E). Similar to the measurements in the sedimented solids from Feb. 22nd, 2021, post-grit wastewater the change in the N1 and N2 copies/L is more likely attributed to a higher pellet weight of 1.11 ± 0.06 g resulting from solids sedimented with 60 mg/L Fe^{3+} dosages compared to 0.51 ± 0.09 g from solids

sedimented without coagulation treatment. This confirms that coagulation did not affect the SARS-CoV-2 N1 and N2 viral measurements in sedimented solids.

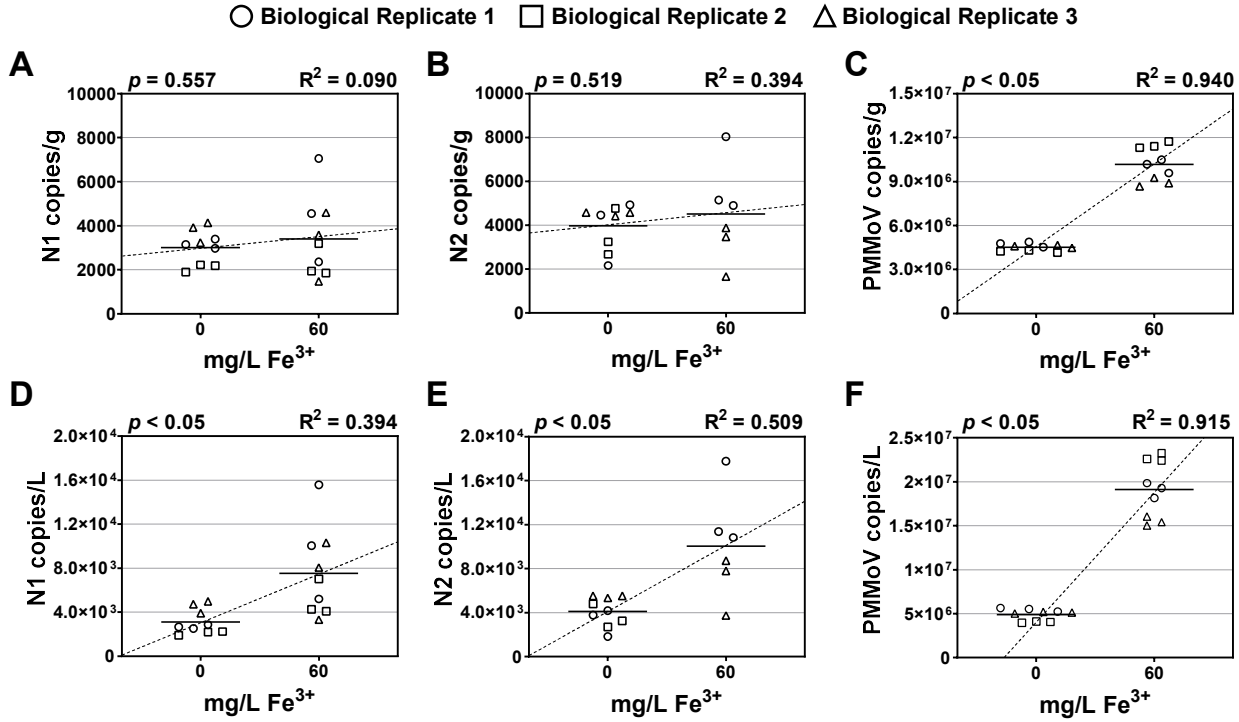

Figure 2.6: Effect of 0 and 60 mg/L Fe^{3+} on: (A) N1 copies/g extracted mass, (B) N2 copies/g extracted mass, (C) PMMoV copies/g extracted mass, (D) N1 copies/L, (E) N2 copies/L, and (F) PMMoV copies/L.

PMMoV viral copies/g and copies/L were measured in the sedimented solids fraction from post-grit wastewater collected on May 2nd, 2021. Significantly higher measurements of PMMoV copies/g and copies/L were measured in sedimented solids at 60 mg/L Fe^{3+} compared to sedimented solids without treatment with coagulant ($p < 0.05$) along with very strong linear association with ferric sulfate dosage ($R^2 = 0.940$ and $R^2 = 0.915$; as described in Statistical Analysis section of the manuscript) (Figure 2.6 C and F, respectively). As previously discussed, while a higher PMMoV RNA concentration is likely attributed to more solids being sedimented with 60 mg/L Fe^{3+} dosage, providing a concentrated solids pelleted weight of 0.94 ± 0.06 g compared to 0.54 ± 0.05 g of sedimented solids without coagulant (from the samples collected on May 2nd, 2021), it is important to consider the possibility of virus partitioning between the wastewater solid and liquid phases due to changes in the virus' or wastewater colloids surface charge (Ye et al., 2016). Previous studies have suggested considerable portions of PMMoV RNA

detected in the supernatant fraction of the wastewater (Kitamura et al., 2021), while others suggested that the solids fraction is enriched with PMMoV RNA (Kim et al., 2021). Although PMMoV measurement in wastewater solids fraction is sufficient as a SARS-CoV-2 normalization tool due to its low variability and enrichment in the solids fraction of wastewaters (D'Aoust et al., 2021b; Kitajima et al., 2018; Wu et al., 2020), the effects of variability in wastewater qualities, such as the presence or absence of metal ions, on the preferential partitioning of viruses in the solid and liquid phases were not previously explored. Whether PMMoV recovery is enhanced in the solid phase due to changes in ionic forces is also unknown. Studies that applied ferric-based (Farrah and Preston, 1985; John et al., 2011; Payment et al., 1984; Randazzo et al., 2019; Sobsey et al., 1997) and aluminum-based (Bar-Or et al., 2020; Barril et al., 2021; Randazzo et al., 2020b, 2020a) precipitation methods for virus recovery did not investigate differences in viral biomass between the wastewater solids and liquid fractions. Therefore, this study considers RT-qPCR processing of the liquid fraction for viral signal measurements of both SARS-CoV-2 and PMMoV RNA.

RT-qPCR analysis was conducted on the supernatant collected after the jar test 30 min sedimentation period from post-grit wastewater collected on both Mar. 23rd and May 2nd, 2021, using the same viral extraction methodology that was used for RNA measurement in the solids fraction. From the samples collected on Mar. 23rd, only supernatant samples collected directly from the beakers were examined, and all six samples showed no SARS-CoV-2 N1 and N2 measurements, and PMMoV measurements were below detection limits. This is likely because the supernatant in this study was processed without further concentration with centrifugal filter devices which were used in previous studies that involved testing SARS-CoV-2 and PMMoV in wastewater liquid fractions (Ahmed et al., 2020b; Kitamura et al., 2021; Petala et al., 2021).

The supernatant fractions were tested once more for SARS-CoV-2 and PMMoV RNA from post-grit wastewater collected on May 2nd, but this time the samples were not diluted during the RT-qPCR procedure for PMMoV detection in the supernatant fraction. Once again, the RT-qPCR of the supernatant fractions for all six samples showed no detectable signals of SARS-CoV N1 and N2 gene regions. This corresponds to the previous finding that showed significantly higher SARS-CoV-2 RNA concentrations in the solids fraction compared to the liquid fraction (Kim et al., 2021; Li et al., 2021) and supports previous findings that SARS-CoV-2 RNA predominates in the wastewater solids fraction (Chik et al., 2021; D'Aoust et al., 2021b; Graham et al., 2021; Kitamura

et al., 2021; Peccia et al., 2020; Rosario et al., 2009). However, PMMoV viral copies were successfully measured in the concentrated supernatant fractions from both the beakers following sedimentation (settled supernatant) and decanted supernatant resulting from the concentration of sedimented solids (centrifuged supernatant) from post-grit wastewater collected on May 2nd, 2021. This aligns with previous observations that unenveloped viruses, such as PMMoV, tend to bind poorly to wastewater colloids compared to enveloped viruses like SARS-CoV-2 (Kampf et al., 2020; Kitamura et al., 2021; Kumar et al., 2021; Ye et al., 2016). For the settled supernatant, measurements of PMMoV viral signals ranged from 5.8 x 10^5 – 2.1 x 10^6 copies/L (average of 1.05 x 10^6 ± 4.58 x 10^5 copies/L) in samples with 0 mg/L Fe^{3+} dosage, and from 1.2 x 10^5 copies/L – 7.6 x 10^5 (avg. 3.62 x 10^5 ± 2.42 x 10^5 copies/L) in settled supernatant from samples with 60 mg/L Fe^{3+} dosage (Figure 2.7 A). For the centrifuged supernatant, measurements of PMMoV viral signals ranged from 7.5 x 10^5 – 2.2 x 10^6 copies/L (avg. 1.3 x 10^6 ± 5.1 x 10^5 copies/L) in samples with 0 mg/L Fe^{3+} dosage, and from 7.6 x 10^4 – 6.2 x 10^5 copies/L (avg. 2.7 x 10^5 ± 1.7 x 10^5 copies/L) in samples with 60 mg/L Fe^{3+} dosage (Figure 2.7 B). The PMMoV copies/L measurements in both the settled and centrifuged supernatant fractions were shown to be significantly reduced ($p < 0.05$) in samples with 60 mg/L Fe^{3+} dosages compared to samples that were not treated with a coagulant with moderate to strong linear association with the ferric sulfate dosage (R^2 = 0.498 and R^2 = 0.662; as described in the Statistical Analysis section of the manuscript) (Figure 2.7 A and B, respectively). Notably, the settled supernatant TS measurements between samples with no coagulant (avg. 417 ± 8 mg/L TS) and with 60 mg/L Fe^{3+} dosages (avg. 437 ± 4 mg/L TS) have no significant difference (p = 0.02), suggesting that the change in the PMMoV viral measurements were not significantly governed by changes in wastewater qualities associated with coagulant dosing. This suggests that positively charged Fe^{3+} not only aggregates negatively charged wastewater colloids to initiate coagulation (Crittenden et al., 2012; Ye et al., 2016) but also neutralizes negatively charged PMMoV viral particles and causes them to bind to wastewater colloids. This causes the partitioning of PMMoV viral particles from the bulk liquid phase to the solid phase due to neutralization by the Fe^{3+} ions.

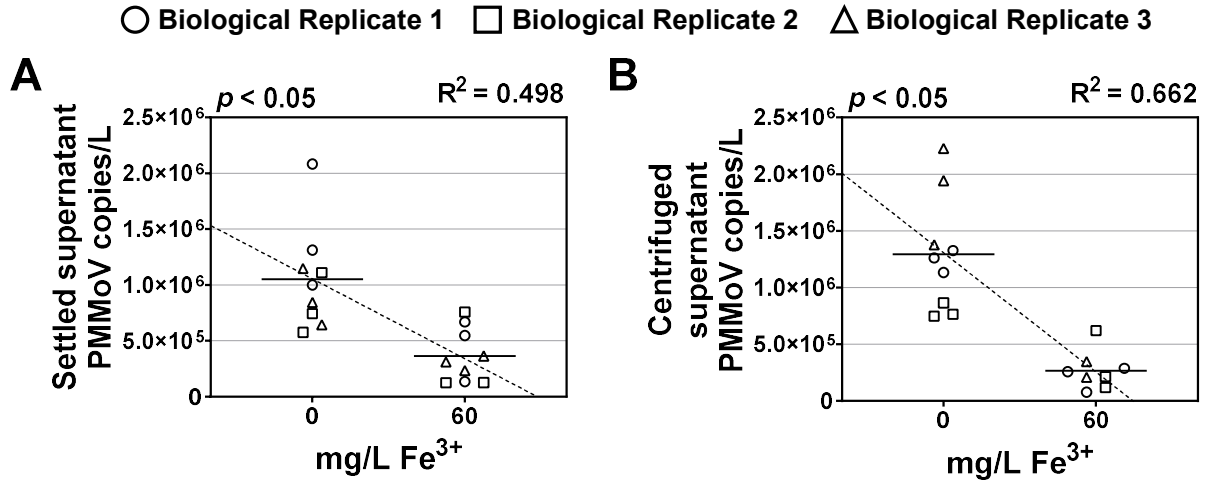

Figure 2.7: Effect of 0 and 60 mg/L Fe^{3+} on: (A) PMMoV copies/L in settled supernatant (supernatant collected directly from beakers after jar tests), and (B) PMMoV copies/L in centrifuged supernatant (decanted supernatant collected after centrifugation of solids for sample concentration).

Partitioning of SARS-CoV-2 and PMMoV viral particles from the bulk supernatant fractions (settled and centrifuged supernatant) to the wet solids fraction with 60 mg/L as Fe^{3+} dosage is visually illustrated (Figure 2.8). In post-grit wastewater samples collected on May 2nd, 2021, 100% of the SARS-CoV-2 RNA was exclusively detected in the wet solids fraction with negligible detection of the signal in the settled supernatant and centrifuged supernatant fractions in both the untreated and treated samples by the coagulant (Figure 2.8 A). PMMoV RNA was similarly found to be enriched in the wet solids fraction of the post-grit wastewater (Figure 2.8 B); this is consistent with the previous finding that measured significantly higher PMMoV RNA in wastewater solids fraction compared to the liquid fraction (Kim et al., 2021). Solids from post-grit samples that were not treated by coagulant were shown to contain 96.35% ± 0.67% of the total PMMoV copies (Figure 2.8 B). Partitioning of PMMoV RNA could still be observed in the samples treated with 60 mg/L Fe^{3+} for which an additional 3.48% ± 0.48% of total PMMoV viral copies transferred from the unsettled and settled supernatant fractions to the solids fraction; as such, when treated with 60 mg/L as Fe^{3+} dosage, the solids fraction contained 99.83% ± 0.11% of the total PMMoV biomass (Figure 2.8 B). With PMMoV biomass being largely localized in the solids phase, this makes it an effective normalizing biomarker for the SARS-CoV-2 N1 and N2 gene regions in WWS. Normalization against PMMoV in WWS applications is particularly important as it better reflects the community prevalence of COVID-19 infections by accounting for variations in

wastewater physico-chemical properties, fecal mass flux, and PCR amplification (D'Aoust et al., 2021b; Graham et al., 2021; Kitamura et al., 2021; Wolfe et al., 2021a; Wu et al., 2021).

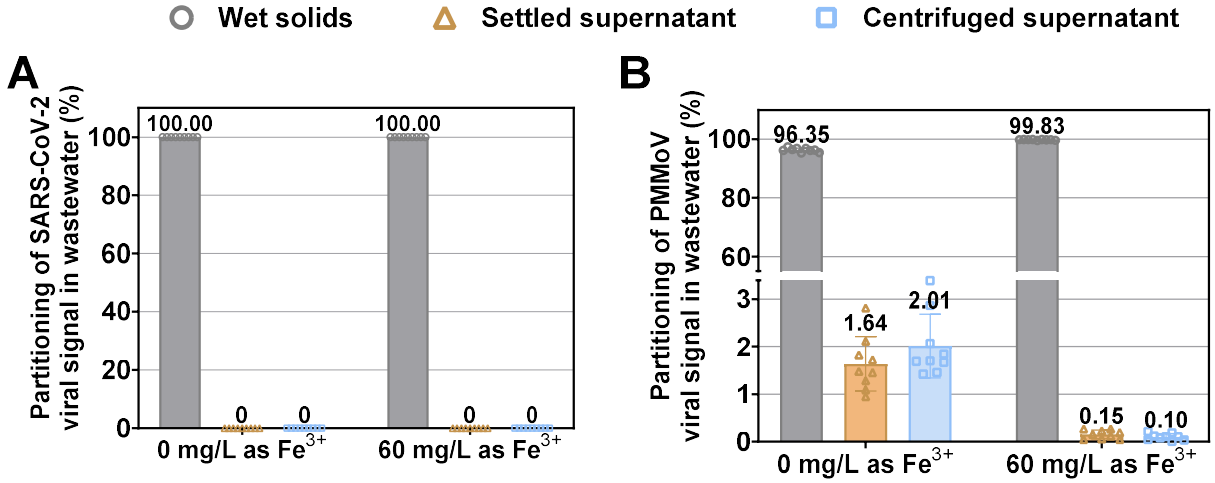

Figure 2.8: Comparison of the partitioning of (A) SARS-CoV-2 and (B) PMMoV genomic copies. The bars represent the standard deviation (SD) of each measurement and the number on top of each bar is the mean percentage for the measurements.

2.5 Conclusion and Recommendations

Over the past year and a half since the detection of the first COVID-19 cases, WWS including analyzing wastewater solids from primary municipal sludge has emerged as an effective disease surveillance tool for monitoring active COVID-19 cases (D'Aoust et al., 2021b; Graham et al., 2021; Peccia et al., 2020). In this investigation, the effect of the commonly used metal coagulant Fe^{3+} on SARS-CoV-2 and PMMoV viral signals was examined for potential implications on the effectiveness of WWS using primary sludge.

Coagulation due to increasing Fe^{3+} did not significantly influence the average measurements of SARS-CoV-2 N1 and N2 viral copies. However, the PMMoV signal for wet solids showed a significantly higher signal with increasing concentrations of Fe^{3+}. This change in PMMoV copies might significantly affect the normalization of SARS-CoV-2 viral copies in wastewater determined through WWS and result in underestimating the community prevalence of SARS-CoV-2. Various factors can be attributed to this observation, including a higher fraction of settled solids associated with coagulation that are likely to contain higher concentrations of PMMoV copies/g and PMMoV copies/L. Indirect pH reduction associated with adding ferric sulfate was not associated with trends

observed for PMMoV copies and had no significant impact on PMMoV-normalized viral N1 and N2 copies. However, changes in the behaviour of PMMoV RNA due to pH should be further examined. Another possible explanation for the behaviour that was observed was the reduction of electrostatic forces associated with the decrease in negative charges between PMMoV and wastewater colloids caused by adding Fe^{3+}, thereby resulting in PMMoV RNA partitioning from the liquid phase to the solid phase.

2.6 Declaration of Competing Interests

The authors declare that no competing financial interests or personal relationships influenced the work reported in this manuscript.

2.7 Acknowledgements

The authors wish to acknowledge the help and assistance of the University of Ottawa, the Ottawa Hospital, the Children's Hospital of Eastern Ontario, the Children's Hospital of Eastern Ontario's Research Institute, Public Health Ontario and all of their employees who were involved in this project. Their time, facilities, resources, and feedback are greatly appreciated.

2.8 Funding

This research was supported by the Province of Ontario's Wastewater Surveillance Initiative (WSI). It was also supported by a CHEO (Children's Hospital of Eastern Ontario) CHAMO (Children's Hospital Academic Medical Organization) grant, which was awarded to Dr. Alex E. MacKenzie.

2.9 References

Ahmed, W., Angel, N., Edson, J., Bibby, K., Bivins, A., O'Brien, J.W., Choi, P.M., Kitajima, M., Simpson, S.L., Li, J., Tscharke, B., Verhagen, R., Smith, W.J.M., Zaugg, J., Dierens, L., Hugenholtz, P., Thomas, K. V., Mueller, J.F., 2020a. First confirmed detection of SARS-CoV-2 in untreated wastewater in Australia: A proof of concept for the wastewater surveillance of COVID-19 in the community. Sci. Total Environ. 728, 138764.

https://doi.org/10.1016/j.scitotenv.2020.138764

Ahmed, W., Bertsch, P.M., Bivins, A., Bibby, K., Farkas, K., Gathercole, A., Haramoto, E., Gyawali, P., Korajkic, A., McMinn, B.R., Mueller, J.F., Simpson, S.L., Smith, W.J.M., Symonds, E.M., Thomas, K. V., Verhagen, R., Kitajima, M., 2020b. Comparison of virus concentration methods for the RT-qPCR-based recovery of murine hepatitis virus, a surrogate for SARS-CoV-2 from untreated wastewater. Sci. Total Environ. 739, 139960. https://doi.org/10.1016/J.SCITOTENV.2020.139960

American Water Works Association, 2011. Operational Control of Coagulation and Filtration Processes AWWA MANUAL M37, Third Edit. ed. American Water Works Association, Denver, CO, USA.

APHA American Public Health Association, 2017. Standard Methods for the Examination of Water and Wastewater, 23rd ed. Washington, DC.

Arora, S., Nag, A., Sethi, J., Rajvanshi, J., Saxena, S., Shrivastava, S.K., Gupta, A.B., 2020. Sewage surveillance for the presence of SARS-CoV-2 genome as a useful wastewater based epidemiology (WBE) tracking tool in India. Water Sci. Technol. 82, 2823–2836. https://doi.org/10.2166/wst.2020.540

Balboa, S., Mauricio-Iglesias, M., Rodriguez, S., Martínez-Lamas, L., Vasallo, F.J., Regueiro, B., Lema, J.M., 2020. The fate of SARS-CoV-2 in WWTPs points out the sludge line as a suitable spot for monitoring. medRxiv 2020.05.25.20112706. https://doi.org/10.1101/2020.05.25.20112706

Bar-Or, I., Yaniv, K., Shagan, M., Ozer, E., Erster, O., Mendelson, E., Mannasse, B., Shirazi, R., Kramarsky-Winter, E., Nir, O., Abu-Ali, H., Ronen, Z., Rinott, E., Lewis, Y.E., Friedler, E., Bitkover, E., Paitan, Y., Berchenko, Y., Kushmaro, A., 2020. Regressing SARS-CoV-2 sewage measurements onto COVID-19 burden in the population: A proof-of-concept for quantitative environmental surveillance. medRxiv 1–11. https://doi.org/10.1101/2020.04.26.20073569

Barril, P.A., Pianciola, L.A., Mazzeo, M., Ousset, M.J., Jaureguiberry, M.V., Alessandrello, M., Sánchez, G., Oteiza, J.M., 2021. Evaluation of viral concentration methods for SARS-CoV-2 recovery from wastewaters. Sci. Total Environ. 756, 144105. https://doi.org/10.1016/j.scitotenv.2020.144105

Bivins, A., North, D., Ahmad, A., Ahmed, W., Alm, E., Been, F., Bhattacharya, P., Bijlsma, L., Boehm, A.B., Brown, J., Buttiglieri, G., Calabro, V., Carducci, A., Castiglioni, S., Cetecioglu Gurol, Z., Chakraborty, S., Costa, F., Curcio, S., De Los Reyes, F.L., Delgado Vela, J., Farkas, K., Fernandez-Casi, X., Gerba, C., Gerrity, D., Girones, R., Gonzalez, R., Haramoto, E., Harris, A., Holden, P.A., Islam, M.T., Jones, D.L., Kasprzyk-Hordern, B., Kitajima, M., Kotlarz, N., Kumar, M., Kuroda, K., La Rosa, G., Malpei, F., Mautus, M., McLellan, S.L., Medema, G., Meschke, J.S., Mueller, J., Newton, R.J., Nilsson, D., Noble, R.T., Van Nuijs, A., Peccia, J., Perkins, T.A., Pickering, A.J., Rose, J., Sanchez, G., Smith, A., Stadler, L., Stauber, C., Thomas, K., Van Der Voorn, T., Wigginton, K., Zhu, K., Bibby, K., 2020. Wastewater-Based Epidemiology: Global Collaborative to Maximize Contributions in the Fight against COVID-19. Environ. Sci. Technol. https://doi.org/10.1021/acs.est.0c02388

Carliell-Marquet, C., Smith, J., Oikonomidis, I., Wheatley, A., 2010. Inorganic profiles of chemical phosphorus removal sludge. Proc. Inst. Civ. Eng. Manag. 163, 65–77. https://doi.org/10.1680/WAMA.2010.163.2.65

CDC, 2020. Real-Time RT-PCR diagnostic panel for emergency use only. CDC EUA.

Charles P. Gerba, 1984. Applied and theoretical aspects of virus adsorption to surfaces. Adv. Appl. Microbiol. 30, 133–168.

Chik, A.H.S., Glier, M.B., Servos, M., Mangat, C.S., Pang, X.L., Qiu, Y., D'Aoust, P.M., Burnet, J.B., Delatolla, R., Dorner, S., Geng, Q., Giesy, J.P., McKay, R.M., Mulvey, M.R., Prystajecky, N., Srikanthan, N., Xie, Y., Conant, B., Hrudey, S.E., 2021. Comparison of approaches to quantify SARS-CoV-2 in wastewater using RT-qPCR: Results and implications from a collaborative inter-laboratory study in Canada. J. Environ. Sci. 107, 218–229. https://doi.org/10.1016/j.jes.2021.01.029

Combs, L.G., Warren, J.E., Huynh, V., Castaneda, J., Golden, T.D., Roby, R.K., 2015. The effects of metal ion PCR inhibitors on results obtained with the Quantifiler® Human DNA Quantification Kit. Forensic Sci. Int. Genet. 19, 180–189. https://doi.org/10.1016/j.fsigen.2015.06.013

Cornel, P., Schaum, C., 2009. Phosphorus recovery from wastewater: needs, technologies and costs. Water Sci. Technol. 59, 1069–1076. https://doi.org/10.2166/WST.2009.045

Crittenden, J.C., Trussell, R.R., Hand, D.W., Howe, K.J., Tchobanoglous, G., 2012. MWH's water treatment : principles and design, Third. ed. John Wiley and Sons.

Cuevas-Ferrando, E., Randazzo, W., Pérez-Cataluña, A., Sánchez, G., 2020. HEV Occurrence in Waste and Drinking Water Treatment Plants. Front. Microbiol. 10. https://doi.org/10.3389/fmicb.2019.02937

D'Aoust, P.M., Graber, T.E., Mercier, E., Montpetit, D., Alexandrov, I., Neault, N., Baig, A.T., Mayne, J., Zhang, X., Alain, T., Servos, M.R., Srikanthan, N., MacKenzie, M., Figeys, D., Manuel, D., Jüni, P., MacKenzie, A.E., Delatolla, R., 2021a. Catching a resurgence: Increase in SARS-CoV-2 viral RNA identified in wastewater 48 h before COVID-19 clinical tests and 96 h before hospitalizations. Sci. Total Environ. 770. https://doi.org/10.1016/j.scitotenv.2021.145319

D'Aoust, P.M., Mercier, E., Montpetit, D., Jia, J.J., Alexandrov, I., Neault, N., Baig, A.T., Mayne, J., Zhang, X., Alain, T., Langlois, M.A., Servos, M.R., MacKenzie, M., Figeys, D., MacKenzie, A.E., Graber, T.E., Delatolla, R., 2021b. Quantitative analysis of SARS-CoV-2 RNA from wastewater solids in communities with low COVID-19 incidence and prevalence. Water Res. 188, 116560. https://doi.org/10.1016/j.watres.2020.116560

D'Aoust, P.M., Towhid, S.T., Mercier, É., Hegazy, N., Tian, X., Bhatnagar, K., Zhang, Z., Mackenzie, A.E., Graber, T.E., Delatolla, R., 2021c. COVID-19 monitoring in rural communities: First comparison of lagoon and pumping station samples for wastewater-based epidemiology. Environ. Sci. Water Res. Technol. https://doi.org/https://doi.org/10.1016/j.scitotenv.2021.149618

Dalecka, B., Mezule, L., 2018. Study of potential PCR inhibitors in drinking water for Escherichia coli identification. Agron. Res. 16, 1351–1359.

https://doi.org/10.15159/AR.18.118

Davis, M.L., 2010. Water and Wastewater Engineering: Design Principles and Practice. McGraw-Hill Education.

Dong, T., Shewa, W.A., Murray, K., Dagnew, M., 2019. Optimizing chemically enhanced primary treatment processes for simultaneous carbon redirection and phosphorus removal. Water (Switzerland) 11. https://doi.org/10.3390/w11030547

ECCC, 2011. Municipal Water Use Report.

ECCC, 2010. Optimization Guidance Manual for Sewage Works .

Farrah, S.R., Preston, D.R., 1985. Concentration of viruses from water by using cellulose filters modified by in situ precipitation of ferric and aluminum hydroxides. Appl. Environ. Microbiol. 50, 1502–1504. https://doi.org/10.1128/AEM.50.6.1502-1504.1985

Feng, S., Roguet, A., McClary-Gutierrez, J.S., Newton, R.J., Kloczko, N., Meiman, J.G., McLellan, S.L., 2021. Evaluation of sampling frequency and normalization of SARS-CoV-2 wastewater concentrations for capturing COVID-19 burdens in the community. medRxiv 2021.02.17.21251867. https://doi.org/10.1101/2021.02.17.21251867

Gonzalez, R., Curtis, K., Bivins, A., Bibby, K., Weir, M.H., Yetka, K., Thompson, H., Keeling, D., Mitchell, J., Gonzalez, D., 2020. COVID-19 surveillance in Southeastern Virginia using wastewater-based epidemiology. Water Res. 186, 116296. https://doi.org/10.1016/j.watres.2020.116296

Graham, K.E., Loeb, S.K., Wolfe, M.K., Catoe, D., Sinnott-Armstrong, N., Kim, S., Yamahara, K.M., Sassoubre, L.M., Mendoza Grijalva, L.M., Roldan-Hernandez, L., Langenfeld, K., Wigginton, K.R., Boehm, A.B., 2021. SARS-CoV-2 RNA in Wastewater Settled Solids Is Associated with COVID-19 Cases in a Large Urban Sewershed. Environ. Sci. Technol. 55, 488–498. https://doi.org/10.1021/acs.est.0c06191

Haramoto, E., Kitajima, M., Kishida, N., Konno, Y., Katayama, H., Asami, M., Akiba, M., 2013. Occurrence of pepper mild mottle virus in drinking water sources in Japan. Appl. Environ. Microbiol. 79, 7413–7418. https://doi.org/10.1128/AEM.02354-13

Jafferali, M.H., Khatami, K., Atasoy, M., Birgersson, M., Williams, C., Cetecioglu, Z., 2021. Benchmarking virus concentration methods for quantification of SARS-CoV-2 in raw wastewater. Sci. Total Environ. 755, 142939. https://doi.org/10.1016/J.SCITOTENV.2020.142939

John, S.G., Mendez, C.B., Deng, L., Poulos, B., Kauffman, A.K.M., Kern, S., Brum, J., Polz, M.F., Boyle, E.A., Sullivan, M.B., 2011. A simple and efficient method for concentration of ocean viruses by chemical flocculation. Environ. Microbiol. Rep. 3, 195–202. https://doi.org/10.1111/J.1758-2229.2010.00208.X

Kampf, G., Todt, D., Pfaender, S., Steinmann, E., 2020. Persistence of coronaviruses on inanimate surfaces and their inactivation with biocidal agents. J. Hosp. Infect. 104, 246–251. https://doi.org/10.1016/j.jhin.2020.01.022

Kim, S., Kennedy, L.C., Wolfe, M.K., Criddle, C.S., Duong, D.H., Topol, A., White, B.J., Kantor, R.S., Nelson, K.L., Steele, J.A., Langlois, K., Griffith, J.F., Zimmer-Faust, A.G.,

McLellan, S.L., Schussman, M.K., Ammerman, M., Wigginton, K.R., Bakker, K.M., Boehm, A.B., 2021. SARS-CoV-2 RNA is enriched by orders of magnitude in solid relative to liquid wastewater at publicly owned treatment works. medRxiv 2021.11.10.21266138. https://doi.org/10.1101/2021.11.10.21266138

Kitajima, M., Sassi, H.P., Torrey, J.R., 2018. Pepper mild mottle virus as a water quality indicator. npj Clean WaterClean Water 1. https://doi.org/10.1038/s41545-018-0019-5

Kitamura, K., Sadamasu, K., Muramatsu, M., Yoshida, H., 2021. Efficient detection of SARS-CoV-2 RNA in the solid fraction of wastewater. Sci. Total Environ. 763, 144587. https://doi.org/10.1016/j.scitotenv.2020.144587

Kuffel, A., Gray, A., Daeid, N.N., 2021. Impact of metal ions on PCR inhibition and RT-PCR efficiency. Int. J. Legal Med. 135, 63–72. https://doi.org/10.1007/s00414-020-02363-4

Kumar, M., Mazumder, P., Mohapatra, S., Kumar Thakur, A., Dhangar, K., Taki, K., Mukherjee, S., Kumar Patel, A., Bhattacharya, P., Mohapatra, P., Rinklebe, J., Kitajima, M., Hai, F.I., Khursheed, A., Furumai, H., Sonne, C., Kuroda, K., 2021. A chronicle of SARS-CoV-2: Seasonality, environmental fate, transport, inactivation, and antiviral drug resistance. J. Hazard. Mater. 405, 124043. https://doi.org/10.1016/j.jhazmat.2020.124043

La Rosa, G., Mancini, P., Bonanno Ferraro, G., Veneri, C., Iaconelli, M., Bonadonna, L., Lucentini, L., Suffredini, E., 2021. SARS-CoV-2 has been circulating in northern Italy since December 2019: Evidence from environmental monitoring. Sci. Total Environ. 750, 141711. https://doi.org/10.1016/j.scitotenv.2020.141711

Lee, M.T., Prudent, A., Marr, L.C., 2016. Partitioning of Viruses in Wastewater Systems and Potential for Aerosolization. Environ. Sci. Technol. Lett. 3, 210–215. https://doi.org/10.1021/ACS.ESTLETT.6B00105

Li, B., Di, D.Y.W., Saingam, P., Jeon, M.K., Yan, T., 2021. Fine-Scale Temporal Dynamics of SARS-CoV-2 RNA Abundance in Wastewater during A COVID-19 Lockdown. Water Res. 197, 117093. https://doi.org/10.1016/J.WATRES.2021.117093

Mao, K., Zhang, K., Du, W., Ali, W., Feng, X., Zhang, H., 2020. The potential of wastewater-based epidemiology as surveillance and early warning of infectious disease outbreaks. Curr. Opin. Environ. Sci. Heal. https://doi.org/10.1016/j.coesh.2020.04.006

Mckinnon, I., Pellegrino, M., Rak-Banville, J., Goss, C., Brant, B., Thorne, G., 2018. Pilot Testing an Alternative Coagulant for the Winnipeg Water Treatment Plant.

Medema, G., Heijnen, L., Elsinga, G., Italiaander, R., Brouwer, A., 2020. Presence of SARS-Coronavirus-2 RNA in Sewage and Correlation with Reported COVID-19 Prevalence in the Early Stage of the Epidemic in the Netherlands. Environ. Sci. Technol. Lett. 7, 511–516. https://doi.org/10.1021/acs.estlett.0c00357

Metcalf and Eddy, 2014. Wastewater Engineering - Treatment and Resource Recovery, 5th ed. McGraw-Hill Education, New York, US.

Michen, B., Graule, T., 2010. Isoelectric points of viruses. J. Appl. Microbiol. 109, 388–397. https://doi.org/10.1111/J.1365-2672.2010.04663.X

Pal, P., 2017. Chemical Treatment Technology, in: Industrial Water Treatment Process

Technology. Butterworth-Heinemann, pp. 21–63. https://doi.org/10.1016/B978-0-12-810391-3.00002-3

Payment, P., Fortin, S., Trudel, M., 1984. Ferric chloride flocculation for nonflocculating beef extract preparations. Appl. Environ. Microbiol. 47, 591–592. https://doi.org/10.1128/AEM.47.3.591-592.1984

Peccia, J., Zulli, A., Brackney, D.E., Grubaugh, N.D., Kaplan, E.H., Casanovas-Massana, A., Ko, A.I., Malik, A.A., Wang, D., Wang, M., Warren, J.L., Weinberger, D.M., Arnold, W., Omer, S.B., 2020. Measurement of SARS-CoV-2 RNA in wastewater tracks community infection dynamics. Nat. Biotechnol. 38, 1164–1167. https://doi.org/10.1038/s41587-020-0684-z

Petala, M., Dafou, D., Kostoglou, M., Karapantsios, T., Kanata, E., Chatziefstathiou, A., Sakaveli, F., Kotoulas, K., Arsenakis, M., Roilides, E., Sklaviadis, T., Metallidis, S., Papa, A., Stylianidis, E., Papadopoulos, A., Papaioannou, N., 2021. A physicochemical model for rationalizing SARS-CoV-2 concentration in sewage. Case study: The city of Thessaloniki in Greece. Sci. Total Environ. 755, 142855. https://doi.org/10.1016/j.scitotenv.2020.142855

Polo, D., Quintela-Baluja, M., Corbishley, A., Jones, D.L., Singer, A.C., Graham, D.W., Romalde, J.L., 2020. Making waves: Wastewater-based epidemiology for COVID-19 – approaches and challenges for surveillance and prediction. Water Res. 186, 116404. https://doi.org/10.1016/j.watres.2020.116404

Randazzo, W., Cuevas-Ferrando, E., Sanjuán, R., Domingo-Calap, P., Sánchez, G., 2020a. Metropolitan wastewater analysis for COVID-19 epidemiological surveillance. Int. J. Hyg. Environ. Heal. 230. https://doi.org/10.1101/2020.04.23.20076679

Randazzo, W., Piqueras, J., Zoran Evtoski, ·, Sastre, G., Sancho, R., Gonzalez, C., Sánchez, G., 2019. Interlaboratory Comparative Study to Detect Potentially Infectious Human Enteric Viruses in Influent and Effluent Waters. Food Environ. Virol. 11, 350–363. https://doi.org/10.1007/s12560-019-09392-2

Randazzo, W., Truchado, P., Cuevas-Ferrando, E., Simón, P., Allende, A., Sánchez, G., 2020b. SARS-CoV-2 RNA in wastewater anticipated COVID-19 occurrence in a low prevalence area. Water Res. 181. https://doi.org/10.1016/j.watres.2020.115942

Rock, C., Alum, A., Abbaszadegan, M., 2010. PCR inhibitor levels in concentrates of biosolid samples predicted by a new method based on excitation-emission matrix spectroscopy. Appl. Environ. Microbiol. 76, 8102–8109. https://doi.org/10.1128/AEM.02339-09

Rosario, K., Symonds, E.M., Sinigalliano, C., Stewart, J., Breitbart, M., Petersburg, S., 2009. Pepper Mild Mottle Virus as an Indicator of Fecal Pollution. Appl. Environ. Microbiol. 75, 7261–7267. https://doi.org/10.1128/AEM.00410-09

Schrader, C., Schielke, A., Ellerbroek, L., Johne, R., 2012. PCR inhibitors – occurrence, properties and removal. J. Appl. Microbiol. 113, 1014–1026. https://doi.org/10.1111/J.1365-2672.2012.05384.X

Shewa, W.A., Dagnew, M., 2020. Revisiting chemically enhanced primary treatment of wastewater: A review. Sustainability 12, 1–19. https://doi.org/10.3390/SU12155928

Shirasaki, N., Matsushita, T., Matsui, Y., Murai, K., 2017. Assessment of the efficacy of membrane filtration processes to remove human enteric viruses and the suitability of bacteriophages and a plant virus as surrogates for those viruses. Water Res. 115, 29–39. https://doi.org/10.1016/j.watres.2017.02.054

Simpson, A., Topol, A., White, B., Wolfe, M.K., Wigginton, K., Boehm, A.B., 2021. Effect of storage conditions on SARS-CoV-2 RNA quantification in wastewater solids. medRxiv 2021.05.04.21256611. https://doi.org/10.1101/2021.05.04.21256611

Sims, N., Kasprzyk-Hordern, B., 2020. Future perspectives of wastewater-based epidemiology: Monitoring infectious disease spread and resistance to the community level. Environ. Int. https://doi.org/10.1016/j.envint.2020.105689

Sobsey, M.D., Gerba, C.P., Wallis, Craig, D Joseph L Melnick, A.N., C P Gerba, M.D., Wallis, C, Melnick, J.L., 1997. Concentration of enteroviruses from large volumes of turbid estuary water. Can. J. Microbiol. 23, 770–778.

Thompson, J.R., Nancharaiah, Y. V., Gu, X., Lee, W.L., Rajal, V.B., Haines, M.B., Girones, R., Ng, L.C., Alm, E.J., Wuertz, S., 2020. Making waves: Wastewater surveillance of SARS-CoV-2 for population-based health management. Water Res. 184, 116181. https://doi.org/10.1016/j.watres.2020.116181

Toronto Water, 2009. Update on the Supply Shortage of Iron Salts for Wastewater Treatment.

U.S. EPA, 2000. Wastewater Technology Fact Sheet - Chemical Precipitation, Environmental Protection Agency. Washington, DC.

Vega, E., 2006. Attachment and survival of viruses on lettuce (lactuca sativa l. Var. Capitata l.): Role of physicochemical and biotic factors. Texas A&M University.

Walshe, G.E., Pang, L., Flury, M., Close, M.E., Flintoft, M., 2010. Effects of pH, ionic strength, dissolved organic matter, and flow rate on the co-transport of MS2 bacteriophages with kaolinite in gravel aquifer media. Water Res. 44, 1255–1269. https://doi.org/10.1016/j.watres.2009.11.034

Westhaus, S., Weber, F.A., Schiwy, S., Linnemann, V., Brinkmann, M., Widera, M., Greve, C., Janke, A., Hollert, H., Wintgens, T., Ciesek, S., 2021. Detection of SARS-CoV-2 in raw and treated wastewater in Germany – Suitability for COVID-19 surveillance and potential transmission risks. Sci. Total Environ. 751, 141750. https://doi.org/10.1016/J.SCITOTENV.2020.141750

Wetter, C., Conti, M., Altschuh, D., Tabillion, R., Regenmortel, M.H.V. van, 1984. Pepper Mild Mottle Virus, a Tobamovirus Infecting Pepper Cultivars in Sicily. Phytopathology 74, 405–420. https://doi.org/10.1094/phyto-74-405

Whitney, O.N., Kennedy, L.C., Fan, V.B., Hinkle, A., Kantor, R., Greenwald, H., Crits-Christoph, A., Al-Shayeb, B., Chaplin, M., Maurer, A.C., Tjian, R., Nelson, K.L., 2021. Sewage, Salt, Silica, and SARS-CoV-2 (4S): An Economical Kit-Free Method for Direct Capture of SARS-CoV-2 RNA from Wastewater. Environ. Sci. Technol. 55, 4880–4888. https://doi.org/10.1021/acs.est.0c08129

Wolfe, M.K., Archana, A., Catoe, D., Coffman, M.M., Dorevich, S., Graham, K.E., Kim, S.,

Mendoza Grijalva, L., Roldan-Hernandez, L., Silverman, A.I., Sinnott-Armstrong, N., Vugia, D.J., Yu, A.T., Zambrana, W., Wigginton, K.R., Boehm, A.B., 2021a. Scaling of SARS-CoV-2 RNA in Settled Solids from Multiple Wastewater Treatment Plants to Compare Incidence Rates of Laboratory-Confirmed COVID-19 in Their Sewersheds. Environ. Sci. Technol. Lett. 8, 398–404. https://doi.org/10.1021/acs.estlett.1c00184

Wolfe, M.K., Topol, A., Knudson, A., Simpson, A., White, B., Vugia, D.J., Yu, A.T., Li, L., Balliet, M., Stoddard, P., Han, G.S., Wigginton, K.R., Boehm, A.B., 2021b. High frequency, high throughput quantification of SARS-CoV-2 RNA in wastewater settled solids at eight publicly owned treatment works in Northern California shows strong association with COVID-19 incidence. medRxiv 2021.07.16.21260627. https://doi.org/10.1101/2021.07.16.21260627

Wu, F., Xiao, A., Zhang, J., Moniz, K., Endo, N., Armas, F., Bushman, M., Chai, P.R., Duvallet, C., Erickson, T.B., Foppe, K., Ghaeli, N., Gu, X., Hanage, W.P., Huang, K.H., Lee, W.L., Matus, M., McElroy, K.A., Rhode, S.F., Wuertz, S., Thompson, J., Alm, E.J., 2021. Wastewater Surveillance of SARS-CoV-2 across 40 U.S. states. medRxiv 1–13. https://doi.org/10.1101/2021.03.10.21253235

Wu, F., Zhang, J., Xiao, A., Gu, X., Lee, W.L., Armas, F., Kauffman, K., Hanage, W., Matus, M., Ghaeli, N., Endo, N., Duvallet, C., Poyet, M., Moniz, K., Washburne, A.D., Erickson, T.B., Chai, P.R., Thompson, J., Alm, E.J., 2020. SARS-CoV-2 Titers in Wastewater Are Higher than Expected from Clinically Confirmed Cases. Am. Soc. Microbiol. 5. https://doi.org/10.1128/msystems.00614-20

Xagoraraki, I., Yin, Z., Svambayev, Z., 2014. Fate of Viruses in Water Systems. J. Environ. Eng. 140, 04014020–1. https://doi.org/10.1061/(ASCE)EE.1943-7870.0000827

Ye, Y., Ellenberg, R.M., Graham, K.E., Wigginton, K.R., 2016. Survivability, Partitioning, and Recovery of Enveloped Viruses in Untreated Municipal Wastewater. Environ. Sci. Technol. 50, 5077–5085. https://doi.org/10.1021/ACS.EST.6B00876

Yeoman, S., Stephenson, T., Lester, J.., Perry, R., 1988. The Removal of Phosphorus During Wastewater Treatment: A Review. Environ. Pollut. 49, 183–233. https://doi.org/10.1016/0269-7491(88)90209-6.

2.10 Supplementary Materials

Table 2.3S: List of PCR primer and probe sets utilized in this study

Primer/probe & supplier	Sequence	Reference
2019-nCov_N1 forward primer (IDT)	GAC CCC AAA ATC AGC GAA AT	(CDC, 2020)
2019-nCoV_N1 reverse primer (IDT)	TCT GGT TAC TGC CAG TTG AAT CTG	(CDC, 2020)
2019-nCoV_N1 probe (IDT)	6-FAM-ACC CCG CAT/ZEN/ TAC GTT TGG TGG ACC-IOWA BLACK FQ	(CDC, 2020)
2019-nCoV_N2 forward primer (IDT)	TTA CAA ACA TTG GCC GCA AA	(CDC, 2020)
2019-nCoV_N2 reverse primer (IDT)	GCG CGA CAT TCC GAA GAA	(CDC, 2020)
2019-nCoV_N2 probe (IDT)	6-FAM-ACA ATT TGC/ZEN/CCC CAG CGC TTC AG-IOWA BLACK FQ	(CDC, 2020)
PMMoV forward primer (ABI)	GAG TGG TTT GAC CTT AAC GTT GA	(Haramoto et al., 2013)
PMMoV reverse primer (ABI)	TTG TCG GTT GCA ATG CAA GT	(Haramoto et al., 2013)
PMMoV probe (ABI)	6-FAM-CCT ACC GAA GCA AAT G-MGB	(Haramoto et al., 2013)

Table 2.4S: Analysis of correlation between total pellet weight (g) and PMMoV viral copies/g extracted mass.

mg/L Fe^{3+}	Pellet Weight (g)		
	Biological Replicate 1	Biological Replicate 2	Biological Replicate 3
0	0.6682	0.6770	0.8000
5	0.9314	0.8154	0.6674
15	0.8845	0.6971	0.8416
30	0.9696	0.9932	1.0426
60	0.8943	1.2417	1.0134

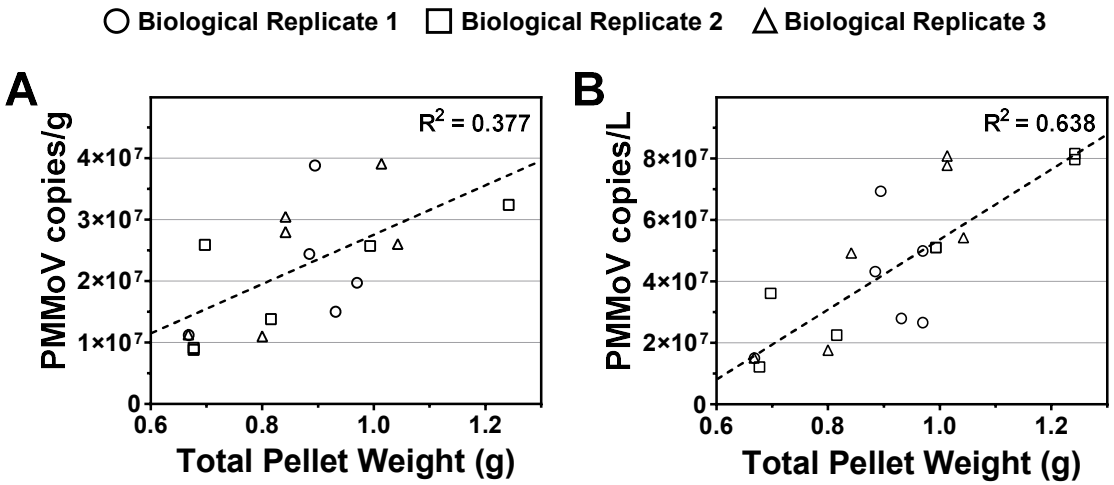

Figure 2.9S: Correlation between the total pellet weight after concentration of sedimented solids and A) PMMoV copies/g and B) PMMoV Copies/g

Science of the Total Environment, 853, (2022), 158458

Chapter 3.

Understanding the Dynamic Relation Between Wastewater SARS-CoV-2 Signal & Clinical Metrics Throughout the Pandemic

Nada Hegazy[1], Aaron Cowan[1], Patrick M. D'Aoust[1], Élisabeth Mercier[1], Syeda Tasneem Towhid[1], Jian-Jun Jia[1], Shen Wan[1], Zhihao Zhang[1], Md Pervez Kabir[1], Wanting Fang[1], Tyson E. Graber[2], Alex E. MacKenzie[2], Stéphanie Guilherme[1], and Robert Delatolla[1]*

1: Department of Civil Engineering, University of Ottawa
161 Louis Pasteur Street, Ottawa, ON, K1N 6N5, Canada

2: Children's Hospital of Eastern Ontario Research Institute
401 Smyth Rd., Ottawa, ON, K1H 5B2, Canada

*Corresponding author: Tel: (613) 562-5800 Ext.2677; E-mail: Robert.Delatolla@uOttawa.ca

Abstract

Wastewater surveillance (WWS) of SARS-CoV-2 was proven to be a reliable and complementary tool for population-wide monitoring of COVID-19 disease incidence but was not as rigorously explored as an indicator for disease burden throughout the pandemic. Prior to global mass immunization campaigns and during the spread of the wildtype COVID-19 and the Alpha variant of concern (VOC), viral measurement of SARS-CoV-2 in wastewater was a leading indicator for both COVID-19 incidence and disease burden in communities. As the two-dose vaccination rates escalated during the spread of the Delta VOC in Jul. 2021 through Dec. 2021, relations weakened between wastewater signal and community COVID-19 disease incidence and maintained a strong relationship with clinical metrics indicative of disease burden (new hospital admissions, ICU admissions, and deaths). Further, with the onset of the vaccine-resistant Omicron BA.1 VOC in Dec. 2021 through Mar. 2022, wastewater again became a strong indicator of both

disease incidence and burden during a period of limited natural immunization (no recent infection), vaccine escape, and waned vaccine effectiveness. Lastly, with the populations regaining enhanced natural and vaccination immunization shortly prior to the onset of the Omicron BA.2 VOC in mid-Mar 2022, wastewater is shown to be a strong indicator for both disease incidence and burden. Hospitalization-to-wastewater ratio is further shown to be a good indicator of VOC virulence when widespread clinical testing is limited. In the future, WWS is expected to show moderate indication of incidence and strong indication of disease burden in the community during future potential seasonal vaccination campaigns.

Keywords: WWS, laboratory positive cases, hospital admissions, deaths, vaccination

3.1 Introduction

Wastewater surveillance (WWS) is a population-wide approach that uses municipal wastewater for real-time surveillance of public health status. Historically, WWS has played a role in the Global Polio Eradication Initiative (GPEI) in 1988 to monitor poliovirus outbreaks around the world (Asghar et al., 2014). Wastewater monitoring has further proven to effectively forecast disease outbreaks caused by norovirus (Prevost et al., 2015; Santiso-Bellón et al., 2020) and hepatitis A (Hellmér et al., 2014). During the spread of the wildtype and the B.1.1.7 (Alpha) Coronavirus disease 2019 (COVID-19) between March 2020 and May 2021, WWS rapidly emerged as a reliable and complementary indicator of severe acute respiratory syndrome coronavirus 2 (SARS-CoV-2) infections in various communities around the world.

At the time of writing this article (Jun. 2022), WWS of COVID-19 is active worldwide in nearly 60 countries at over 3000 sites (COVIDPoops19, 2022; Naughton et al., 2021) and is playing an increasingly significant role in the real-time monitoring of SARS-CoV-2 infection dynamics throughout the world (Ahmed et al., 2020; Bar-Or et al., 2020; Gonzalez et al., 2020; Haramoto et al., 2020; Kocamemi et al., 2020; La Rosa et al., 2021; Medema et al., 2020; Nemudryi et al., 2020; Peccia et al., 2020; Randazzo et al., 2020; Rimoldi et al., 2020; Sherchan et al., 2020; Wu et al., 2021; Wurtzer et al., 2020; Zhang et al., 2021). Various studies identified a significant correlation between the wildtype and the early variant of concern (VOC) B.1.1.7 (Alpha) (dominant in Canada from Mar. 2021 to Jul. 2021) SARS-CoV-2 RNA measurements in wastewater and laboratory reported COVID-19 positive cases of nasopharyngeal testing results with an anticipation of 0 – 4

day (lead time of viral detection in wastewater from the respective clinical metric), thereby establishing wastewater signal of SARS-CoV-2 RNA as an effective early indicator for disease incidence (D'Aoust et al., 2021a; Gerrity et al., 2021; Gonzalez et al., 2020; Graham et al., 2021; Medema et al., 2020; Peccia et al., 2020). Additionally, a strong relation between wastewater measurements of wildtype and the B.1.1.7 (Alpha) VOC SARS-CoV-2 RNA viral signal and hospitalization of patients with severe COVID-19 symptoms was reported with a lead time of 19 – 21 days (Peccia et al., 2020; Saguti et al., 2021) and 3 – 9 days based on mathematical modelling predictions (Galani et al., 2022; Kaplan et al., 2021). Mathematical modelling predictions further demonstrated wastewater is an indicator for intensive care unit (ICU) admissions with a lead time of 3 – 8 days (Galani et al., 2022). With such a considerable time gap between viral measurements in wastewater and reported hospitalizations and ICU admissions, the application of WWS for COVID-19 surveillance provided to be an early prediction of health care demands for COVID-19-related symptoms, while providing insight into disease burden through its relation to hospitalizations and ICU admissions during the dominance of the wildtype SARS-CoV-2 strain and the B.1.1.7 (Alpha) VOC

With the progression of the COVID-19 pandemic and the predomination of new VOCs such as the B.1.617.2 (Delta) VOC (dominant in Canada from Jul. 2021 to Dec. 2021), B.1.1.529.1 (first Omicron BA.1 sub-lineage dominant in Canada from Dec. 2021 to Mar. 2022), initiation of mass vaccination immunization campaigns, and population wide SARS-CoV-2 diagnosis using nasopharyngeal testing becoming less applied in many countries, COVID-19 laboratory positive cases was shown to become a less representative metric of community incidence and less correlated to wastewater viral signal measurements (D'Aoust et al., 2022; Nattino et al., 2022; Xiao et al., 2021). Although early WWS work indicates strong relation between viral signal measurements in wastewater and hospital admission, there remains a knowledge gap with respect to the predictability of WWS as a metric of community disease burden throughout the pandemic. Particularly, the relation between wastewater signal and new hospital admissions, ICU admissions, and COVID-19-caused deaths during the progression of the pandemic has not currently been as rigorously explored compared to laboratory positive COVID-19 cases, and hence the effects of the relation to disease burden throughout the pandemic is less evident. Further into the pandemic, over 16 weeks having passed since 60% of the total population in Canada received two doses of the COVID-19 vaccine (Aug. 3rd, 2021) (Mathieu et al., 2021), the increasingly infectious B.1.1.529.1

(Omicron BA.1) was identified as a new VOC (Nov. 26th, 2021) entering the community and rapidly overtook the B.1.617.2 (Delta) VOC (WHO, 2021). The effectiveness of the widely used mRNA vaccine against symptomatic disease from the B.1.1.529.1 (Omicron BA.1) VOC was found to wane over time from 45.9 to 88% after 2 – 9 weeks from receiving two doses of mRNA vaccine to only 14.9 – 36.3% after ≥ 25 weeks (Andrews et al., 2022; Iorio A. et al., 2022; Lin et al., 2021; Tartof et al., 2021). The mRNA-based vaccine booster (third dose) was found to once more increase vaccine-induced immunization against symptomatic disease up to 75% at 2 weeks, 56.6% at 4 to 5 weeks, and 43.7% at 10 to 11 weeks from third dose reception (Iorio A. et al., 2022). As such, in light of the B.1.1.529.1 (Omicron BA.1) VOC spread in Canada, vaccine booster dose rollout increased rapidly between Jan. 2022 and Feb. 2022. As of Feb. 27nd, 2022, 45.7% of the total population in Canada received a booster vaccine dose (Government of Canada, 2022); optimizing vaccination immunization in almost half of the population prior to entering the sixth surge of the COVID-19 pandemic by mid-March, 2022, driven by the B.1.1.529.2 (Omicron BA.2) VOC. Recent city-wide WWS studies during periods of mass vaccination display divergence of wastewater SARS-CoV-2 measurements from laboratory positive cases prior to waning of vaccine effectiveness during the onset of the B.1.1.529.1 (Omicron BA.1) VOC (Cutrupi et al., 2022; Nattino et al., 2022). However, a gap of knowledge exists with respect to WWS functioning as a predictor and indicator of disease burden during periods of peak vaccination immunization (with a significant portion of the population receiving two vaccine doses 2 – 4 weeks prior to or during the onset of a predominating VOC), and during periods of limited natural immunization and waning vaccination immunization (with a significant portion of the population last receiving two vaccine doses beyond 20 weeks of the onset of the predominating VOC). With significant WWS efforts ongoing across the globe for over 24 months, there is a present opportunity to explore how WWS reflects clinical epidemiological metrics based on timely distribution of vaccines (limited waning of vaccine effectiveness), and whether the vaccine is effective for the dominant VOC (limited vaccine-escape).

It was previously proposed by Xiao et al. (2021) to use wastewater signal/laboratory positive cases (WC) as a means for estimating true disease incidence and virulence (Xiao et al., 2021). However, continuous and population-wide representative SARS-CoV-2 diagnosis using polymerase chain reaction (PCR) testing has presently become less applied in many countries due to the economic impact of testing and small cohorts of populations becoming eligible for PCR

testing. As such, there currently exists a high likelihood of underreporting of COVID-19 laboratory positive cases in many countries, and hence the ability to continue to relate WWS measurements to population-wide, representative laboratory COVID-19 positive testing results for estimating community VOC virulence has diminished and will likely continue to diminish across the world. This highlights the need to determine whether the relationships between wastewater and hospital admissions are a good indicator of VOC virulence in the absence of population-wide clinical testing through a hospitalization-to-wastewater (HW) ratio. Hence, the objective of this research is to evaluate the relationship between SARS-CoV-2 wastewater viral measurements and four public health metrics throughout the pandemic in two long-standing monitored locations in Canada. The four specific public health metrics that will be related to WWS are i) laboratory positive cases, ii) new hospital admissions, iii) ICU admissions, and iv) COVID-19-caused deaths. These relations will be evaluated during the period preceding significant natural and vaccinated immunity and following significant natural and vaccinated immunity to elucidate the use of wastewater in the future for SARS-CoV-2 surveillance and the use during future potential seasonal vaccination campaigns. This research also aims to determine whether hospitalization-to-wastewater (HW) ratio is an effective means to track changes in disease virulence.

3.2 Materials and Methods

3.2.1 Wastewater sampling locations and characteristics

Twenty-four-hour composite samples of primary clarified sludge were collected from the City of Ottawa's (Ontario, Canada) sole water resource recovery facilities (WRRF), Robert O. Pickard Environmental Centre (ROPEC), and from the City of Hamilton's (Ontario, Canada) largest WRRF that services over 80% of the community's population (Woodward Avenue Treatment Plant). Primary clarified sludge samples were first collected on Apr. 8th, 2020, from the Ottawa WRRF, and July 18th, 2020, from the Hamilton WRRF. Daily sample collection and SARS-CoV-2 RNA extraction were ongoing in Ottawa from Sep. 10th, 2020, up until the time of writing of this article (Jun. 2022). A sampling frequency of 3 to 4 days per week was performed in Hamilton. For the duration of the study period, a total of 940 samples were analyzed: 648 of those samples being from the Ottawa WRRF and 292 samples from the Hamilton Woodward WRRF. The Ottawa WRRF services approximately 936,382 people and has an average daily capacity of 545 million

litres. The Hamilton Woodward WRRF services approximately 485,017 people and has an average daily capacity of 409 million litres. Composite samples from both WRRFs were collected, immediately kept on ice and transported to the University of Ottawa laboratory for analysis. Typical primary sludge characteristics from the Ottawa and Hamilton (Woodward) WRRFs across 2020 are shown in Table 3.1. It is noted that the characteristics of the primary sludges do not change significantly in the cities year to year.

Table 3.1: Yearly average primary sludge characteristics (2020) at Ottawa WRRF and Hamilton Woodward WRRF

	Yearly average Ottawa WRRF primary sludge characteristics (avg. ± standard dev.)	**Yearly average Hamilton Woodward WRRF primary sludge characteristics (avg. ± standard dev.)**
Chemical Oxygen Demand (mg/L)	49,959.4 ± 8221.1	41,150.0 ± 12264.3
Total Kjeldahl nitrogen (mg N/L)	1,202.1 ± 187.4	1,453.0 ± 381.2
Total phosphorus (mg P/L)	376.1 ± 59.7	506.5 ± 104.0
Conductivity (uS/cm)	1,968.5 ± 203.5	1,492.8 ± 319.9

3.2.2 RNA extraction and RT-qPCR quantification of SARS-CoV-2, PMMoV, and Variants of Concern in wastewater

40 mL of well-mixed, 24-hour composite primary sludge samples from Ottawa and Hamilton were concentrated by centrifugation at 10,000 x g for 45 min at 4°C. The resulting pellet was well-mixed and 0.250 ± 0.05 g of the resulting pellet was immediately processed for viral extraction using Qiagen's RNeasy PowerMicrobiome extraction kit (PN 26000-50, MD, USA) on a QIAcube Connect automated extraction platform with a modified methodology previously described (D'Aoust et al., 2021b, 2021c). Quantification of SARS-CoV-2 RNA was performed by RT-qPCR targeting the N1 and N2 gene regions (D'Aoust et al., 2021b, 2021c). The RT-qPCR quantification of the Alpha (B.1.1.7) VOC was performed according to Graber et al. (2021), and the RT-qPCR quantification of Delta (B.1.617.2) VOC was performed according to D'Aoust et al. (2022). Analysis for Omicron BA.1 (B.1.1.529.1) in comparison to Omicron BA.2 (B.1.1.529.2) were performed using the sequences shown in Supplemental Material (Table 3.7S). Using a CFX Opus Real-Time PCR system (Bio-Rad, Hercules, CA), reverse-transcriptase incubation was performed at 50°C for 15 min, followed by polymerase activation at 95°C for 2 min, and 40 cycles of denaturation at 95°C /5 s, then annealing/elongation at 60°C/30 s. Additional RT-qPCR

quantifications of the pepper mild mottle virus (PMMoV) were performed with 1/10 dilution of the same samples. Each PCR reaction consisted of 3 µL of RNA template. All primer and probes used in this study are shown in Supplemental Material (Table 3.7S). To check for inhibition, the samples were diluted by a factor of four and then a factor of ten and were compared with undiluted samples for the corresponding decline in PMMoV signal. The assay limit of detection (ALOD; ≥ 95% detection) is approximately 2 copies/reaction. RNA extraction and RT-qPCR were performed in separate laboratories in Class 2 biosafety cabinets to avoid contamination. The measured copies of SARS-CoV-2 (N1 and N2 gene regions) per reaction were normalized against measured PMMoV copies from respective samples.

3.2.3 Epidemiological data

Daily laboratory confirmed positive COVID-19 cases by report date and daily new hospital admissions due to COVID-19 infection in Ottawa between Apr. 8th, 2020, and Feb. 22nd, 2022, were obtained from Public Health Ontario's COVID-19 online data tool (Public Health Ontario, 2022a) and Ottawa Public Health's online COVID-19 dashboard (Ottawa Public Health, 2022), respectively. Laboratory positive COVID-19 cases and daily hospital admissions from COVID-19 infection in Hamilton between July 18th, 2020 and Feb. 13nd, 2022, were obtained from the City of Hamilton online COVID-19 database (City of Hamilton, 2022). Further epidemiological daily measurements representing disease burden including ICU admissions and reported deaths due to COVID-19 complications were obtained from the Ottawa Public Health's online COVID-19 dashboard (Ottawa Public Health, 2022) and from Hamilton's public health dashboard (City of Hamilton, 2022). In this study, the laboratory positive cases, daily hospital admissions, ICU admissions, and reported deaths are expressed in per-capita bases (per 100,000 inhabitants) respectively for both communities. Vaccination information for both Ottawa and Hamilton was obtained from Public Health Ontario's COVID-19 tool (Public Health Ontario, 2022a).

3.2.4 Statistical analysis

Spearman's Rank correlation analyses between the 5-day and 3-day midpoint average of the wastewater viral signal measurements in Ottawa and Hamilton, respectively, and the 5-day midpoint average of the four sets of epidemiological data (laboratory positive cases, hospital admissions, ICU admissions, and deaths). Spearman's coefficients (ρ) values ranging from 0.00 –

0.19 would suggest very weak correlations, 0.20 – 0.39 suggest weak correlations, 0.40 – 0.59 suggest a moderate correlation, 0.60 – 0.79 suggest strong correlation and 0.80 – 1.00 suggest an extraordinarily strong correlation. To determine whether a lag time (△t), measured in days, exists between the wastewater SARS-CoV-2 measurements and epidemiological metrics, a time step analysis was performed by offsetting wastewater SARS-CoV-2 measurements forward in time by a period of 1 – 25 days. The forward time step (lag time of the epidemiological metric) with the strongest correlation between the data sets, along with visual alignment in recorded peaks, was considered when selecting the optimal lag time between wastewater measurements and epidemiological data.

3.3 Results and Discussion

3.3.1 Relation between WWS signal and epidemiological metrics prior to significant natural and vaccination immunization, wildtype and Alpha (B.1.1.7) surges

The wildtype SARS-CoV-2 and Alpha (B.1.1.7) VOC were dominant in Ottawa and Hamilton between Apr. 8th 2020 – Jul. 31st, 2021. The Alpha (B.1.1.7) was first detected in Ontario, Canada in Dec., 2020, quickly overtaking the original wild type SARS-CoV-2 that dominated infections in Canada since Jan. 2020 (Tuite et al., 2021). As of Mar. 23rd, 2021, over 50% of the total wastewater signal analyzed in Ottawa was attributed to the Alpha (B.1.1.7) VOC (D'Aoust et al., 2022). From Apr. 8th, 2020 to Aug. 29th, 2021, in Ottawa, and July 14th, 2020 to Oct. 9th, 2021, in Hamilton, less than 70% of the total population in both cities qualified as "fully vaccinated" (two doses of approved vaccine) against COVID-19 (Public Health Ontario, 2022a). Prior to significant community vaccination immunization, the asymptomatic proportion is believed to have ranged from 17.9% to 57% relative to symptomatic individuals (Kimball et al., 2020; Mizumoto et al., 2020; Sah et al., 2021). The proportion of symptomatic individuals likely to display moderate and severe illness are 56.7% and 0.9%, respectively (Inokuchi et al., 2021). A time step analysis demonstrates a good relationship between the measured SARS-CoV-2 wastewater viral signal (normalized with PMMoV) and laboratory positive cases and hence community disease incidence, with a 5-day lead time in Ottawa (△t = 5d) (ρ = 0.821) and a 10-day lead time (△t = 10d) in Hamilton (ρ = 0.655) when under 70% of both populations were fully immunized (Table 3.2, Figure 3.1 A and B). These findings are in agreement with reported observations from previous WWS

work performed prior to mass vaccination immunization (D'Aoust et al., 2021a; Gerrity et al., 2021; Gonzalez et al., 2020; Graham et al., 2021; Medema et al., 2020; Peccia et al., 2020).

A similar time step analysis further identified WWS as a good indicator for disease burden prior to significant vaccination immunization based on hospital admissions from COVID-19, and additionally based on ICU admissions, and deaths due to complications from COVID-19. A strong positive correlation exists between PMMoV normalized SARS-CoV-2 viral signal and hospital admissions with a 10-day lead time in the viral signal measurements in Ottawa (ρ = 0.808), and with a 14-day lead time in Hamilton (ρ = 0.682) (Table 3.2). This is further confirmed visually (Figure 3.1 C and D) and aligns with an observation from previous work demonstrating SARS-CoV-2 viral signal measurements preceding hospital admissions by over 10 days (D'Aoust et al., 2021a). PMMoV-normalized SARS-CoV-2 viral signal was further found to have a strong positive correlation with COVID-19 patients in ICU with $\triangle$t = 10d in Ottawa (ρ = 0.708); and a weak positive correlation exists between wastewater measurements and ICU admissions with $\triangle$t = 14d in Hamilton (ρ = 0.352) (Table 3.2, Figure 3.1 E and F, respectively). Finally, wastewater measurements maintain a strong positive relation with COVID-19-caused deaths in Ottawa with $\triangle$t = 19d (ρ = 0.730) (Table 3.2, Figure 3.1 G) and a moderate positive correlation with reported deaths in Hamilton with $\triangle$t = 20d (ρ = 0.574) (Table 3.2). The weak correlations between wastewater signal and epidemiological metrics in the city of Hamilton compared to the city of Ottawa are partially attributable to a lower frequency of wastewater testing in the city of Hamilton. Although weak positive correlations were found between wastewater measurements and reported ICU admissions and deaths in Hamilton, an apparent similarity in the trends between wastewater measurements and reported deaths in Hamilton is visually confirmed (Figure 3.1 F and H). With these findings, it can be concluded that WWS provides affirmative information attributed to both incidence of COVID-19 infections, and disease burden prior to significant vaccination immunization.

Table 3.2: Correlations (Spearman's ρ) between normalized SARS-CoV-2 RNA signal (N1-N2 copies/copies PMMoV) and laboratory positive cases, hospital admissions, ICU admissions, and deaths in Ottawa and Hamilton, prior to significant natural and vaccination immunization.

Under 70% of the total population fully vaccinated, Apr. 8th, 2020 – Aug. 29th (Ottawa)/Oct. 9th (Hamilton), 2021, wildtype and Alpha surges

Ottawa		5-day midpoint avg. laboratory positive cases	5-day midpoint avg. hospital admissions	5-day midpoint avg. ICU admissions	5-day midpoint avg. deaths
	Lead time ($\triangle$t)	5d	10d	10d	19d
	Spearman's ρ	0.821	0.808	0.708	0.730
Hamilton		3-day midpoint avg. laboratory positive cases	3-day midpoint avg. hospital admissions	3-day midpoint avg. ICU admissions	3-day midpoint avg. deaths
	Lead time ($\triangle$t)	10d	14d	14d	20d
	Spearman's ρ	0.655	0.682	0.352	0.574

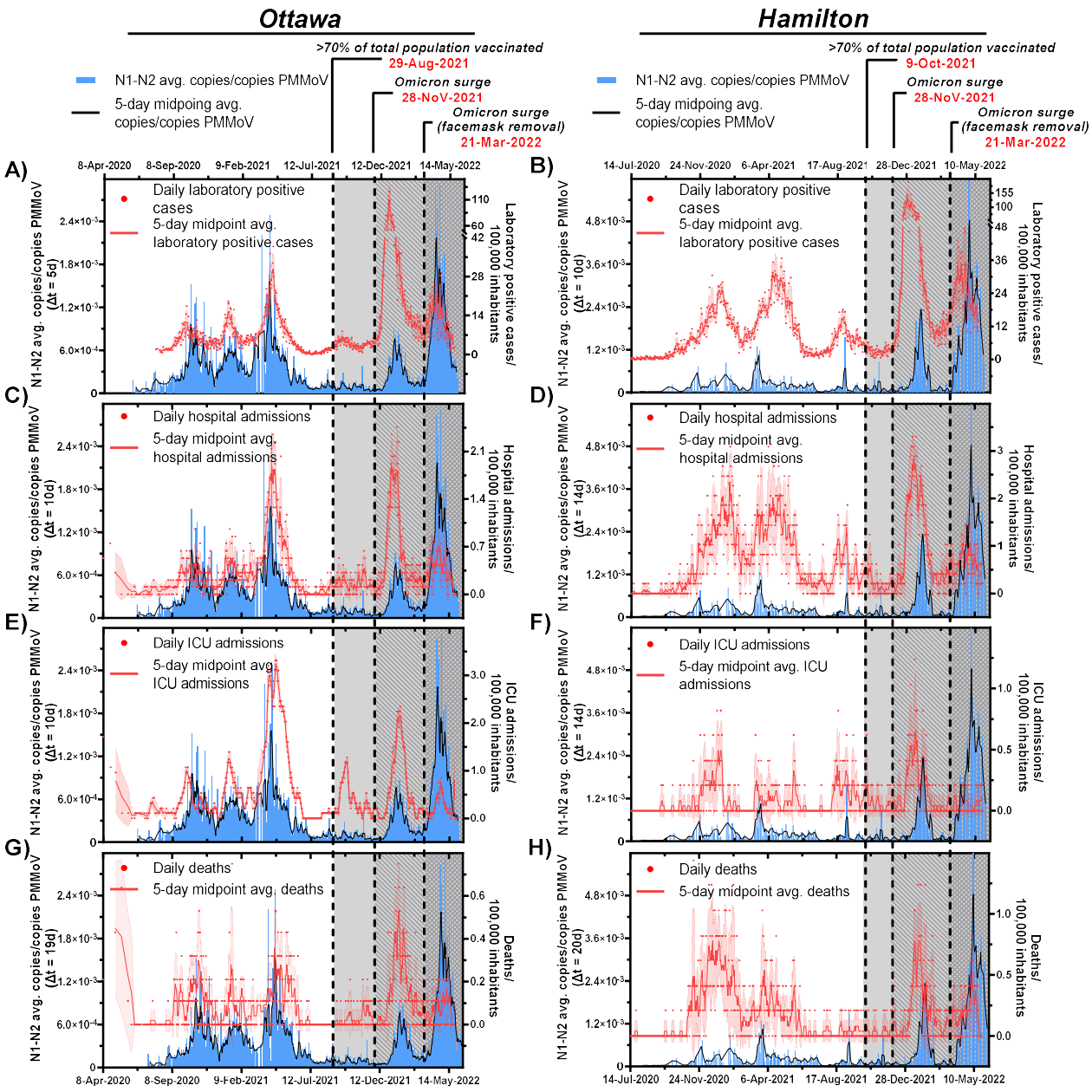

Figure 3.1: Relation between SARS-CoV-2 wastewater signal (advanced by respective "△t" time lag on the x-axis) and A) clinical COVID-19 positive cases/100,000 inhabitants in Ottawa and B) clinical COVID-19 positive cases/100,000 inhabitants in Hamilton, C) hospital admissions/100,000 inhabitants in Ottawa and D) hospitalization admissions/100,000 inhabitants in Hamilton, E) ICU admissions/100,000 inhabitants in Ottawa and F) ICU admissions/100,000 inhabitants in Hamilton, and G) COVID-19 caused deaths/100,000 inhabitants in Ottawa, and H) COVID-19 caused deaths/100,000 inhabitants in Hamilton from Apr. 8th, 2020 to May. 26th, 2022.

**Laboratory positive cases in Ottawa and Hamilton are underreported due to updated PCR eligibility in Ontario as of Dec. 31st, 2021*

3.3.2 Relation between WWS signal and epidemiological metrics post significant natural and vaccination immunization and prior to vaccination waning, Delta (B.1.617.2) surge and prior to Omicron (B.1.1.529) surge

As of Aug. 29th, 2021, in Ottawa, and Oct. 9th, 2021, in Hamilton, ≥ 70% of the total population in these communities were characterized as having reached significant vaccination immunity (2 approved vaccine doses) against COVID-19 (Public Health Ontario, 2022a). Amidst the mass vaccination campaign in both communities, the Delta (B.1.617.2) overtook the B.1.1.7 (Alpha) VOC as the dominant strain by Jul. 2021 in Ontario (Fisman and Tuite, 2021); by Jul. 31st, 2021, 50% of total wastewater signal analyzed in Ottawa was attributed to the Delta (B.1.617.2) VOC and remained dominant until Dec. 12th, 2021 (D'Aoust et al., 2022). Compared to the preceding B.1.1.7 (Alpha) VOC, the B.1.617.2 (Delta) VOC is distinguished as more transmissible and virulent (Kannan et al., 2021; Y. Liu et al., 2022; Planas et al., 2021) with higher risk of hospitalization to unvaccinated individuals (Paredes et al., 2021). To establish whether significant vaccination immunization affects the predictive nature and relation of wastewater measurements to community incidence and disease burden, the relationships between wastewater and epidemiological metrics/100,000 inhabitants (laboratory positive cases, new hospital admissions, ICU admissions, and deaths) were further evaluated using a time step analysis once significant vaccination immunization to just before the initial detection of the B.1.1.529.1 (Omicron BA.1) VOC in Ontario in Nov. 28th, 2021 (Public Health Ontario, 2022b). With significant vaccination immunization just being achieved in the communities, the majority of SARS-CoV-2 infections are less likely to exhibit severe COVID-19 symptoms leading to hospitalization or fatality due to lower viral loads (Levine-Tiefenbrun et al., 2021). Furthermore, with vaccine efficacy against the Delta (B.1.617.2) VOC being over 75% at 12 weeks since reception of a second COVID-19 mRNA vaccine dose (Iorio A. et al., 2022), waning immunity was assumed to not be prevalent in either Ottawa or Hamilton between Aug. 29th, 2021 (Ottawa)/Oct. 9th, 2021 (Hamilton) and prior to the onset of the Omicron BA.1 (B.1.1.529.1) VOC on Nov. 28th, 2021.

During the periods of high natural and vaccination immunization between Aug. 29th, 2021 (Ottawa)/Oct. 9th, 2021 (Hamilton) and Nov. 28th, 2021, and prior to vaccination waning, the wastewater viral signal along with epidemiological data fluctuated at low levels as the B.1.617.2 (Delta) VOC spread through in the cities (Figure 3.2). Weak to moderate correlations were observed between the PMMoV-normalized SARS-CoV-2 viral signal measurements in wastewater

and laboratory positive cases/100,000 inhabitants (Table 3.3). The weak correlations showed time steps of $\triangle t$ = 0d in Ottawa (ρ = 0.189) and $\triangle t$ = 0d in Hamilton (ρ = -0.029). This is further visually confirmed with wastewater signals remaining at low levels despite slight increases in laboratory positive case counts/100,000 inhabitants in both Ottawa and Hamilton communities (Figure 3.2 A and B, respectively). A similar divergence of wastewater viral measurements from laboratory COVID-19 positive cases was observed in recent WWS work during period of peak vaccination immunization (Bivins and Bibby, 2021; Cutrupi et al., 2022; Nattino et al., 2022). This indicates that wastewater is no longer leading laboratory COVID-19 positive case counts in a community with recent, significant vaccination immunity.

While there was no change in PCR testing eligibility in Ontario during the B.1.617.2 (Delta) VOC surge, it is hypothesized that this loss in relation between wastewater signal and laboratory confirmed positive cases in both communities is attributed to reduced disease severity during the B.1.617.2 (Delta) VOC surge. As such, a similar time-step analysis was conducted between wastewater and epidemiological metrics reflective of disease burden (hospital admissions, ICU admissions, and deaths). A higher, but weak positive correlation exists between wastewater viral signals and hospital admissions/100,000 inhabitants at $\triangle t$ = 11d in Ottawa (ρ = 0.364) (Table 3.3), and at $\triangle t$ = 5d in Hamilton (ρ = 0.312) (Table 3.3). While the weak correlations between wastewater and the two clinical metrics are likely attributed to wastewater data fluctuating at low levels, the trends between the PMMoV-normalized viral signals and new hospital admission/100,000 inhabitants in Ottawa and Hamilton display better visual alignment at $\triangle t$ = 11d (ρ = 0.364) (Figure 3.2 C) and $\triangle t$ = 5d (ρ = 0.312) (Figure 3.2 D), respectively, compared to the overlayed trends of wastewater and laboratory positive cases (Figure 3.2 A and B). Furthermore, the weaker correlation between wastewater signal and hospital admissions/100,000 inhabitants in Hamilton, compared to the wastewater signals in Ottawa, may be due to the lower frequency of wastewater testing in Hamilton compared to Ottawa. A weak positive correlation was observed between PMMoV-normalized SARS-CoV-2 viral signal and ICU admissions/100,000 inhabitants in Ottawa at $\triangle t$ = 14d (ρ = 0.316) (Table 3.3, Figure 3.2 E) and in Hamilton at $\triangle t$ = 7d (ρ = 0.524) (Table 3.3, Figure 3.2 F). Finally, a moderate positive correlation was observed between PMMoV-normalized SARS-CoV-2 viral signal and reported daily deaths/100,000 inhabitants at $\triangle t$ = 25d in Ottawa (ρ = 0.501) (Table 3.3, Figure 3.2 G), and at $\triangle t$ = 23d in Hamilton (ρ = 0.097) (Table 3.3, Figure 3.2 H). Since no more than 0.2 COVID-19-related deaths/100,000 inhabitants were

reported in Ottawa and Hamilton, the correlations between the wastewater measurements and reported deaths prior to the Omicron BA.1 (B.1.1.529.1) surge are presumed inconclusive. The results show a decline in the relation between wastewater and laboratory positive cases/100,000 inhabitants with ≥ 70% of the total population of both communities being recently fully vaccinated against COVID-19 and vaccination occurring prior to anticipated vaccine waning. Comparatively, hospitalization and ICU admissions exhibit a better relationship with the PMMoV-normalized viral signal measurements. These findings suggest the possibility of wastewater being a less strong lead indicator of disease incidence during possible, future COVID-19 seasonal vaccination campaigns while being a strong lead indicator of community disease burden.

Table 3.3: Correlations between normalized SARS-CoV-2 RNA signal (N1-N2 avg. copies/copies PMMoV) and laboratory positive cases, hospital admissions, ICU admissions, and deaths/100,000 inhabitants in Ottawa and Hamilton, post significant natural and vaccination immunization during the onset of the B.1.617.2 (Delta) VOC.

Over 70% of the total population was fully vaccinated, Aug. 29th (Ottawa)/Oct.9th (Hamilton), 2021 – Nov. 27th, 2021, Delta surge

Ottawa		5-day midpoint avg. laboratory positive cases	5-day midpoint avg. hospital admissions	5-day midpoint avg. ICU admissions	5-day midpoint avg. deaths
	Lead time (△t)	0d	11d	14d	25d
	Spearman's ρ	0.189	0.364	0.316	0.501
Hamilton		3-day midpoint avg. laboratory positive cases	3-day midpoint avg. hospital admissions	3-day midpoint avg. ICU admissions	3-day midpoint avg. deaths
	Lead time (△t)	0d	5d	7d	23d
	Spearman's ρ	-0.029	0.312	0.524	0.097

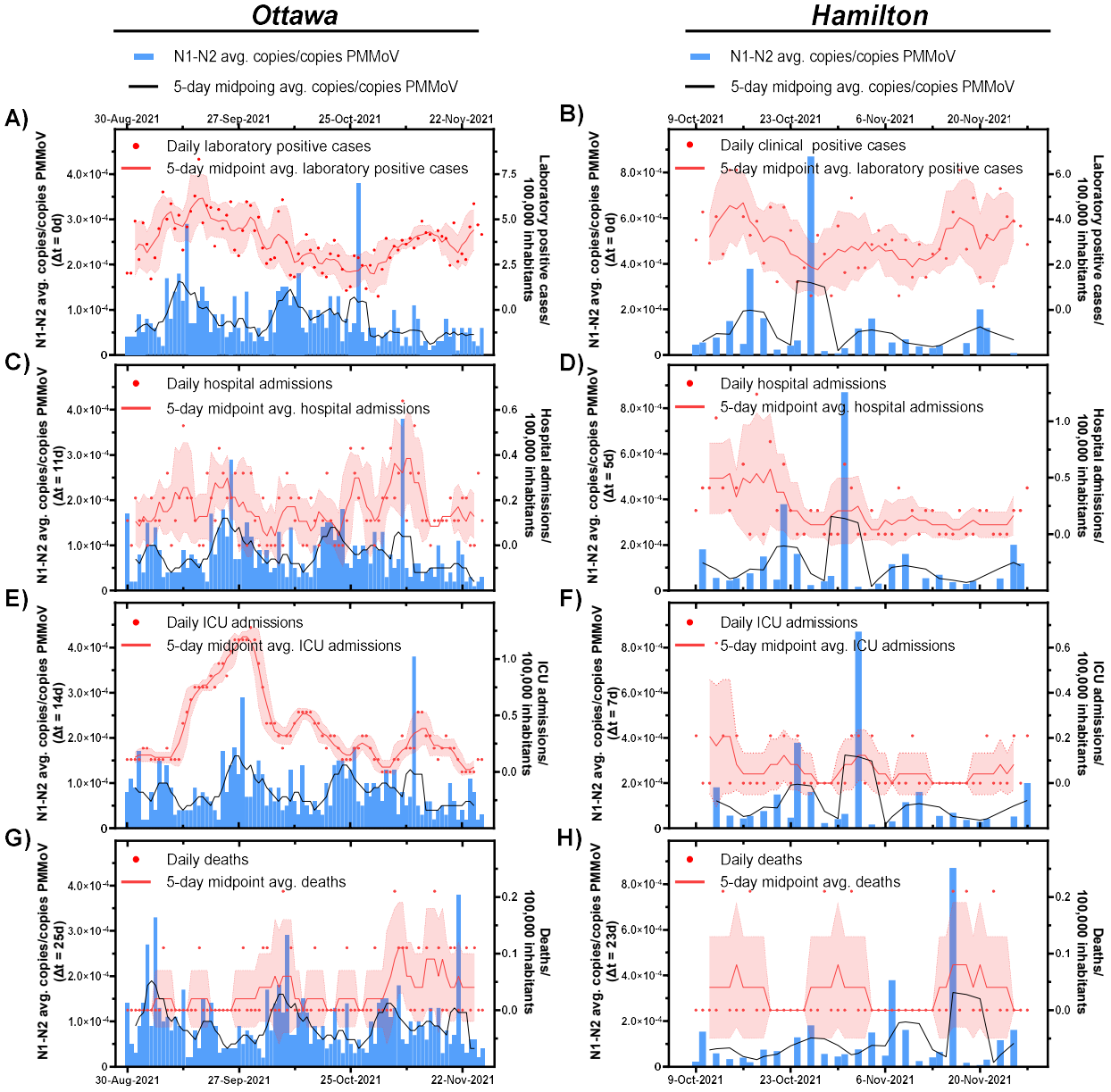

Figure 3.2: Relation between SARS-CoV-2 wastewater signal (advanced by respective "△t" time lag on the x-axis) and A) clinical COVID-19 positive cases/100,000 inhabitants in Ottawa and B) clinical COVID-19 positive cases/100,000 inhabitants in Hamilton, C) hospital admissions/100,000 inhabitants in Ottawa and D) hospitalization admissions/100,000 inhabitants in Hamilton, E) ICU admissions/100,000 inhabitants in Ottawa and F) ICU admissions/100,000 inhabitants in Hamilton, and G) COVID-19-caused deaths/100,000 inhabitants in Ottawa, and H) COVID-19 caused deaths/100,000 inhabitants in Hamilton post 70% vaccination of total population and prior to Omicron surge (Aug. 30th, 2021 – Nov. 27th, 2021, in Ottawa, and Oct 9th, 2021 – Nov. 27th, 2021, in Hamilton)

3.3.3 Relation between WWS signal and epidemiological metrics during community vaccination waning, Omicron BA.1 (B.1.1.529.1) surge

The Omicron subvariant BA.1 (B.1.1.529.1) VOC was first detected in the Canadian province of Ontario on Nov. 28th, 2021 (Public Health Ontario, 2022b). As of Dec. 12th, 2021, 50% of total wastewater signal was attributed to the Omicron BA.1 (B.1.1.529.1) VOC in Ottawa's wastewater (Figure 3.6S in Supplemental Material) and as of Dec. 26th, 2021, 50% of laboratory positive cases were reportedly infected with Omicron BA.1 (B.1.1.529.1) in Hamilton (Public Health Ontario, 2022a). The Omicron BA.1 (B.1.1.529.1) VOC remained dominant in both communities until Mar. 27th, 2022. One of the unique properties of the Omicron BA.1 (B.1.1.529.1) VOC is its higher vaccine-escape capabilities, resulting in reduced protection by vaccination immunization against onset disease severity and higher contagion compared to the Delta (B.1.617.2) VOC (Hogan et al., 2021; L. Liu et al., 2022; Smith-Jeffcoat et al., 2022; Wang et al., 2022). Additionally, at the onset of Omicron BA.1 (B.1.1.529.1), over 15 weeks have passed since ≥ 70% of the total population in the Ottawa and Hamilton communities achieved full vaccination immunization (two doses of approved vaccine). Evidence suggests waning of vaccine effectiveness against symptomatic disease from the Omicron BA.1 (B.1.1.529.1) from 75% at 2 weeks, to 14.9 – 36.3% at ≥ 25 weeks from the reception of a second COVID-19 mRNA vaccine dose (Andrews et al., 2022; Iorio A. et al., 2022; Lin et al., 2021; Tartof et al., 2021). Thus, subjecting both communities to waned vaccine-induced immunity against the highly infections Omicron BA.1 (B.1.1.529.1) VOC. This particularly puts the most frail groups in the community (the elderly, immunocompromised, and unvaccinated) at a greater risk of severe COVID-19-related complications and morbidity during the onset of Omicron BA.1 (B.1.1.529.1). A booster (third dose) of the mRNA-based vaccine was found to increase vaccine-induced immunization against symptomatic disease up to 75% at 2 weeks, 56.6% at 4 – 5 weeks, and 43.7% at 10 – 11 weeks from reception of the third vaccine dose (Iorio A. et al., 2022). As such, a booster COVID-19 vaccine dose campaign was initiated on Dec. 13, 2021, to provide improved vaccine-induced immunity against the Omicron BA.1 (B.1.1.529.1) VOC, with priority given to the most frail groups in the community. The Omicron BA.1 (B.1.1.529.1) VOC is further distinguished from the preceding VOCs by its shorter incubation period (the duration between infection and onset of symptoms) (Lee et al., 2021; Public Health Ontario, 2022c; Smith-Jeffcoat et al., 2022), and its shorter serial interval (the time from symptom onset in primary infector and symptom onset in secondarily infected case) (Backer et al., 2022;

Public Health Ontario, 2022c). The implications of these novel characteristics on the relation between wastewater viral signal and the clinical metrics representing disease incidence and disease burden require further exploration.

With the onset of the Omicron BA.1 (B.1.1.529.1) VOC from Nov. 28th, 2021, through Feb. 22nd, 2022, measurements of the PMMoV-normalized SARS-CoV-2 RNA in wastewater from both Ottawa and Hamilton exhibited an abrupt rise along with laboratory positive case counts, new hospital admissions, ICU admissions, and deaths/100,000 inhabitants (Figure 3.1). A similar resurgence in SARS-CoV-2 viral signal measurements in wastewater and laboratory COVID-19 positive case counts was observed in Israel 17 weeks after 60% of the total population received two mRNA vaccine doses during the onset of the Delta (B.1.617.2) VOC (Yaniv et al., 2021). At the peak of the Omicron BA.1 (B.1.1.529.1) surge, clinical case counts and hospital admissions/100,000 inhabitants reached a record high of 125 laboratory positive cases/100,000 inhabitants and 2.4 hospital admissions/100,000 inhabitant after the wildtype and Alpha (B.1.1.7) surges (Apr. 8th, 2020 – Aug. 29th, 2021) (Figure 3.1). On Dec. 31st, 2021, PCR testing eligibility in the Canadian province of Ontario changed from population-wide testing to only symptomatic and high-risk individuals being eligible for testing (Government of Ontario, 2021). Prior to this change in testing eligibility, a strong positive correlation between PMMoV-normalized SARS-CoV-2 viral signal and laboratory positive cases/100,000 inhabitants were observed in Ottawa at $\triangle t = 0d$ ($\rho = 0.861$), and at $\triangle t = 0d$ in Hamilton ($\rho = 0.727$) (Table 3.4). Following the Dec. 31st, 2021, change in testing eligibility, the relation between wastewater viral signal and reported laboratory positive cases/100,000 inhabitants has notably diminished due to reduced clinical testing and underreporting of the laboratory positive case counts in both Ottawa and Hamilton; this is further visually confirmed (Figure 3.3 A and B). On the contrary, PMMoV-normalized SARS-CoV-2 viral signal remained in strong agreement with new hospital admissions/100,000 inhabitants at $\triangle t = 4d$ in Ottawa ($\rho = 0.947$), and at $\triangle t = 3d$ in Hamilton ($\rho = 0.837$) (Table 3.4) from Nov. 28th, 2021, through Feb. 22nd, 2022; this is further visually confirmed (Figure 3.3 C and D), demonstrating WWS efforts consistently leading new hospital admissions. However, the lead time between PMMoV-normalized viral signal and new hospital admissions/100,000 inhabitants is notably shorter during the onset of the Omicron BA.1 (B.1.1.529.1) VOC in Ottawa and Hamilton compared to the onset of the Alpha (B.1.1.7) VOC that displayed lead times of 10 and 14 days in Ottawa and Hamilton, respectively (Table 3.2, Figure 3.1 A and B). This is likely attributed to the

shorter incubation period ranging between 2 – 8 days in individuals infected with the Omicron BA.1 (B.1.1.529.1) VOC compared to the preceding VOCs (Lee et al., 2021; Smith-Jeffcoat et al., 2022). Furthermore, PMMoV-normalized SARS-CoV-2 viral signal measurements maintains a strong positive relation with reported ICU admissions/100,000 inhabitants at $\triangle t$ = 14d in Ottawa (ρ = 0.911), and at $\triangle t$ = 2d in Hamilton (ρ = 0.673) (Table 3.4, Figure 3.3 E and F, respectively). The differences in the lead times of the PMMoV-normalized SARS-CoV-2 viral signals to the ICU admissions/100,000 inhabitants between Ottawa and Hamilton are likely attributed to the lower ICU admissions/100,000 inhabitants in Hamilton compared to Ottawa (Figure 3.3 E and F, respectively). Finally, a strong positive correlation further exists between PMMoV-normalized SARS-CoV-2 viral signal and reported deaths/100,000 inhabitants at $\triangle t$ = 18d in Ottawa (ρ = 0.905), and at $\triangle t$ = 9d in Hamilton (ρ = 0.663) (Table 3.4, Figure 3.3 G and H), supporting the indication of disease burden. Thus, findings suggest that during the onset of the Omicron BA.1 (B.1.1.529.1) VOC with its vaccine-escape capabilities and waned natural and vaccination immunization, wastewater viral signal measurements were strong indicators of disease burden in both the Ottawa and Hamilton communities.

Table 3.4: Correlations between midpoint avg. of N1-N2 copies/copies PMMoV and laboratory positive cases, hospital admissions, ICU admissions, and deaths/100,000 inhabitants in Ottawa and Hamilton, respectively, post significant natural and vaccination immunization and during the onset of the Omicron BA.1 (B.1.1.529.1) VOC.

Over 70% of the total population fully vaccinated, Nov. 28th, 2021 – Feb 22nd, 2022, Omicron BA.1 surge

Ottawa		5-day midpoint avg. laboratory positive cases	5-day midpoint avg. hospital admissions	5-day midpoint avg. ICU admissions	5-day midpoint avg. deaths
	Lead time ($\triangle t$)	0d	4d	14d	18d
	Spearman's ρ	0.861	0.947	0.911	0.905
Hamilton		3-day midpoint avg. laboratory positive cases	3-day midpoint avg. hospital admissions	3-day midpoint avg. ICU admissions	3-day midpoint avg. deaths
	Lead time ($\triangle t$)	0d	3d	2d	9d
	Spearman's ρ	0.727	0.837	0.673	0.663

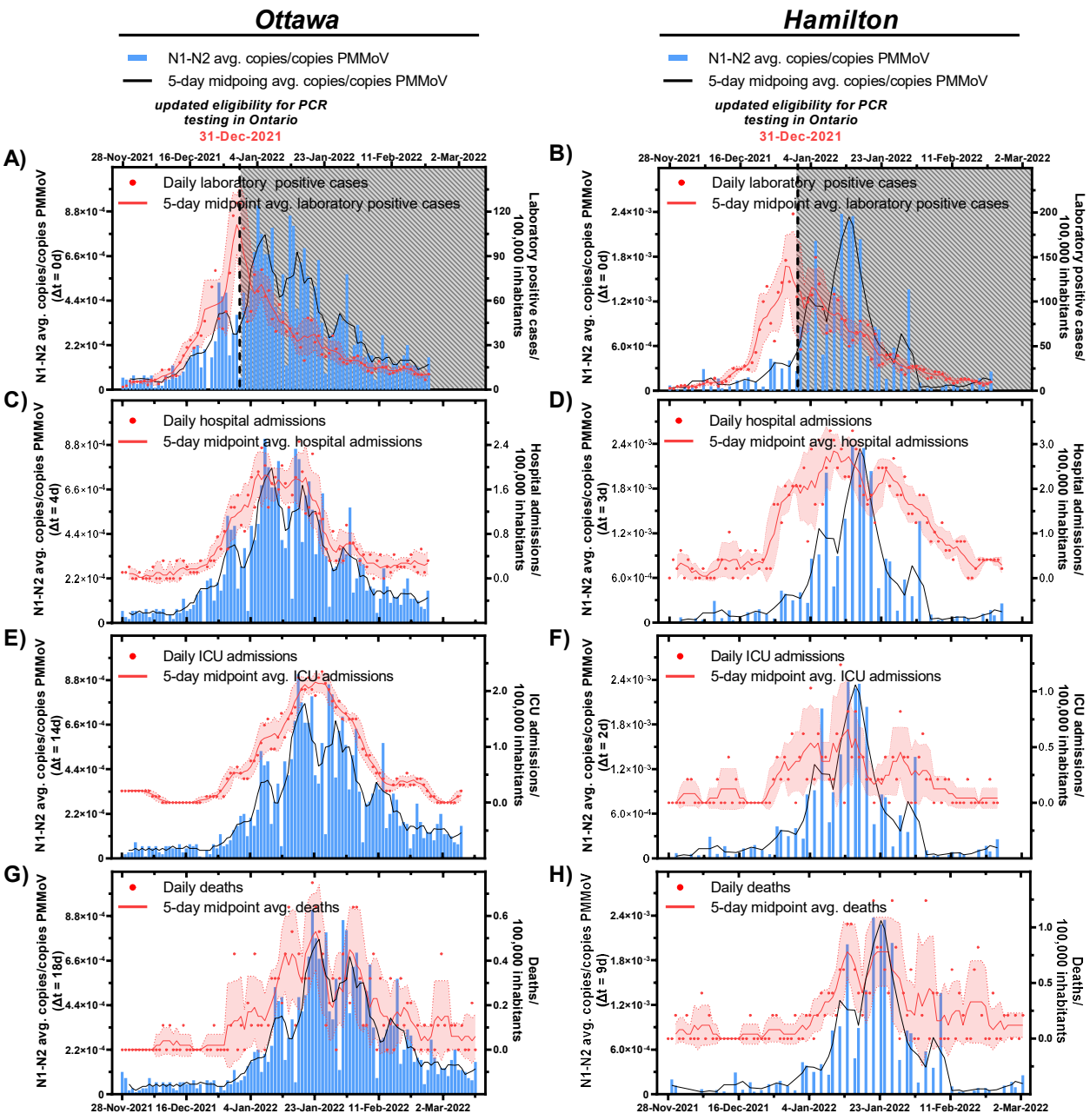

Figure 3.3: Relation between SARS-CoV-2 wastewater signal (advanced by respective "△t" time lag on the x-axis) and A) laboratory COVID-19 positive cases/100,000 inhabitants in Ottawa and B) laboratory COVID-19 positive cases/100,000 inhabitants in Hamilton, C) hospital admissions/100,000 inhabitants in Ottawa and D) hospitalization admissions/100,000 inhabitants in Hamilton, E) ICU admissions/100,000 inhabitants in Ottawa and F) ICU admissions/100,000 inhabitants in Hamilton, and G) COVID-19 caused deaths/100,000 inhabitants in Ottawa, and H) COVID-19 caused deaths/100,000 inhabitants in Hamilton during the Omicron BA.1 (B.1.1.529.1) surge (Nov. 28th, 2021, to Feb. 22nd, 2022).

**Laboratory positive cases in Ottawa and Hamilton are underreported due to updated PCR eligibility in Ontario as of Dec. 31st, 2021*

3.3.4 Relation between WWS signal and epidemiological metrics following gained natural immunity via recent surge, Omicron BA.2 (B.1.1.529.2) post protection surge

A facemask mandate and other public health protections such as gathering limits, and proof vaccination requirements were present throughout the entirety of the studied period until Mar. 21st, 2022, when facemasks were no longer required in most indoor public settings (except for public transit, health care settings, long-term care homes, and congregate settings) (Government of Ontario, 2022). Facemasks were proven to provide the highest level of personal protection against contracting COVID-19 in indoor public settings (Andrejko et al., 2022). However, immediately following the removal of facemask mandates on Mar. 21st, 2022, a steep rise in the PMMoV-normalized SARS-CoV-2 viral signal measurements was observed in both Ottawa and Hamilton as the Omicron BA.1 (B.1.1.529.1) VOC resurges, along with a concurring surge of the highly transmissible Omicron BA.2 (B.1.1.529.2) subvariant. As of Mar. 27th, 2022, 50% of total wastewater signal in Ottawa's wastewater was attributed to the Omicron BA.2 (B.1.1.529.2) VOC (Figure 3.7S in Supplemental Material) in Ottawa; the Omicron BA.2 (B.1.1.529.2) VOC remained dominant until the end of this study. During the Omicron BA.2 (B.1.1.529.2) surge since Mar. 27th, 2022, the 5-day average PMMoV-normalized SARS-CoV-2 measurement reached the highest recorded peak throughout the entirety of the study period after the previous highest peak measured during the Alpha (B.1.1.7) surge in both Ottawa and Hamilton (Figure 3.1). Unusually during this surge, however, all the four studied epidemiological metrics per 100,000 inhabitants (laboratory positive cases, hospital admissions, ICU admissions, and deaths) exhibited lower values compared to those recorded during the preceding Alpha (B.1.1.7) and Omicron BA.1 (B.1.1.529.1) surges in both communities (Figure 3.1), even though evidence suggests a similar risk for individual infected with the Omicron BA.1 and BA.2 subvariants to be hospitalized and develop severe COVID-19 symptoms (Wolter et al., 2022). This observation is dissimilar to those made during the previous surges where all the clinical metrics reached peaks that were proportional to the wastewater measurements during the preceding wildtype, Alpha (B.1.1.7), Delta (B.1.617.2), and Omicron BA.1 (B.1.1.529.1) surges (Figure 3.1). This is likely attributed to enhanced natural immunization in the most frail members of the community (the elderly and immunocompromised) due to reinfection (at least 90 days after first infection) from the Omicron BA.1 (B.1.1.529.1) surge (Abu-Raddad et al., 2021), and enhanced vaccination immunization from receiving a booster COVID-19

vaccine dose which provides up to 90% protection against severe or fatal disease by the Omicron BA.2 (B.1.1.529.2) VOC at 7 weeks since reception of a third COVID-19 mRNA vaccine dose (Iorio A. et al., 2022); resulting in a lower hospitalization and fatality outcomes throughout the course of the Omicron BA.2 (B.1.1.529.2) surge.

A moderate positive correlation between PMMoV-normalized SARS-CoV-2 viral signal and laboratory positive cases/100,000 inhabitants was observed in Ottawa at $\triangle t = 0d$ ($\rho = 0.579$), while a stronger correlation was observed at $\triangle t = 0d$ ($\rho = 0.847$) in Hamilton (Table 3.5). It is noteworthy that during this period, PCR eligibility in Ontario was still limited to only symptomatic and high-risk individuals. It is thus very likely that the reported laboratory positive cases in both studied communities are underreported, and a stronger correlation could have been observed as shown previously during the Omicron BA.1 (B.1.1.529.1) surge before Dec. 31st, 2021 (Table 3.4, Figure 3.3 A and B). According to personal communications, personnel from a high-risk occupational setting who were still eligible for PCR testing of COVID-19 in Ontario post-Dec. 31st, 2021, reported a higher magnitude of positive COVID-19 test results during the Omicron BA.2 (B.1.1.529.2) compared to the previous Omicron BA.1 (B.1.1.529.1) surge. The trends displayed by those institutions displayed a similar visual trend with the wastewater viral signal with a lead time of approximately 5 days from the PMMoV-normalized viral signal measured in wastewater, further suggesting an underestimation of the true population-wide laboratory positive cases/100,000 inhabitants in both Ottawa and Hamilton. This further aligns with evidence of higher transmissibility of the Omicron BA.2 (B.1.1.529.2) sub-lineage compared to the preceding BA.1 (B.1.1.529.1) sub-lineage (Lyngse et al., 2022). Therefore, even as clinical testing eligibility was restricted and testing results are less representative of community incidence, wastewater viral signal measurement likely remained an indicator of incidence during the Omicron BA.2 (B.1.1.529.2) surge.

Findings from the previous wildtype, Alpha (B.1.1.7), Delta (B.1.617.2), and the first Omicron BA.1 (B.1.1.529.1) surges have suggested that wastewater was a reliable indicator of disease burden based on its relationship with the clinical metrics of hospitalization, ICU admissions, and deaths/100,000 inhabitants. During the Omicron BA.2 (B.1.1.529.2) surge, although the PMMoV-normalized SARS-CoV-2 viral signal measurements displayed strong correlations with new hospital admissions/100,000 inhabitants at $\triangle t = 5d$ in Ottawa ($\rho = 0.784$)

and at △t = 3d in Hamilton (ρ= 0.612) (Table 3.5), they are notably weaker compared to the correlations from the previous Omicron BA.1 (B.1.1.529.1) surge (ρ = 0.947 at △t = 4d in Ottawa and ρ = 0.837 at △t = 3d in Hamilton) prior to the removal of facemask mandate in both communities (Table 3.4). This is likely because hospitalizations/100,000 inhabitants during this Omicron BA.2 (B.1.1.529.2) surge fluctuate more irregularly at lower counts (between 0 and 1.6) (Figure 3.5 C and D) compared to the previous Omicron BA.1 (B.1.1.529.1) surge where hospital admissions/100,000 inhabitants ranged from 0 to 2.4 (Figure 3.4 C and D). Furthermore, a moderate positive correlation exists between the PMMoV-normalized viral signal measurements in wastewater and ICU admissions/100,000 inhabitants at △t = 14d in Ottawa (ρ = 0.557) and at △t = 2d in Hamilton (ρ = 0.445) (Table 3.5). Lastly, a weak positive correlation was observed between the PMMoV-normalized viral signal and COVID-19-related deaths/100,000 inhabitants at △t = 18d in Ottawa (ρ = 0.356) and at △t = 16d in Hamilton (ρ = 0.252) (Table 3.5). COVID-19 caused deaths during the Omicron BA.2 (B.1.1.529.2) surge does not visually exhibit a notable curve-like trend with increasing wastewater viral signal in both Ottawa (Figure 3.4 G) and Hamilton (Figure 3.4 H), unlike what was been previously observed with preceding VOC surges prior to Mar. 21st, 2022 (Figure 3.1). Compared to the previous Omicron BA.1 (B.1.1.529.1) surge, not only are the correlations weaker between the clinical metrics/100,000 inhabitants indicative of disease burden (hospitalization, ICU admissions, and deaths) and wastewater viral signal during the Omicron BA.2 (B.1.1.529.2) surge, but the magnitudes of all the three metrics are reportedly lower (Figure 3.1). It is hypothesized that the lower hospitalizations, ICU admissions, and deaths/100,000 inhabitants during the Omicron BA.2 (B.1.1.529.2) surge are attributed to enhanced natural immunization and enhanced vaccination immunization against severe disease outcomes. Another contributor to higher hospitalizations/100,000 inhabitants between Dec. 2021 and Feb. 2022 during the Omicron BA.1 (B.1.1.529.1) surge compared to Mar. 2022 onwards during the Omicron BA.2 (B.1.1.529.2) surge could be a form of morbidity or mortality displacement in which the most frail members of the population are affected by the first Omicron BA.1 (B.1.1.529.1) surge. Due to reduced protection posed by Omicron's vaccine-escape capabilities, the most frail people in the community (the elderly, immunocompromised) who were protected from previous VOCs may have had severe COVID-19-related complications (hospitalization, ICU admission, or death) early in the Omicron BA.1 (B.1.1.529.1) surge. During the onset of the Omicron BA.2 (B.1.1.529.2) from Mar. 2022 onwards, those frail members of the community have either

succumbed to the illness or had recovered leaving a less-frail population for which significant natural and vaccination immunization may still convey protection from severe outcomes. Therefore, during the surge of a less virulent VOC in a community with significant natural and vaccination immunization, wastewater is shown to be less of an indicator of disease burden.

Post significant vaccination immunization, between the past 3 – 4 months of authoring this article (Jun. 2022), the WWS link to disease incidence was weakened, but the link to hospitalizations/100,000 inhabitants was not. During the post protection Omicron BA.2 (B.1.1.529.2) surge, wastewater is shown to be an indicator of incidence and infections of a less virulent VOC, and less of an indicator of disease burden either due to significant natural and vaccination immunization or due to morbidity displacement.

Table 3.5: Correlations between midpoint avg. of N1-N2 copies/copies PMMoV and laboratory positive cases, hospital admissions, ICU admissions, and deaths/100,000 inhabitants in Ottawa and Hamilton, respectively, post significant natural and vaccination immunization and during the onset of the Omicron BA.2 (B.1.1.529.2) VOC.

Over 70% of the total population fully vaccinated Mar. 21st, 2022 – May 26th, 2022, 2022, Omicron surge

Ottawa		5-day midpoint avg. laboratory positive cases	5-day midpoint avg. hospital admissions	5-day midpoint avg. ICU admissions	5-day midpoint avg. deaths
	Lead time (△t)	0d	5d	14d	18d
	Spearman's ρ	0.579	0.784	0.557	0.356
Hamilton		3-day midpoint avg. laboratory positive cases	3-day midpoint avg. hospital admissions	3-day midpoint avg. ICU admissions	3-day midpoint avg. deaths
	Lead time (△t)	0d	3d	2d	16d
	Spearman's ρ	0.847	0.612	0.445	0.252

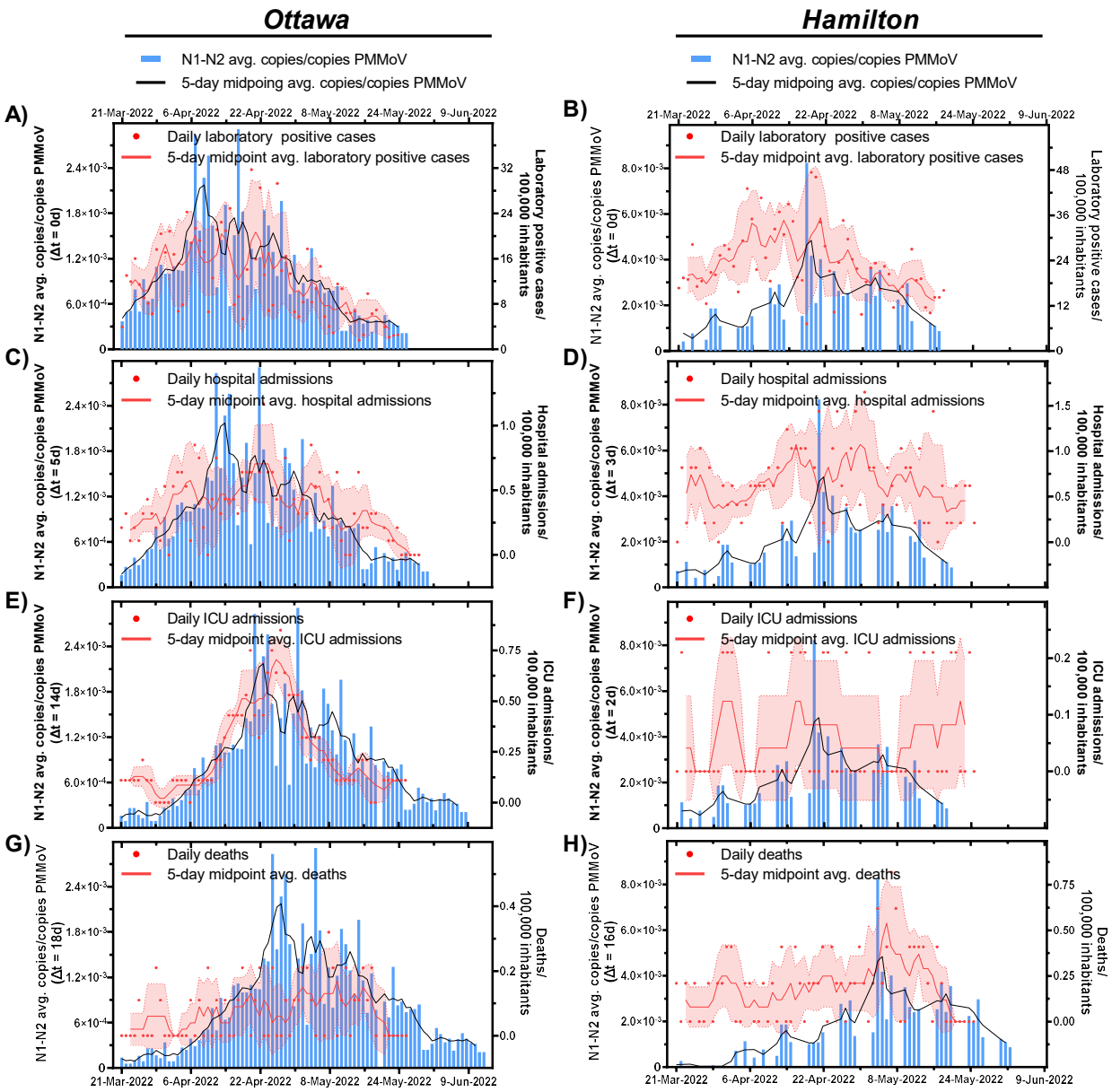

Figure 3.4: Relation between SARS-CoV-2 wastewater signal (advanced by respective "△t" time lag on the x-axis and A) laboratory COVID-19 positive cases/100,000 inhabitants in Ottawa and B) laboratory COVID-19 positive cases/100,000 inhabitants in Hamilton, C) hospital admissions/100,000 inhabitants in Ottawa and D) hospitalization admissions/100,000 inhabitants in Hamilton, E) ICU admissions/100,000 inhabitants in Ottawa and F) ICU admissions/100,000 inhabitants in Hamilton, and G) COVID-19 caused deaths/100,000 inhabitants in Ottawa, and H) COVID-19 caused deaths/100,000 inhabitants in Hamilton during the Omicron BA.2 (B.1.1.529.2) surge post removal of protection/face masking protection (Mar. 21th, 2022 to May 26th, 2022).

**Laboratory positive cases in Ottawa and Hamilton are underreported due to updated PCR eligibility in Ontario as of Dec. 31st, 2021*

3.3.5 Progression of hospitalization data as an indicator of disease virulence

Wastewater signal as a predictor and indicator of community disease burden is demonstrated during wildtype SARS-CoV-2 and the spread of the B.1.1.7 (Alpha), B.1.617.2 (Delta), and B.1.1.529.1 (Omicron BA.1 – prior to protection removal) VOCs, but not during the B.1.1.529.2 (Omicron BA.2 – post protection/facemask removal). During the onset of the wildtype SARS-CoV-2 between Dec. 2020 and Mar. 2021, wastewater viral signal was a predictor and indicator of both incidence (laboratory positive cases) and disease burden (hospital admissions) in both Ottawa (Figure 3.1 A and C) and Hamilton (Figure 3.1 B and D). The B.1.1.7 (Alpha) VOC further caused infectious surges of COVID-19 disease between Mar. 23rd, 2021 and July 31st, 2021 while vaccine rollout was still limited and only 2.2% and 2.7% of the Ottawa and Hamilton population were fully vaccinated against COVID-19 (2 approved vaccine doses) by Mar. 23rd, 2021 (onset of B.1.1.7 (Alpha) VOC), respectively (Public Health Ontario, 2022a). With the majority of the population in both communities lacking natural and vaccination immunity, the B.1.1.7 (Alpha) surge had the highest morbidity outcome (i.e., the highest counts of hospital admissions, ICU admissions, and deaths/100,000 inhabitants due to COVID-19 complications) throughout the studied period (Figure 3.1). The elevated magnitude of the corresponding hospitalization-to-wastewater (HW) ratio is further indicative of the virulence of the B.1.1.7 (Alpha) VOC in both communities (Figure 3.5). In the course of the wildtype COVID-19 and the B.1.1.7 (Alpha) VOC surge, the wastewater signal strongly correlated to both COVID-19 positive laboratory positive cases/100,000 inhabitants and hospital admissions/100,000 inhabitants in Ottawa and Hamilton (Figure 3.1). Thus, prior to significant vaccination immunization, wastewater functioned as an effective predictor and indicator of both incidence (laboratory positive cases) and disease burden (hospital admissions) with virulent dominant VOC.

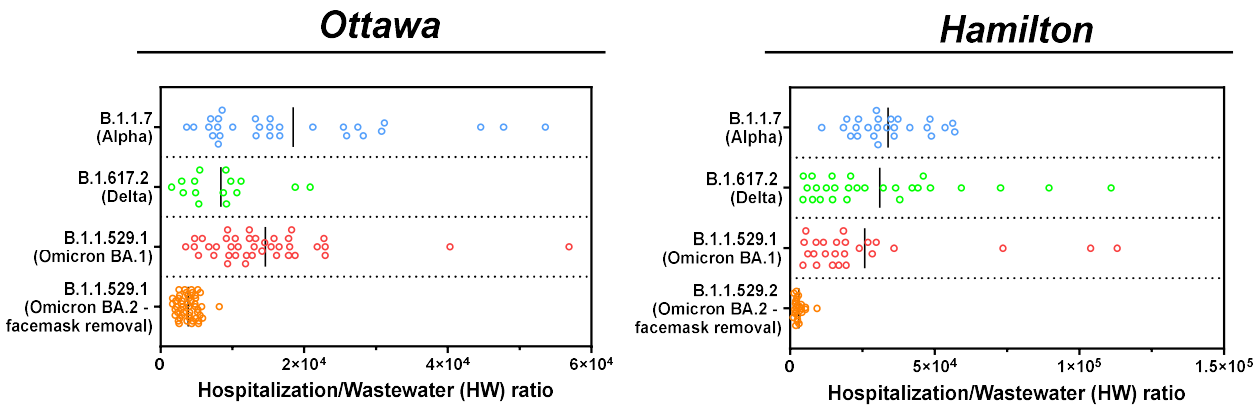

Figure 3.5: Comparison of hospitalization to wastewater ratio amplitude during the onset of the B.1.1.7 (Alpha), B.1.617 (Delta), B.1.1.529.1 (Omicron BA.1), and B.1.1.529.2 (Omicron BA.2 – post facemask removal) VOCs in Ottawa and Hamilton.

Although vaccine rollout was limited during the onset of the B.1.1.7 (Alpha) VOC, vaccination rates increased rapidly from Jun. 2021 through Aug. 2021 concurrently as the more transmissible B.1.617.2 (Delta) VOC surged through the cities from Jul. 31st, 2021 to Dec. 12th, 2021. By 23rd Jul. 23rd/Aug. 5th, 2021, at least 60% of the total population in Ottawa/Hamilton were fully immunized (2 approved vaccine doses) and by Aug. 29th/Oct. 9th, 2021, in Ottawa/Hamilton, at least 70% of the total population were fully immunized (Public Health Ontario, 2022a). With significant vaccination immunization achieved in both cities less than 2 – 4 weeks from the onset of the B.1.617.2 (Delta) VOC, both communities benefited from peak vaccination immunity. There was further the benefit of enhanced natural immunity for recovered individuals previously infected with the B.1.1.7 (Alpha) VOC during its dominance. Consequently, both studied communities experienced the lowest laboratory confirmed positive cases/100,000 inhabitants (Figure 3.1 A and B) and hospital admissions/100,000 inhabitants (Figure 3.1 C and D) throughout the entire studied period during the B.1.617.2 (Delta) VOC surge. With lower proportions of symptomatic infections occurring in the general population during the B.1.617.2 (Delta) VOC surge, the link between wastewater signal and COVID-19 incidence was weakened (population-wide PCR testing in Ontario was available during this period) (Figure 3.2 A and B) while the relation to disease burden was preserved (Figure 3.2 C and D). While the lowest hospitalizations/100,000 inhabitants and wastewater signals were experienced in both communities during the dominance of the B.1.617.2 (Delta) VOC, an elevated HW ratio is still observed, reflecting the virulent nature of the B.1.617.2 (Delta) VOC (Figure 3.5).

In Dec. 12th, 2021, the highly infectious B.1.1.529.1 (Omicron BA.1) VOC became dominant in both studied communities. By then, there is a possibility of waning vaccination protection as over 15 weeks have passed since≥70% of the total population in both communities achieved full vaccination immunization, along with the vaccine-escape qualities of the B.1.1.529.1 (Omicron BA.1) VOC. These factors have likely contributed to the highest surge in laboratory positive cases (Figure 3.1 A and B) with the second-highest morbid outcomes (i.e. second highest peaks in hospital admissions, ICU admissions, and COVID-19 related deaths/100,000 inhabitants after the B.1.1.7 (Alpha) VOC) in Ottawa (Figure 3.1 C, E and G) and Hamilton (Figure 3.1 D, F, and H). The virulence of this VOC is further reflected by an elevated HW ratio (Figure 3.5), similarly to the preceding VOCs. During this period (Dec. 12th, 2021 – Mar 27th,. 2022), wastewater viral signal measurements likely have a strong correlation to incidence (by Dec. 31st, 2021, laboratory positive cases/100,000 inhabitants in both communities are underreported due to province-wide updated PCR eligibility in Ontario) and once again maintained a strong correlation to hospitalization/100,000 inhabitants, albeit with shorter lead times of 4 days (Ottawa) and 3 days (Hamilton) (Figure 3.3 C and D), which are likely attributed to the shorter incubation time of the B.1.1.529.1 (Omicron BA.1) VOC compared to the preceding VOCs.

In Mar. 27th, 2022, the highly infections B.1.1.529.2 (Omicron BA.2) VOC predominated the latest surge in Ottawa and Hamilton (Figure 3.1 & Figure 3.4). By early Feb. 2022/early Mar. 2022 (prior to the onset of the B.1.1.529.2 (Omicron BA.2)), 50% of the total population received a booster dose (third dose of approved COVID-19 vaccine) in Ottawa/Hamilton (Public Health Ontario, 2022a); increasing vaccine-induced effectiveness for both communities against the B.1.1.529.1 & B.1.1.529.2 (Omicron BA.1 & BA.2) VOC. Natural immunity is further heightened due to SARS-CoV-2 infections during the previous B.1.1.529.1 (Omicron BA.1). As such, the populations are at peak vaccination and natural immunity during the B.1.1.529.2 (Omicron BA.2); a similar scenario to the B.1.617.2 (Delta) VOC surge. Concurrently, the mandatory facemask requirement in most public indoor spaces was removed province wide as of Mar. 21st, 2022, whilst the B.1.1.529.2 (Omicron BA.2) VOC began to spread through the cities between Mar. 27th, 2022 through the last sampling date of May 26th, 2022. Lower morbidity outcomes were observed during the B.1.1.529.2 (Omicron BA.2) VOC despite being of similar severity to the B.1.1.529.1 (Omicron BA.1) VOC. This is further reflected by a lower magnitude of HW ratio in both Ottawa and Hamilton during the B.1.1.529 (Omicron BA.2) surge, indicative of less virulent dominant VOC

during a period of peak vaccination and natural immunization (Figure 3.5). During this surge, wastewater relation to the clinical metrics/100,000 inhabitants is expected to be similar to that observed during the B.1.617.2 (Delta) surge due to being of similar immunization dynamics. However, the removal of facemask protection during the second Omicron BA.2 (B.1.1.529.2) VOC surge has resulted in a rapid surge in laboratory positive cases/100,000 inhabitants (albeit being underreported due to limited population-wide PCR testing), hence strongly correlating to the wastewater signal in Ottawa (Figure 3.4 A) and Hamilton (Figure 3.4 B). The wastewater viral signal measurements is once more displayed as a strong indicator of hospital admissions/100,000 inhabitants in both communities (Figure 3.4 C and D) with peak vaccination and natural immunity during the Omicron BA.2 (B.1.1.529.2) VOC surge. The evolution of the relation between wastewater and community disease incidence and burden throughout the studied period of the COVID-19 pandemic is summarized in Table 3.6.

Table 3.6: Evolution of WWS relation to clinical epidemiological metrics throughout the studied period of the COVID-19 pandemic

Surge	Vaccination immunity	Natural immunity	WWS relation to clinical metrics	HW ratio
Alpha (Apr. 8th, 2020, to Jul. 31st, 2021)	<70% of total population fully vaccinated (two doses of approved vaccine)	Limited natural immunity as this surge is the first exposure to the COVID-19 disease for the majority of the infections	WWS strong and moderate correlations to both incidence (ρ = 0.821 at $\triangle$t = 5d in Ottawa and ρ = 0.655 at $\triangle$t = 10d in Hamilton) and hospitalizations (ρ = 0.808 at $\triangle$t = 10d in Ottawa and ρ = 0.682 $\triangle$t = 14d in Hamilton)	Elevated ratio, indicative of virulent dominant VOC
Delta (Jul. 31st, 2021 – Dec. 12th, 2021)	Significant vaccination immunity with ≥ 70% of total population fully vaccinated against COVID-19 (two doses of approved vaccine) with limited waned immunity with vaccine efficacy against the Delta VOC being 75% at 17 weeks since reception of a second COVID-19 mRNA vaccine dose	Higher natural immunity, and limited vaccine immune escape (indication of re-infection from Alpha VOC)	WWS very weak correlation to incidence (ρ = 0.189 at $\triangle$t = 0d in Ottawa and ρ = -0.029 at $\triangle$t = 0d in Hamilton) (this shown to decrease) and weak correlation to hospitalizations (ρ = 0.364 at $\triangle$t = 11d in Ottawa and ρ = 0.312 at $\triangle$t = 5d in Hamilton)	Elevated ratio, indicative of virulent dominant VOC
Omicron (BA.1) (Dec. 12th, 2021 – Mar 27th, 2022)	Waned vaccination immunity for individuals receiving two doses of vaccine 5 months from the onset of the Omicron (BA.1) VOC	Limited natural immunity, and significant immune escape via VOC	WWS strong correlation to incidence again (ρ = 0.861 at $\triangle$t = 0d in Ottawa and ρ = 0.727 at $\triangle$t = 0d in Hamilton) and a strong correlation to hospitalizations (ρ = 0.947 at $\triangle$t = 4d in Ottawa and ρ = 0.837 at $\triangle$t = 3d in Hamilton)	Elevated ratio indicative of virulent dominant VOC
Omicron (BA.2) (Mar. 27th, 2022 – May 26th, 2022)	Significant vaccination immunity (due to rollout timing of booster vaccine dose)	Higher natural immunity (indication of re-infection from Omicron BA.1 VOC)	WWS moderate and strong correlation to incidence again (ρ = 0.579 at $\triangle$t = 0d in Ottawa and ρ = 0.847 at $\triangle$t = 0d in Hamilton) and strong correlations to hospitalizations (ρ = 0.784 at $\triangle$t = 5d in Ottawa and ρ = 0.612 at $\triangle$t = 3d in Hamilton) (weaker compared to preceding the Omicron BA.1 surge due to lower morbidity)	Low ratio, indicative of less virulent dominant VOC

3.4 Conclusions

This study demonstrates the dynamic progression of WWS of SASR-CoV-2 as predictor and indicator of disease incidence and disease burden in various stages of the pandemic. During periods with limited/waned vaccinated or natural immunity (when the wildtype COVID-19, the Alpha (B.1.1.7) and the Omicron BA.1 (B.1.1.529.1) VOCs predominated), wastewater is a strong predictor and indicator for both disease incidence and burden. During periods with peak vaccination immunization (when the Delta (B.1.617.2) and the Omicron BA.2 (B.1.1.529.2) VOCs predominated), wastewater weakened as an indictor of laboratory positive cases, but is a strong indicator for disease burden. The morbidity outcomes experienced by the studied communities were reflected by the HW ratio during the surges of the respective VOCs. While both the Omicron BA.1 and BA.2 are characterized with similar virulence, the studied communities experienced lower morbidity outcomes during the Omicron BA.2 surge due to significant natural and vaccination immunization. This is further reflected by a low HW ratio. In future cases where individuals would require seasonal vaccination for COVID-19 such that vaccination waning becomes limited, and while the vaccine is effective for the dominant VOC, WWS is expected to show moderate indication of incidence and strong indication of disease burden in the community. The wastewater to hospitalization data is also a good indicator of virulence when widespread clinical testing is limited.

3.5 Declaration of Competing Interests

The authors declare that no competing financial interests or personal relationships influenced the work reported in this manuscript.

3.6 Acknowledgements

The authors wish to acknowledge the help and assistance of the University of Ottawa, the Ottawa Hospital, the Children's Hospital of Eastern Ontario, the Children's Hospital of Eastern Ontario's Research Institute, Ottawa Public Health, City of Hamilton, Public Health Hamilton, Public Health Ontario, and all of their employees who were involved in this project. In particular, we would like to acknowledge the contributions of Cameron McDermaid and Monir Taha of Ottawa Public Health. Their time, facilities, resources, and feedback are greatly appreciated.

3.7 Funding

This research was supported by the Province of Ontario's Wastewater Surveillance Initiative (WSI). It was also supported by a CHEO (Children's Hospital of Eastern Ontario) CHAMO (Children's Hospital Academic Medical Organization) grant, which was awarded to Dr. Alex E. MacKenzie.

3.8 References

Abu-Raddad, L.J., Chemaitelly, H., Bertollini, R., 2021. Severity of SARS-CoV-2 Reinfections as Compared with Primary Infections. N. Engl. J. Med. 385, 2487–2489. https://doi.org/10.1056/NEJMc2108120

Ahmed, W., Angel, N., Edson, J., Bibby, K., Bivins, A., O'Brien, J.W., Choi, P.M., Kitajima, M., Simpson, S.L., Li, J., Tscharke, B., Verhagen, R., Smith, W.J.M., Zaugg, J., Dierens, L., Hugenholtz, P., Thomas, K. V., Mueller, J.F., 2020. First confirmed detection of SARS-CoV-2 in untreated wastewater in Australia: A proof of concept for the wastewater surveillance of COVID-19 in the community. Sci. Total Environ. 728, 138764. https://doi.org/10.1016/j.scitotenv.2020.138764

Andrejko, K.L., Pry, J.M., Myers, J.F., Fukui, N., DeGuzman, J.L., Openshaw, J., Watt, J.P., Lewnard, J.A., Jain, S., Team, C.C.-19 C.-C.S., Team, C.C.-19 C.-C.S., Abdulrahim, Y., Barbaduomo, C.M., Bermejo, M.I., Cheunkarndee, J., Cornejo, A.F., Corredor, S., Dabbagh, N., Dong, Z.N., Dyke, A., Fang, A.T., Felipe, D., Frost, P.M., Ho, T., Javadi, M.H., Kaur, A., Lam, A., Li, S.S., Miller, M., Ni, J., Park, H., Poindexter, D.J., Samani, H., Saretha, S., Spencer, M., Spinosa, M.M., Tran, V.H., Walas, N., Wan, C., Xavier, E., 2022. Effectiveness of Face Mask or Respirator Use in Indoor Public Settings for Prevention of SARS-CoV-2 Infection — California, February–December 2021. Morb. Mortal. Wkly. Rep. 71, 212. https://doi.org/10.15585/MMWR.MM7106E1

Andrews, N., Stowe, J., Kirsebom, F., Toffa, S., Rickeard, T., Gallagher, E., Gower, C., Kall, M., Groves, N., O'Connell, A.-M., Simons, D., Blomquist, P.B., Zaidi, A., Nash, S., Aziz, N.I.B.A., Thelwall, S., Dabrera, G., Myers, R., Amirthalingam, G., Gharbia, S., Barrett, J.C., Elson, R., Ladhani, S.N., Ferguson, N., Zambon, M., Campbell, C.N.J., Brown, K., Hopkins, S., Chand, M., Ramsay, M., Bernal, J.L., 2022. Covid-19 Vaccine Effectiveness against the Omicron (B.1.1.529) Variant. N. Engl. J. Med. 386, 1532–1546. https://doi.org/10.1056/NEJMOA2119451

Asghar, H., Diop, O.M., Weldegebriel, G., Malik, F., Shetty, S., El Bassioni, L., Akande, A.O., Al Maamoun, E., Zaidi, S., Adeniji, A.J., Burns, C.C., Deshpande, J., Oberste, M.S., Lowther, S.A., 2014. Environmental Surveillance for Polioviruses in the Global Polio Eradication Initiative. J. Infect. Dis. 210, S294–S303.

https://doi.org/10.1093/INFDIS/JIU384

Backer, J.A., Eggink, D., Andeweg, S.P., Veldhuijzen, I.K., Maarseveen, N. van, Vermaas, K., Vlaemynck, B., Schepers, R., Hof, S. van den, Reusken, C.B.E.., Wallinga, J., 2022. Shorter serial intervals in SARS-CoV-2 cases with Omicron BA.1 variant compared to Delta variant in the Netherlands, 13 - 26 December 2021. med 2003–2005. https://doi.org/10.1101/2022.01.18.22269217

Bar-Or, I., Yaniv, K., Shagan, M., Ozer, E., Erster, O., Mendelson, E., Mannasse, B., Shirazi, R., Kramarsky-Winter, E., Nir, O., Abu-Ali, H., Ronen, Z., Rinott, E., Lewis, Y.E., Friedler, E., Bitkover, E., Paitan, Y., Berchenko, Y., Kushmaro, A., 2020. Regressing SARS-CoV-2 sewage measurements onto COVID-19 burden in the population: A proof-of-concept for quantitative environmental surveillance. medRxiv 1–11. https://doi.org/10.1101/2020.04.26.20073569

Bivins, A., Bibby, K., 2021. Wastewater Surveillance during Mass COVID-19 Vaccination on a College Campus. Environ. Sci. Technol. Lett. 8, 792–798. https://doi.org/10.1021/acs.estlett.1c00519

CDC, 2020. Real-Time RT-PCR diagnostic panel for emergency use only. CDC EUA.

City of Hamilton, 2022. Status of Cases in Hamilton | City of Hamilton, Ontario, Canada [WWW Document]. URL https://www.hamilton.ca/coronavirus/status-cases-in-hamilton (accessed 1.17.22).

COVIDPoops19, 2022. Summary of global SARS-CoV-2 wastewater monitoring efforts by UC Merced researchers [WWW Document]. Univ. Calif. Merced. URL https://ucmerced.maps.arcgis.com/apps/dashboards/c778145ea5bb4daeb58d31afee389082 (accessed 6.6.22).

Cutrupi, F., Cadonna, M., Manara, S., Postinghel, M., La Rosa, G., Suffredini, E., Foladori, P., 2022. The wave of the SARS-CoV-2 Omicron variant resulted in a rapid spike and decline as highlighted by municipal wastewater surveillance. Environ. Technol. Innov. 28, 102667. https://doi.org/10.1016/j.eti.2022.102667

D'Aoust, P.M., Graber, T.E., Mercier, E., Montpetit, D., Alexandrov, I., Neault, N., Baig, A.T., Mayne, J., Zhang, X., Alain, T., Servos, M.R., Srikanthan, N., MacKenzie, M., Figeys, D., Manuel, D., Jüni, P., MacKenzie, A.E., Delatolla, R., 2021a. Catching a resurgence: Increase in SARS-CoV-2 viral RNA identified in wastewater 48 h before COVID-19 clinical tests and 96 h before hospitalizations. Sci. Total Environ. 770. https://doi.org/10.1016/j.scitotenv.2021.145319

D'Aoust, P.M., Mercier, E., Montpetit, D., Jia, J.J., Alexandrov, I., Neault, N., Baig, A.T., Mayne, J., Zhang, X., Alain, T., Langlois, M.A., Servos, M.R., MacKenzie, M., Figeys, D., MacKenzie, A.E., Graber, T.E., Delatolla, R., 2021b. Quantitative analysis of SARS-CoV-2 RNA from wastewater solids in communities with low COVID-19 incidence and prevalence. Water Res. 188, 116560. https://doi.org/10.1016/j.watres.2020.116560

D'Aoust, P.M., Tian, X., Towhid, S.T., Xiao, A., Mercier, E., Hegazy, N., Jia, J.-J., Wan, S., Kabir, M.P., Fang, W., Fuzzen, M., Hasing, M., Yang, M.I., Sun, J., Plaza-Diaz, J., Zhang, Z., Cowan, A., Eid, W., Stephenson, S., Servos, M.R., Wade, M.J., MacKenzie, A.E., Peng,

H., Edwards, E.A., Pang, X.-L., Alm, E.J., Graber, T.E., Delatolla, R., 2022. Wastewater to clinical case (WC) ratio of COVID-19 identifies insufficient clinical testing, onset of new variants of concern and population immunity in urban communities. medRxiv 2022.04.19.22274052. https://doi.org/10.1101/2022.04.19.22274052

D'Aoust, P.M., Towhid, S.T., Mercier, É., Hegazy, N., Tian, X., Bhatnagar, K., Zhang, Z., Mackenzie, A.E., Graber, T.E., Delatolla, R., 2021c. COVID-19 monitoring in rural communities: First comparison of lagoon and pumping station samples for wastewater-based epidemiology. Environ. Sci. Water Res. Technol. https://doi.org/https://doi.org/10.1016/j.scitotenv.2021.149618

Fisman, D.N., Tuite, A.R., 2021. Evaluation of the relative virulence of novel SARS-CoV-2 variants: a retrospective cohort study in Ontario, Canada. Can. Med. Assoc. J. 193, E1619–E1625. https://doi.org/10.1503/CMAJ.211248

Fuzzen, M., Harper, N.B.J., Dhiyebi, H.A., Srikanthan, N., Hayat, S., Peterson, W., Yang, I., Sun, J.X., Edwards, E.A., Giesy, J.P., Mangat, C.S., Tyson, E., Delatolla, R., Servos, M.R., Unit, W.S., Chemistry, A., Centre, T., 2022. Multiplex RT-qPCR assay (N200) to detect and estimate prevalence of multiple SARS-CoV-2 Variants of Concern in wastewater Abstract Wastewater-based surveillance (WBS) has become an effective tool around the globe for indirect monitoring of COVID-19 in. medRxiv 1–27. https://doi.org/10.1101/2022.04.12.22273761

Galani, A., Aalizadeh, R., Kostakis, M., Markou, A., Alygizakis, N., Lytras, T., Adamopoulos, P.G., Peccia, J., Thompson, D.C., Kontou, A., Karagiannidis, A., Lianidou, E.S., Avgeris, M., Paraskevis, D., Tsiodras, S., Scorilas, A., Vasiliou, V., Dimopoulos, M.A., Thomaidis, N.S., 2022. SARS-CoV-2 wastewater surveillance data can predict hospitalizations and ICU admissions. Sci. Total Environ. 804, 150151. https://doi.org/10.1016/J.SCITOTENV.2021.150151

Gerrity, D., Papp, K., Stoker, M., Sims, A., Frehner, W., 2021. Early-pandemic wastewater surveillance of SARS-CoV-2 in Southern Nevada: Methodology, occurrence, and incidence/prevalence considerations. Water Res. X 10, 100086. https://doi.org/10.1016/j.wroa.2020.100086

Gonzalez, R., Curtis, K., Bivins, A., Bibby, K., Weir, M.H., Yetka, K., Thompson, H., Keeling, D., Mitchell, J., Gonzalez, D., 2020. COVID-19 surveillance in Southeastern Virginia using wastewater-based epidemiology. Water Res. 186, 116296. https://doi.org/10.1016/j.watres.2020.116296

Government of Canada, 2022. COVID-19 vaccination coverage in Canada [WWW Document]. URL https://health-infobase.canada.ca/covid-19/vaccination-coverage/ (accessed 6.1.22).

Government of Ontario, 2022. Statement from Ontario's Chief Medical Officer of Health | Ontario Newsroom [WWW Document]. URL https://news.ontario.ca/en/statement/1001732/statement-from-ontarios-chief-medical-officer-of-health (accessed 5.18.22).

Government of Ontario, 2021. Updated Eligibility for PCR Testing and Case and Contact Management Guidance in Ontario | Ontario Newsroom [WWW Document]. URL

https://news.ontario.ca/en/backgrounder/1001387/updated-eligibility-for-pcr-testing-and-case-and-contact-management-guidance-in-ontario (accessed 1.16.22).

Graber, T.E., Mercier, É., Bhatnagar, K., Fuzzen, M., D'Aoust, P.M., Hoang, H.D., Tian, X., Towhid, S.T., Plaza-Diaz, J., Eid, W., Alain, T., Butler, A., Goodridge, L., Servos, M., Delatolla, R., 2021. Near real-time determination of B.1.1.7 in proportion to total SARS-CoV-2 viral load in wastewater using an allele-specific primer extension PCR strategy. Water Res. 205, 117681. https://doi.org/10.1016/J.WATRES.2021.117681

Graham, K.E., Loeb, S.K., Wolfe, M.K., Catoe, D., Sinnott-Armstrong, N., Kim, S., Yamahara, K.M., Sassoubre, L.M., Mendoza Grijalva, L.M., Roldan-Hernandez, L., Langenfeld, K., Wigginton, K.R., Boehm, A.B., 2021. SARS-CoV-2 RNA in Wastewater Settled Solids Is Associated with COVID-19 Cases in a Large Urban Sewershed. Environ. Sci. Technol. 55, 488–498. https://doi.org/10.1021/acs.est.0c06191

Haramoto, E., Kitajima, M., Kishida, N., Konno, Y., Katayama, H., Asami, M., Akiba, M., 2013. Occurrence of pepper mild mottle virus in drinking water sources in Japan. Appl. Environ. Microbiol. 79, 7413–7418. https://doi.org/10.1128/AEM.02354-13

Haramoto, E., Malla, B., Thakali, O., Kitajima, M., 2020. First environmental surveillance for the presence of SARS-CoV-2 RNA in wastewater and river water in Japan. Sci. Total Environ. 737, 140405. https://doi.org/10.1016/J.SCITOTENV.2020.140405

Hellmér, M., Paxéus, N., Magnius, L., Enache, L., Arnholm, B., Johansson, A., Bergström, T., Norder, H., 2014. Detection of pathogenic viruses in sewage provided early warnings of hepatitis A virus and norovirus outbreaks. Appl. Environ. Microbiol. 80, 6771–6781. https://doi.org/10.1128/AEM.01981-14

Hogan, A.B., Wu, S.L., Doohan, P., Watson, O.J., Winskill, P., Charles, G., Barnsley, G., Riley, E.M., Khoury, D.S., Ferguson, N.M., Ghani, A.C., 2021. Report 48: The value of vaccine booster doses to mitigate the global impact of the Omicron SARS-CoV-2 variant. https://doi.org/10.25561/93034

Inokuchi, R., Morita, K., Iwagami, M., Watanabe, T., Tamiya, N., 2021. Changes in the proportion and severity of patients with fever or common cold symptoms utilizing an after-hours house call medical service during the COVID-19 pandemic in Tokyo, Japan: a retrospective cohort study. BMC Emerg. Med. 21. https://doi.org/10.1186/s12873-021-00458-8

Iorio A., Little J., Linkins L., Abdelkader W., Bennett D., Lavis JN., 2022. COVID-19 Living Evidence Synthesis 6.31: What is the efficacy and effectiveness of available COVID-19 vaccines in general and specifically for variants of concern?

Kannan, S.R., Spratt, A.N., Cohen, A.R., Naqvi, S.H., Chand, H.S., Quinn, T.P., Lorson, C.L., Byrareddy, S.N., Singh, K., 2021. Evolutionary analysis of the Delta and Delta Plus variants of the SARS-CoV-2 viruses. J. Autoimmun. 124, 102715. https://doi.org/10.1016/J.JAUT.2021.102715

Kaplan, E.H., Wang, D., Wang, M., Malik, A.A., Zulli, A., Peccia, J., 2021. Aligning SARS-CoV-2 indicators via an epidemic model: application to hospital admissions and RNA detection in sewage sludge. Health Care Manag. Sci. 24, 320–329.

https://doi.org/10.1007/s10729-020-09525-1

Kimball, A., Hatfield, K.M., Arons, M., James, A., Taylor, J., Spicer, K., Bardossy, A.C., Oakley, L.P., Tanwar, S., Chisty, Z., Bell, J.M., Methner, M., Harney, J., Jacobs, J.R., Carlson, C.M., McLaughlin, H.P., Stone, N., Clark, S., Brostrom-Smith, C., Page, L.C., Kay, M., Lewis, J., Russell, D., Hiatt, B., Gant, J., Duchin, J.S., Clark, T.A., Honein, M.A., Reddy, S.C., Jernigan, J.A., Baer, A., Barnard, L.M., Benoliel, E., Fagalde, M.S., Ferro, J., Smith, H.G., Gonzales, E., Hatley, N., Hatt, G., Hope, M., Huntington-Frazier, M., Kawakami, V., Lenahan, J.L., Lukoff, M.D., Maier, E.B., McKeirnan, S., Montgomery, P., Morgan, J.L., Mummert, L.A., Pogosjans, S., Riedo, F.X., Schwarcz, L., Smith, D., Stearns, S., Sykes, K.J., Whitney, H., Ali, H., Banks, M., Balajee, A., Chow, E.J., Cooper, B., Currie, D.W., Dyal, J., Healy, J., Hughes, M., McMichael, T.M., Nolen, L., Olson, C., Rao, A.K., Schmit, K., Schwartz, N.G., Tobolowsky, F., Zacks, R., Zane, S., 2020. Asymptomatic and Presymptomatic SARS-CoV-2 Infections in Residents of a Long-Term Care Skilled Nursing Facility — King County, Washington, March 2020. MMWR. Morb. Mortal. Wkly. Rep. 69, 377–381. https://doi.org/10.15585/MMWR.MM6913E1

Kocamemi, B.A., Kurt, H., Sait, A., Sarac, F., Saatci, A.M., Pakdemirli, B., 2020. SARS-CoV-2 Detection in Istanbul Wastewater Treatment Plant Sludges. medRxiv 2020.05.12.20099358. https://doi.org/10.1101/2020.05.12.20099358

La Rosa, G., Mancini, P., Bonanno Ferraro, G., Veneri, C., Iaconelli, M., Bonadonna, L., Lucentini, L., Suffredini, E., 2021. SARS-CoV-2 has been circulating in northern Italy since December 2019: Evidence from environmental monitoring. Sci. Total Environ. 750, 141711. https://doi.org/10.1016/j.scitotenv.2020.141711

Lee, J.J., Choe, Y.J., Jeong, H., Kim, M., Kim, S., Yoo, H., Park, K., Kim, C., Choi, S., Sim, J.W., Park, Y., Huh, I.S., Hong, G., Kim, M.Y., Song, J.S., Lee, J., Kim, E.J., Rhee, J.E., Kim, I.H., Gwack, J., Kim, Jungyeon, Jeon, J.H., Lee, W.G., Jeong, S., Kim, Jusim, Bae, B., Kim, J.E., Kim, H., Lee, H.Y., Lee, S.E., Kim, J.M., Park, H., Yu, M., Choi, J., Kim, Jia, Lee, H., Jang, E.J., Lim, D., Lee, S., Park, Y.J., 2021. Importation and Transmission of SARS-CoV-2 B.1.1.529 (Omicron) Variant of Concern in Korea, November 2021. J. Korean Med. Sci. 36, 2–5. https://doi.org/10.3346/JKMS.2021.36.E346

Levine-Tiefenbrun, M., Yelin, I., Katz, R., Herzel, E., Golan, Z., Schreiber, L., Wolf, T., Nadler, V., Ben-Tov, A., Kuint, J., Gazit, S., Patalon, T., Chodick, G., Kishony, R., 2021. Decreased SARS-CoV-2 viral load following vaccination. Nat. Med. 27, 790–792. https://doi.org/10.1038/s41591-021-01316-7

Lin, D.-Y., Gu, Y., Wheeler, B., Young, H., Holloway, S., Sunny, S.K., Moore, Z., Zeng, D., 2021. Effectiveness of Covid-19 Vaccines in the United States Over 9 Months: Surveillance Data from the State of North Carolina. medRxiv 2021.10.25.21265304. https://doi.org/10.1101/2021.10.25.21265304

Liu, L., Iketani, S., Guo, Y., Chan, J.F.W., Wang, M., Liu, Liyuan, Luo, Y., Chu, H., Huang, Yiming, Nair, M.S., Yu, J., Chik, K.K.H., Yuen, T.T.T., Yoon, C., To, K.K.W., Chen, H., Yin, M.T., Sobieszczyk, M.E., Huang, Yaoxing, Wang, H.H., Sheng, Z., Yuen, K.Y., Ho, D.D., 2022. Striking antibody evasion manifested by the Omicron variant of SARS-CoV-2. Nature 602, 676–681. https://doi.org/10.1038/S41586-021-04388-0

Liu, Y., Liu, J., Johnson, B.A., Xia, H., Ku, Z., Schindewolf, C., Widen, S.G., An, Z., Weaver, S.C., Menachery, V.D., Xie, X., Shi, P.-Y., 2022. Delta spike P681R mutation enhances SARS-CoV-2 fitness over Alpha variant. Cell Rep. 39, 110829. https://doi.org/10.1016/J.CELREP.2022.110829

Lyngse, F.P., Kirkeby, C.T., Denwood, M., Christiansen, L.E., Mølbak, K., Møller, C.H., Skov, R.L., Krause, T.G., Rasmussen, M., Sieber, R.N., Johannesen, T.B., Lillebaek, T., Fonager, J., Fomsgaard, A., Møller, F.T., Stegger, M., Overvad, M., Spiess, K., Mortensen, L.H., 2022. Transmission of SARS-CoV-2 Omicron VOC subvariants BA.1 and BA.2: Evidence from Danish Households. medRxiv 2022.01.28.22270044. https://doi.org/10.1101/2022.01.28.22270044

Mathieu, E., Ritchie, H., Ortiz-Ospina, E., Roser, M., Hasell, J., Appel, C., Giattino, C., Rodés-Guirao, L., 2021. A global database of COVID-19 vaccinations. Nat. Hum. Behav. 5, 947–953. https://doi.org/10.1038/S41562-021-01122-8

Medema, G., Heijnen, L., Elsinga, G., Italiaander, R., Brouwer, A., 2020. Presence of SARS-Coronavirus-2 RNA in Sewage and Correlation with Reported COVID-19 Prevalence in the Early Stage of the Epidemic in the Netherlands. Environ. Sci. Technol. Lett. 7, 511–516. https://doi.org/10.1021/acs.estlett.0c00357

Mizumoto, K., Kagaya, K., Zarebski, A., Chowell, G., 2020. Estimating the asymptomatic proportion of coronavirus disease 2019 (COVID-19) cases on board the Diamond Princess cruise ship, Yokohama, Japan, 2020. Eurosurveillance 25. https://doi.org/10.2807/1560-7917.ES.2020.25.10.2000180

Nattino, G., Castiglioni, S., Cereda, D., Della Valle, P.G., Pellegrinelli, L., Bertolini, G., Pariani, E., 2022. Association Between SARS-CoV-2 Viral Load in Wastewater and Reported Cases, Hospitalizations, and Vaccinations in Milan, March 2020 to November 2021. JAMA - J. Am. Med. Assoc. 327, 1922–1924. https://doi.org/10.1001/jama.2022.4908

Naughton, C.C., Roman, F.A., Grace Alvarado, A.F., Tariqi, A.Q., Deeming, M.A., Bibby, K., Bivins, A., Rose, J.B., Medema, G., Ahmed, W., Katsivelis, P., Allan, V., Sinclair, R., Zhang, Y., Kinyua, M.N., Author cnaughton, C., 2021. Show us the Data: Global COVID-19 Wastewater Monitoring Efforts, Equity, and Gaps. medRxiv 2021.03.14.21253564. https://doi.org/10.1101/2021.03.14.21253564

Nemudryi, A., Nemudraia, A., Wiegand, T., Surya, K., Buyukyoruk, M., Cicha, C., Vanderwood, K.K., Wilkinson, R., Wiedenheft, B., 2020. Temporal Detection and Phylogenetic Assessment of SARS-CoV-2 in Municipal Wastewater. Cell Reports Med. 1, 100098. https://doi.org/10.1016/J.XCRM.2020.100098

Ottawa Public Health, 2022. Daily COVID-19 Dashboard - Ottawa Public Health [WWW Document]. URL https://www.ottawapublichealth.ca/en/reports-research-and-statistics/daily-covid19-dashboard.aspx (accessed 5.26.22).

Paredes, M.I., Lunn, S.M., Famulare, M., Frisbie, L.A., Painter, I., Burstein, R., Roychoudhury, P., Xie, H., Bakhash, S.A.M., Perez, R., Lukes, M., Ellis, S., Sathees, S., Mathias, P.C., Greninger, A., Starita, L.M., Frazar, C.D., Ryke, E., Zhong, W., Gamboa, L., Threlkeld, M., Lee, J., McDermot, E., Truong, M., Nickerson, D.A., Bates, D.L., Hartman, M.E., Haugen,

E., Nguyen, T.N., Richards, J.D., Rodriguez, J.L., Stamatoyannopoulos, J.A., Thorland, E., Melly, G., Dykema, P.E., MacKellar, D.C., Gray, H.K., Singh, A., Peterson, J.M., Russell, D., Torres, L.M., Lindquist, S., Bedford, T., Allen, K.J., Oltean, H.N., 2021. Associations between SARS-CoV-2 variants and risk of COVID-19 hospitalization among confirmed cases in Washington State: a retrospective cohort study. medRxiv. https://doi.org/10.1101/2021.09.29.21264272

Peccia, J., Zulli, A., Brackney, D.E., Grubaugh, N.D., Kaplan, E.H., Casanovas-Massana, A., Ko, A.I., Malik, A.A., Wang, D., Wang, M., Warren, J.L., Weinberger, D.M., Arnold, W., Omer, S.B., 2020. Measurement of SARS-CoV-2 RNA in wastewater tracks community infection dynamics. Nat. Biotechnol. 38, 1164–1167. https://doi.org/10.1038/s41587-020-0684-z

Peterson, S.W., Lidder, R., Daigle, J., Wonitowy, Q., Dueck, C., Nagasawa, A., Mulvey, M.R., Mangat, C.S., 2022. RT-qPCR detection of SARS-CoV-2 mutations S 69–70 del, S N501Y and N D3L associated with variants of concern in Canadian wastewater samples. Sci. Total Environ. 810, 151283. https://doi.org/10.1016/J.SCITOTENV.2021.151283

Planas, D., Veyer, D., Baidaliuk, A., Staropoli, I., Guivel-Benhassine, F., Rajah, M.M., Planchais, C., Porrot, F., Robillard, N., Puech, J., Prot, M., Gallais, F., Gantner, P., Velay, A., Le Guen, J., Kassis-Chikhani, N., Edriss, D., Belec, L., Seve, A., Courtellemont, L., Péré, H., Hocqueloux, L., Fafi-Kremer, S., Prazuck, T., Mouquet, H., Bruel, T., Simon-Lorière, E., Rey, F.A., Schwartz, O., 2021. Reduced sensitivity of SARS-CoV-2 variant Delta to antibody neutralization. Nature 596, 276–280. https://doi.org/10.1038/s41586-021-03777-9

Prevost, B., Lucas, F.S., Ambert-Balay, K., Pothier, P., Moulin, L., Wurtzer, S., 2015. Deciphering the diversities of astroviruses and noroviruses in wastewater treatment plant effluents by a high-throughput sequencing method. Appl. Environ. Microbiol. 81, 7215–7222. https://doi.org/10.1128/AEM.02076-15

Public Health Ontario, 2022a. Ontario COVID-19 Data Tool | Public Health Ontario [WWW Document]. URL https://www.publichealthontario.ca/en/data-and-analysis/infectious-disease/covid-19-data-surveillance/covid-19-data-tool?tab=vaccine (accessed 5.27.22).

Public Health Ontario, 2022b. Enhanced Epidemiological Summary - Early Dynamics of Omicron in Ontario November 1 to December 23, 2021.

Public Health Ontario, 2022c. COVID-19 Omicron (B.1.1.529) Variant of Concern and Communicability … What We Know So Far 1–15.

Randazzo, W., Truchado, P., Cuevas-Ferrando, E., Simón, P., Allende, A., Sánchez, G., 2020. SARS-CoV-2 RNA in wastewater anticipated COVID-19 occurrence in a low prevalence area. Water Res. 181. https://doi.org/10.1016/j.watres.2020.115942

Rimoldi, S.G., Stefani, F., Gigantiello, A., Polesello, S., Comandatore, F., Mileto, D., Maresca, M., Longobardi, C., Mancon, A., Romeri, F., Pagani, C., Cappelli, F., Roscioli, C., Moja, L., Gismondo, M.R., Salerno, F., 2020. Presence and infectivity of SARS-CoV-2 virus in wastewaters and rivers. Sci. Total Environ. 744, 140911. https://doi.org/10.1016/J.SCITOTENV.2020.140911

Saguti, F., Magnil, E., Enache, L., Churqui, M.P., Johansson, A., Lumley, D., Davidsson, F., Dotevall, L., Mattsson, A., Trybala, E., Lagging, M., Lindh, M., Gisslén, M., Brezicka, T., Nyström, K., Norder, H., 2021. Surveillance of wastewater revealed peaks of SARS-CoV-2 preceding those of hospitalized patients with COVID-19. Water Res. 189, 116620. https://doi.org/10.1016/J.WATRES.2020.116620

Sah, P., Fitzpatrick, M.C., Zimmer, C.F., Abdollahi, E., Juden-Kelly, L., Moghadas, S.M., Singer, B.H., Galvani, A.P., 2021. Asymptomatic SARS-CoV-2 infection: A systematic review and meta-analysis. Proc. Natl. Acad. Sci. U. S. A. 118. https://doi.org/10.1073/PNAS.2109229118/-/DCSUPPLEMENTAL

Santiso-Bellón, C., Randazzo, W., Pérez-Cataluña, A., Vila-Vicent, S., Gozalbo-Rovira, R., Muñoz, C., Buesa, J., Sanchez, G., Díaz, J.R., 2020. Epidemiological Surveillance of Norovirus and Rotavirus in Sewage (2016–2017) in Valencia (Spain). Microorganisms 8, 458. https://doi.org/10.3390/MICROORGANISMS8030458

Sherchan, S.P., Shahin, S., Ward, L.M., Tandukar, S., Aw, T.G., Schmitz, B., Ahmed, W., Kitajima, M., 2020. First detection of SARS-CoV-2 RNA in wastewater in North America: A study in Louisiana, USA. Sci. Total Environ. 743, 140621. https://doi.org/10.1016/J.SCITOTENV.2020.140621

Smith-Jeffcoat, S.E., Pomeroy, M.A., Sleweon, S., Sami, S., Ricaldi, J.N., Gebru, Y., Walker, B., Brady, S., Christenberry, M., Bart, S., Vostok, J., Meyer, S., Seys, S., Markelz, A., Ditto, N., Newbern, V., Thomas, F.J., Thomas, D., Cabredo, E., Kellner, S., Brown, V.R., Tate, J.E., Kirking, H.L., 2022. Multistate Outbreak of SARS-CoV-2 B.1.1.529 (Omicron) Variant Infections Among Persons in a Social Network Attending a Convention — New York City, November 18–December 20, 2021. Morb. Mortal. Wkly. Rep. 71, 238–242. https://doi.org/10.15585/mmwr.mm7107a3

Tartof, S.Y., Slezak, J.M., Fischer, H., Hong, V., Ackerson, B.K., Ranasinghe, O.N., Frankland, T.B., Ogun, O.A., Zamparo, J.M., Gray, S., Valluri, S.R., Pan, K., Angulo, F.J., Jodar, L., McLaughlin, J.M., 2021. Effectiveness of mRNA BNT162b2 COVID-19 vaccine up to 6 months in a large integrated health system in the USA: a retrospective cohort study. Lancet 398, 1407–1416. https://doi.org/10.1016/S0140-6736(21)02183-8

Tuite, A.R., Fisman, D.N., Odutayo, A., Bobos, P., Allen, V., Bogoch, I.I., Brown, A.D., Evans, G.A., Greenberg, A., Maltsev, A., Manuel, D.G., Mcgeer, A., Morris, A.M., Mubareka, S., Munshi, L., Murty, V.K., Patel, S.N., Razak, F., Reid, R.J., Sander, B., Schull, M., Schwartz, B., Slutsky, A.S., 2021. COVID - 19 Hospitalizations, ICU Admissions and Deaths Associated with the New Variants of Concern. Sci. Briefs Ontario COVID-19 Sci. Advis. Table 1, 1–10. https://doi.org/10.47326/ocsat.2020.02.18.1.0

Wang, Y., Zhang, L., Li, Q., Liang, Z., Li, T., Liu, S., Cui, Q., Nie, J., Wu, Q., Qu, X., Huang, W., 2022. The significant immune escape of pseudotyped SARS-CoV-2 variant Omicron. Emerg. Microbes Infect. 11, 1–5. https://doi.org/10.1080/22221751.2021.2017757/SUPPL_FILE/TEMI_A_2017757_SM9424.JPG

WHO, 2021. Classification of Omicron (B.1.1.529): SARS-CoV-2 Variant of Concern [WWW Document]. URL https://www.who.int/news/item/26-11-2021-classification-of-omicron-

(b.1.1.529)-sars-cov-2-variant-of-concern (accessed 6.1.22).

Wolter, N., Jassat, W., DATCOV-Gen author group, Gottberg, A. von, Cohen, C., 2022. Clinical severity of Omicron sub-lineage BA.2 compared to BA.1 in South Africa. medRxiv 2022.02.17.22271030. https://doi.org/10.1101/2022.02.17.22271030

Wu, F., Xiao, A., Zhang, J., Moniz, K., Endo, N., Armas, F., Bushman, M., Chai, P.R., Duvallet, C., Erickson, T.B., Foppe, K., Ghaeli, N., Gu, X., Hanage, W.P., Huang, K.H., Lee, W.L., Matus, M., McElroy, K.A., Rhode, S.F., Wuertz, S., Thompson, J., Alm, E.J., 2021. Wastewater Surveillance of SARS-CoV-2 across 40 U.S. states. medRxiv 1–13. https://doi.org/10.1101/2021.03.10.21253235

Wurtzer, S., Marechal, V., Mouchel, J., Maday, Y., Teyssou, R., Richard, E., Almayrac, J., Moulin, L., 2020. Evaluation of lockdown impact on SARS-CoV-2 dynamics through viral genome quantification in Paris wastewaters. medRxiv 2020.04.12.20062679. https://doi.org/10.1101/2020.04.12.20062679

Xiao, A., Wu, F., Bushman, M., Zhang, J., Imakaev, M., Chai, P.R., Duvallet, C., Endo, N., Erickson, T.B., Armas, F., Arnold, B., Chen, H., Chandra, F., Ghaeli, N., Gu, X., Hanage, W.P., Lee, W.L., Matus, M., McElroy, K.A., Moniz, K., Rhode, S.F., Thompson, J., Alm, E.J., 2021. Metrics to relate COVID-19 wastewater data to clinical testing dynamics. medRxiv 6, 2021.06.10.21258580. https://doi.org/10.1101/2021.06.10.21258580

Yaniv, K., Ozer, E., Lewis, Y., Kushmaro, A., 2021. RT-qPCR assays for SARS-CoV-2 variants of concern in wastewater reveals compromised vaccination-induced immunity. Water Res. 207, 117808. https://doi.org/10.1016/j.watres.2021.117808

Zhang, Y., Cen, M., Hu, M., Du, L., Hu, W., Kim, J.J., Dai, N., 2021. Prevalence and Persistent Shedding of Fecal SARS-CoV-2 RNA in Patients With COVID-19 Infection: A Systematic Review and Meta-analysis. Clin. Transl. Gastroenterol. 12, e00343. https://doi.org/10.14309/CTG.0000000000000343

3.9 Supplementary Material

Table 3.7S: List of PCR primer and probe sets utilized in this study

Primer/probe & supplier	Sequence	Reference
2019-nCov_N1 forward primer (IDT)	GAC CCC AAA ATC AGC GAA AT	(CDC, 2020)
2019-nCoV_N1 reverse primer (IDT)	TCT GGT TAC TGC CAG TTG AAT CTG	(CDC, 2020)
2019-nCoV_N1 probe (IDT)	6-FAM-ACC CCG CAT/ZEN/ TAC GTT TGG TGG ACC-IOWA BLACK FQ	(CDC, 2020)
2019-nCoV_N2 forward primer (IDT)	TTA CAA ACA TTG GCC GCA AA	(CDC, 2020)
2019-nCoV_N2 reverse primer (IDT)	GCG CGA CAT TCC GAA GAA	(CDC, 2020)
2019-nCoV_N2 probe (IDT)	6-FAM-ACA ATT TGC/ZEN/CCC CAG CGC TTC AG-IOWA BLACK FQ	(CDC, 2020)
PMMoV forward primer (ABI)	GAG TGG TTT GAC CTT AAC GTT GA	(Haramoto et al., 2013)
PMMoV reverse primer (ABI)	TTG TCG GTT GCA ATG CAA GT	(Haramoto et al., 2013)
PMMoV probe (ABI)	6-FAM-CCT ACC GAA GCA AAT G-MGB	(Haramoto et al., 2013)
VSV forward primer	ATA AGA TAC CGG GCT TGC AC	(D'Aoust et al., 2021b)
VSV reverse primer	ACA AAG ACA TGC CCG ACA C	(D'Aoust et al., 2021b)
VSV probe (ABI)	**6-FAM**-CCA TGT TGT ATT TGG ACC C-**MGB**	(D'Aoust et al., 2021b)
D3 (non-B.1.1.7) forward primer	ATC TAA ACG AAC AAA CTA AAA TGT CTG AT	(Graber et al., 2021)
D3L (B.1.1.7) forward primer	CAT CTA AAC GAA CAA ACT AAA TGT CTC TA	(Graber et al., 2021)
D63G (B.1.617.2) forward primer (ABI)	TCA CTC AAC ATG GCA AGA AAG G	*Personal communication with M. Fuzzen*
D63G (B.1.617.2) reverse primer (ABI)	GGT AGT AGC CAA TTT GGT CAT CT	*Personal communication with M. Fuzzen*
N63 (non-B.1.617.2) forward primer	CTC ACT CAA CAT GGC AAG AAA G	*Personal communication with M. Fuzzen*
D63G probe	**6-FAM**-CCT TAA ATT CCC TCG ATG ACA AGG CG-**MGB**	*Personal communication with M. Fuzzen*
N200 (B.1.617.2) forward primer	TAG TCG CAA CAG TTC AAG AAA T	(Fuzzen et al., 2022)
N200 (B.1.617.2) reverse primer	CTG GTT CAA TCT GTC AAG CAG	(Fuzzen et al., 2022)
N200 (B.1.617.2) universal probe	**6-FAM-**TCC TGC TAG AAT GGC-**BHQ-1**	(Fuzzen et al., 2022)
N200 (B.1.617.2) delta probe	**CAL Fluor Orange 560**-CAG CAG TAT GGG AAC T-**BHQ-2**	(Fuzzen et al., 2022)
C28311 (P13L) (non-B.1.1.529) forward primer	CCA AAA TCA GCG AAA TGA ACC	(D'Aoust et al., 2022)
C28311T (P13L) (B.1.1.529) forward primer	CCA AAA TCA GCG AAA TGA ACT	(D'Aoust et al., 2022)
N1 (version 2) probe (ABI)	**6-FAM**-CCG CAT TAC GTT TGG TGG ACC C-**MGB**	(D'Aoust et al., 2022)
Sdel69-70 (B.1.1.7) forward primer	CAT TCA ACT CAG GAC TTG TTC TTA CC	(Peterson et al., 2022)
Sdel69-70 (B.1.1.7) reverse primer	GGT AGG ACA GGG TTA TCA AAC CTC	(Peterson et al., 2022)
Sdel69-70 (B.1.1.7) wildtype probe	FAM-ATG CTA TA**C ATG T**CT CTG-MGB	(Peterson et al., 2022)
Sdel69-70 (B.1.1.7) alpha probe	FAM-TCCATGCTATCTCTG-MGB	(Peterson et al., 2022)

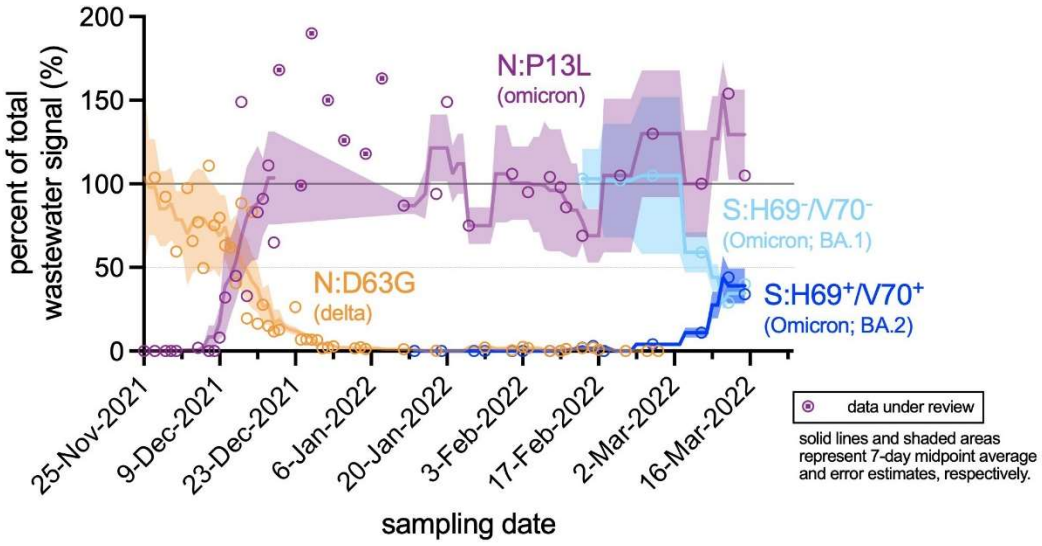

Figure 3.6S: Allelic proportions of B.1.617.2 (Delta), B.1.1.529.1 (Omicron BA.1), and B.1.1.529.2 (Omicron BA.2) VOC found in Ottawa wastewater between Nov. 25th, 2021 to Mar. 16th, 2022

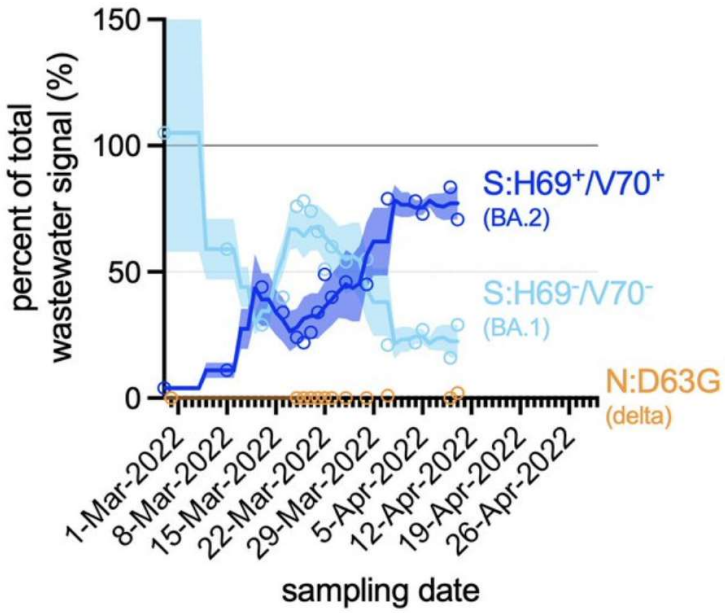

Figure 3.7S: Allelic proportions of B.1.617.2 (Delta), B.1.1.529.1 (Omicron BA.1), and B.1.1.529.2 (Omicron BA.2) VOC found in Ottawa wastewater between Mar. 1st, 2022 to Apr. 10th, 2022

Chapter 4.

Conclusions & Recommendations

4.1 Summary

The objective of this thesis was to examine two key challenges of the wastewater surveillance (WWS) of COVID-19: (i) potential data variability in wastewater samples influenced by ferric sulfate enhanced primary clarification, and (ii) interpretation of WWS data set as a disease metric through different dynamics of the pandemic. Results granted from this work are targeted to optimize the usability of WWS as a complementary epidemiological metric for the spread of the COVID-19 disease in urban communities.

4.2 Conclusions

This thesis examined the effect of a chemical coagulant (ferric sulfate) on the detection of SARS-CoV-2 and the pepper mild mottle virus (PMMoV) viral signal in both the solids and liquid fractions of homogenized influent wastewater at concentrations ranging from 0 to 60 mg/L as Fe^{3+}. The results show that primary sludge settled by a ferric sulfate has no significant impact on the quantification of SARS-CoV-2 N1 and N2 RNA gene regions. However, measurements of PMMoV viral signal were observed to significantly increase as the coagulant concentration increased ($p < 0.05$); consequently, resulting in a significant underestimation of the PMMoV-normalized SARS-CoV-2 viral signal measurements ($p < 0.05$) strongly proportional to increasing ferric sulfate concentration. To determine whether these results are attributed to the pH drop associated with the ferric sulfate addition, an isolated jar test experiment was performed by solely reducing the wastewater sample pH from 7.6 (as recorded from wastewater with 0 mg/L as Fe^{3+}) to 6.6 (as recorded from wastewater with 60 mg/L as Fe^{3+}). Results show that isolated pH reduction had a considerably weak influence on the observations drawn from the preceding coagulation experiments, i.e., the proportional increase of the PMMoV viral signal measurements with

increasing ferric sulfate concentration. Hence, this increase is more likely attributed to the PMMoV viral particles partitioning from the liquid phase to the solids phase of the tested wastewater samples as suggested by Ye et al. (2016) for nonenveloped viruses (Ye et al., 2016). This was further supported by significantly lower measurements of PMMoV viral particles in the supernatant phase when influenced by ferric sulfate concentration of 60 mg/L as Fe^{3+} compared to the measurements with 0 mg/L as Fe^{3+} ($p < 0.05$).

This thesis also examined the evolving interpretation of data acquired from WWS as public health metric. The statistical correlations between wastewater PMMoV-normalized SARS-CoV-2 viral signal and clinical metrics indicative of disease incidence (laboratory-confirmed COVID-19 positive cases), and metrics indicative of disease burden (hospitalization, intensive care unit (ICU) admissions, and deaths) were investigated from the onset of the wildtype and the Alpha variant of concern (VOC) during limited vaccination immunization, through the onset of the Omicron BA.2 VOC. One of the main conclusions drawn from this study is that wastewater demonstrates to be a strong indicator of both disease incidence and disease burden during the period of limited vaccination immunization. However, wastewater was only a moderate indicator of disease incidence, while remains a strong indicator of disease burden during the period of peak vaccination immunization (2-4 weeks after reception of 2 doses of the COVID-19 vaccine). Hospitalization-to-wastewater ratio is further shown to be a good indicator of VOC virulence when widespread clinical testing is limited. In the future, WWS is expected to show a moderate indication of incidence and a strong indication of disease burden in the community during future potential seasonal vaccination campaigns.

4.3 Recommendations for Further Research

The conclusions drawn from this research has lead to the following recommendations for future research to assist in optimizing WWS for surveillance of COVID-19 and other pathogenic diseases:

- **Investigation of other chemical coagulants**

Although the results obtained from ferric sulfate would similarly be reflected by other metal-based coagulants, testing other common coagulants such as alum, ferric chloride, polyaluminum chloride (PACl), polyaluminum sulfate (PAS), and others are recommended as

knowledge of their influence, or lack thereof, on measurement of SARS-CoV-2 and PMMoV viral signals in wastewater solids, remain currently unknown.

- **Testing wastewater samples from water resource recovery facilities (WRRFs) with chemically enhanced primary clarification**

This work was only tested at a laboratory scale to easily manipulate the coagulation conditions that would reflect standard procedures in primary clarification. However, a setup that would be relevant in a large-scale treatment system would need to be tested to better understand the extent of influence from enhanced primary clarification on WWS data through a comparison between influent pre-coagulation, and primary sludge post-coagulation. The Ottawa WRRF from which most samples were collected did not use an enhanced primary clarification process.

- **Continuing to analyze WWS data sets against clinical metrics for SARS-CoV-2**

Analysis of wastewater SARS-CoV-2 trends against public health clinical metrics needs to be continued as the pandemic progresses with the emergence of new VOCs to ensure that all dynamics of the pandemic are captured to improve the robustness of WWS of SARS-CoV-2. This can also be transferred to WWS of other diseases.

4.1 References

Ye, Y., Ellenberg, R. M., Graham, K. E., & Wigginton, K. R. (2016). Survivability, Partitioning, and Recovery of Enveloped Viruses in Untreated Municipal Wastewater. *Environmental Science & Technology*, *50*(10), 5077–5085. https://doi.org/10.1021/ACS.EST.6B00876